USE OF ANIONIC CONTRAST AGENT MAGNETIC RESONANCE IMAGING (ACMRI) AS A NEW TECHNIQUE FOR ASSESSING INTERVERTEBRAL DISC DEGENERATION

by

Joshua Adam Levitz

B.ASc., University of Waterloo, 2005

A THESIS SUBMITTED IN PARTIAL FULFILLMENT OF
THE REQUIREMENTS FOR THE DEGREE OF

MASTER OF APPLIED SCIENCE

in

THE FACULTY OF GRADUATE STUDIES

(Mechanical Engineering)

THE UNIVERSITY OF BRITISH COLUMBIA
(Vancouver)

June 2008

Abstract

Glycosaminoglycan (GAG) depletion is a consistent sign of intervertebral disc degeneration, a cause of lower back pain. Anionic contrast agent MRI (ACMRI) has been able to quantify GAG loss in articular cartilage but it has not yet been tested in the intervertebral disc in a controlled setting. We assessed the feasibility of ACMRI to measure GAG depletion in porcine lumbar intervertebral discs. Three studies were undertaken.

In study 1, we performed in-vitro dynamic diffusion MR imaging to assess the best method to ensure contrast agent uptake occurred in the disc. Signal intensity of discs bathed in contrast agent was measured at various points over a 10 hour scan. We determined that isolating the disc from the spine and manually exposing the cartilaginous endplates enhanced diffusion into the central nucleus. This result was used in our subsequent studies.

Our second study assessed the ability of ACMRI to indirectly assess GAG concentration in the disc. In-vitro contrast agent uptake in healthy and GAG-degenerated discs was measured by calculating T1 times of disc tissue before and after contrast agent exposure. Using Analysis of Variance, we tested the null hypothesis that the magnitude of T1 after contrast uptake and the change in T1 from before to after contrast uptake (ΔT1) was the same in healthy and GAG-depleted discs. The nucleus of degenerated specimens had significantly lower post-contrast T1 times and significantly larger ΔT1 than healthy discs. There were no significant differences found in the annulus of healthy and degenerated discs.

In our final study, we designed a research protocol to correlate axial mechanical properties and ACMRI indices of healthy and GAG-degenerated discs. Loading repeatability tests revealed a one degree of rotational freedom rig, combined with facet joint removal will give reproducible results on repeated tests. Six specimens were tested, and compressive stiffness dropped more in GAG-degenerated discs.

ACMRI may be useful in creating a new quantifiable scale of disc degeneration. It may also help in assessing the efficacy of disc therapeutic techniques, and to study the effect of GAG health on the in-vivo mechanics of the spine.

Table of Contents

List of Figures

List of Tables

Acknowledgements

I first would like to thank Dr. David Wilson for giving me the opportunity to work with such a knowledgeable and inviting group. Being able to really make this project my own was a truly great experience. Thank you for all your guidance.

Thank you to Dr. Tom Oxland and Dr. Brian Kwon for you your consultation and expertise. I could not have made it through this thesis without your guidance.

To Burkhard Maedler and the entire UBC High Field MRI center. You made imaging easy for me. Your help was invaluable in my research.

I would like to thank Caron Fournier for all the hard (and frustrating work) she has put in in the histology lab for me.

To Dr. Wilson's group: Laura Greaves, Laura Given, Emily, JD, Agnes, Amy, and Derek. Its been a great experience working and laughing with all of you. You have provided so much to me over the my time here, and my experience would not have been nearly as positive without you.

Thank you to everyone at DOER. We are lucky to have such a close group and it has been a pleasure to work with all of you.

To Aron, my brother, who has put up with me for my entire Masters. You have more patience then I give you credit for.

And to my parents who have always been there for me in everything I have done. Your support has let me achieve my goals time and time again. Thank you.

1. Introduction

Lower back pain is a prevalent condition which will affect 70-85% of the general population at some point during their lives[8]. It is the leading cause of activity limitation in people under 45. Consequently, determining causes and treatments are essential to maintaining and improving individual quality of life. Although there are a number of potential reasons for the pain, degeneration of the lumbar intervertebral discs is often cited as a leading cause[103].

Intervertebral disc degeneration is generally thought of as an accelerated aging process[5]. In its early stages, it is characterized by a loss of the biochemical structure of the central semi-fluid part of the disc known as the nucleus pulposus. Specifically, there is a loss of glycosaminoglycans, which are negatively charged polysaccharide molecules responsible for compressive load bearing properties of the disc[147]. As degeneration progresses, the disc becomes less hydrated and there is a loss of distinction between the nucleus pulposus and the more cartilaginous outer areas of the disc (called the annulus fibrosus). Following this, annular cracking and/or disc bulging or herniation can occur, as well as a loss of disc height and a complete collapse of the disc in the most severe degenerative cases[165]. Accelerated degeneration may be caused by such factors as genetic influences[15], excessively high or low loading environments[70,71], or nutritional deficiencies caused by impaired diffusion into or out of the disc[95,142].

Medical imaging is commonly used to diagnose degenerative disc disease. Radiographs, CT, and MRI are mostly non-invasive, non-destructive diagnostic modalities able to assess morphologic features of disc degeneration. They are crucial in the assessment of the stage of the disease and thus assist in planning the appropriate therapeutic interventions. Radiographic grading scales have been the clinical standard for years, but MRI has become widely-used recently because of its ability to image soft tissue[139]. There are concerns with imaging techniques, though. These diagnostic methods commonly rely on subjective measures which create interobserver variability problems when two or more people grade the same disc[19,93,139]. The wide range of degenerative change is usually characterized in a basic 3 to 5 level scale[91], and early biochemical changes cannot currently be identified by such modalities. It has been suggested there is a need for a more continuous and quantifiable scale able to identify earlier changes in the disc[11,171]. Current diagnostic measures also have little clinical correlation: Having high grade degeneration does not mean an individual is symptomatic[40,92]. Correlating pain to specific degenerative imaging features may identify precursors or causes of lower back pain. Isolating specific degenerative characteristics on images, as opposed to imaging an array of changes at once (which is currently done), may assist in determining such correlations.

The ability to image the biochemical makeup of the disc, specifically glycosaminoglycan content, would be useful in addressing some weaknesses of current diagnostic measures. Specifically, the ability to indirectly quantify GAG concentrations, independent of observer subjectivity, may resolve the concerns of interobserver variability. Further, as GAG loss is a consistent sign of early disc degeneration, it will help in the diagnosis of

early stage degenerative disc disease (i.e. before gross morphologic signs are present). Identifying early degeneration in this manner may be useful in beginning early treatments to prevent future onset of severe degeneration which may be associated with lower back pain. GAG imaging will also be useful in assessing the efficacy of therapeutic techniques aimed at restoring disc health. For example, it is known that the mechanical environment a disc experiences can affect glycosaminoglycan content[70,71]; there is a range of loads and loading frequencies which may help restore GAG concentration[133,157]. It is feasible to design physiotherapy regimens which exploit such loading ranges and frequencies with the intention of maintaining or restoring GAG concentrations in the degenerating disc. The ability to non-invasively measure GAG concentration will give insight into the success of such regiments.

Anionic contrast agent MRI (ACMRI) is a protocol which may advance imaging of disc degenerative disease by providing an indirect measure of disc biochemical changes. In the protocol, quantitative MRI imaging after administration of negatively charged contrast agent is used to indirectly measure glycosaminoglycan concentration. This approach has been validated in articular cartilage in a protocol called delayed gadolinium enhanced MRI of cartilage (dGEMRIC)[12,13]. Because of its ability to measure glycosaminoglycans indirectly, dGEMRIC can be used to detect early stages of cartilage degeneration which, similar to the intervertebral disc, are characterized by GAG concentration changes. Applying ACMRI in the disc may provide a quantifiable measure of early disc degeneration. This is an advantage over techniques which have aimed to quantify disc degeneration using MRI parameters (i.e. T1 and T2 relaxation times) with

uncharged[128,142] or no contrast agent[9,25] because these have only been able to consistently distinguish more advanced degeneration; these techniques appear to only be effective at diagnosing degeneration once an array of biochemical and morphologic changes have occurred. ACMRI's potential ability to quantify GAG content in early disc degeneration before such gross morphologic changes have occurred sets it apart from the current quantitative MRI techniques.

ACMRI may be useful in the creation of a continuous, quantifiable, and therefore more reliable scale of disc degeneration. It may also assist in tracking the effectiveness of therapeutic techniques aimed at restoring GAG concentration. Further, ACMRI may give us insight into the effect that GAG health has on the in-vivo mechanical properties of the disc, and whether or not GAG regenerating therapies can restore normal spine mechanics.

To assess the feasibility of indirectly measuring GAG content in the disc with ACMRI, it must first be validated in a controlled environment. MRI of discs with isolated GAG depletion is the key to the validation. This can be done in an in-vitro model with chemicals specifically targeting GAG molecules, and is the basis for our research presented here.

The objectives of this study :

1. To answer the research question: In order to create an in-vitro model for testing the feasibility of ACMRI in the intervertebral disc, what is the best anatomical

preparation method to ensure equilibrium contrast agent diffusion occurs into the in-vitro disc in a reasonable amount of time during undisturbed soaking?

2. To answer the research question: Are MRI T1 relaxation times after equilibration of anionic contrast agent sensitive to glycosaminoglycan differences in the intervertebral disc?
3. To create an axial mechanics testing protocol which will be used to detect differences between healthy and GAG-degenerated disc mechanics, and correlate the mechanical properties with ACMRI indices.

2. Background

2.1. Anatomy of the Lumbar Spine

2.1.1. Vertebrae

The 5 lumbar vertebrae are the largest of the vertebrae from any spinal level (Figure 2.1). The spinal cord runs through the vertebral foramen, which is enclosed by the bony arch posteriorly, and the vertebral body anteriorly. The bony arch consists of the two pedicles which connect the arch to the body, the transverse processes, the laminae, the facet joints, and the spinous process. The facet joint, which is a synovial joint, is composed of the superior articular process of one vertebra and the inferior articular process of the superior vertebra. Unlike the cervical and thoracic vertebrae, there are no articulating surfaces on the transverse process or the body of the lumbar vertebrae [49,110].

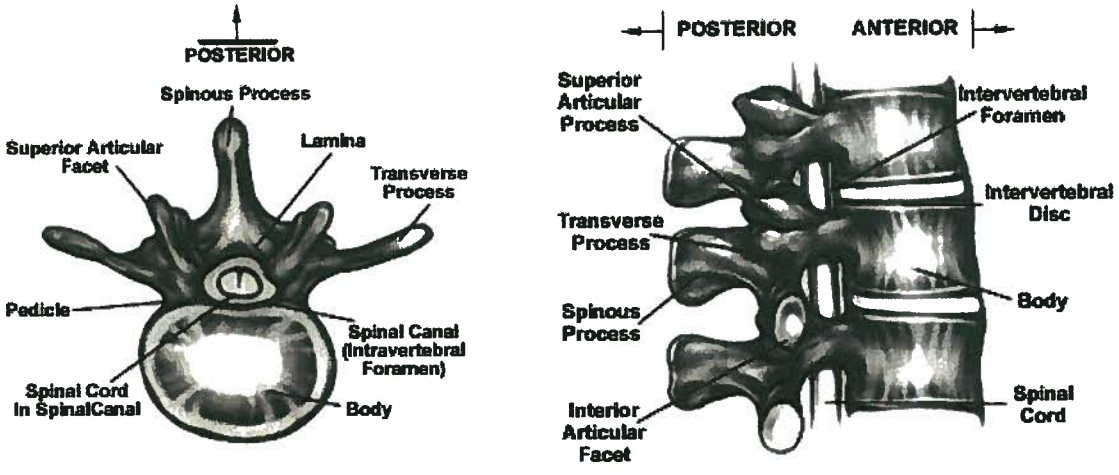

Figure 2.1: Superior (left) and lateral (right) view of the lumbar spine.

Ref: www.back.com

The intervertebral foramen between two adjacent vertebrae are the entrance and exit routes for the spinal nerves going to and coming from the spinal canal. Nerve root

compression caused by an intrusion of surrounding structures (i.e. intervertebral disc) into this space can result in leg and/or back pain.

2.1.2. Ligaments

A number of ligaments are present between the lumbar vertebrae (Figure 2.2). Anteriorly, the intervertebral discs are reinforced by the anterior longitudinal ligament, and posteriorly by the posterior longitudinal ligament. The ligamentum flavum, interspinous ligament and supraspinous ligament all act to connect different bony structures associated with the bony arch. The facet joints are connected by a capsular ligament[163]. The ligaments provide stabilization to the spine, and are important in the resistance of tensile forces. They must allow physiologic motion between vertebrae, while protecting the spinal cord by limiting excessive movement of the vertebral column, in both physiologic and highly dynamic situations[178].

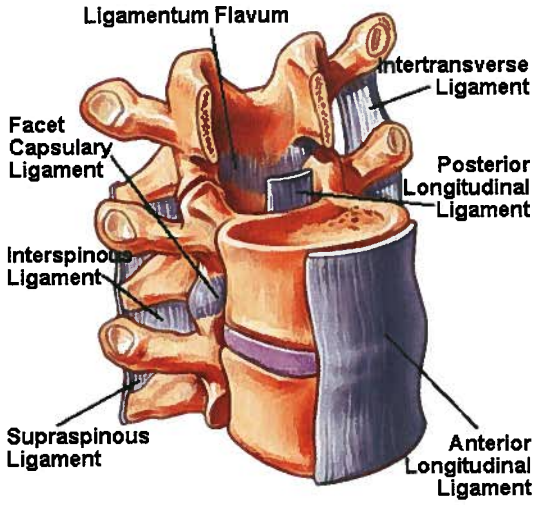

Figure 2.2: Ligaments of the Lumbar Spine

Ref: www.spineuniverse.com

2.1.3. Muscles

The muscles of the lumbar spine can be divided into the superficial and deep layers. The erector spinae, which is the spinal extensor of the superficial layer, is divided into three main muscles: The spinalis, the longissimus, and the iliocostalis divisions. The division of these three muscles is more distinct in the cervical and thoracic spinal regions than in the lumbar region; the group of muscles is often called the sacrospinalis muscles in the lumbar spine. Bilateral activation of the erector spinae causes spinal extension, while activation of only one side of the muscles causes lateral bending. Deep to these muscles are the muscles which connect and stabilize the vertebrae. These include the semispinalis, the multifidus, interspinales, intertransversarii, and the rotators. Acting in various combinations, these muscles produce slight extension or rotation of the spinal column. They also act to adjust and stabilize the vertebrae. These are important pathologically, as injury or imbalance in these muscles can be a cause of lower back pain[110].

2.1.4. The Cauda Equina

The spinal cord runs through the vertebral foramen, beginning at the medulla oblongata at the base of the skull. The cord consists of three main layers: From lateral to medial these are the Dura mater, the Arachnoid mater, and the Pia mater which is adherent to the cord itself. Because the vertebral column grows faster than the cord during childhood development, the cord in the fully developed body ends at approximately the L1-L2 level. From here, a collection of nerves called the Cauda Equina exits the cord and runs through the vertebral foramen in order to communicate with the pelvic and lower extremity

regions. Cauda Equina Syndrome, which is a compression of the nerves in this area, is rarer than spinal cord compression[86] but can cause serious lower back and extremity pain.

2.1.5. The Intervertebral Disc

The intervertebral disc (IVD) is the largest avascular structure in the body, which allows movement and flexibility in the otherwise rigid spine. As seen in Figure 2.3, the discs are bound laterally by the longitudinal ligaments of the spine, and axially by cartilaginous endplates of the vertebrae. The discs themselves consist of an inner cartilaginous nucleus pulposus, and an outer fibrous annulus fibrosus, and overall are classified as a fibrocartilaginous structure[18]. At adulthood, the disc consists of an extracellular matrix interspersed by a small number of cells which only make up approximately 1% of the total disc volume[147]. As will be explained in section 2.1.5.1, there are morphological differences between the cells in the different regions of the disc, and this contributes to different load bearing characteristics and matrix composition between the regions.

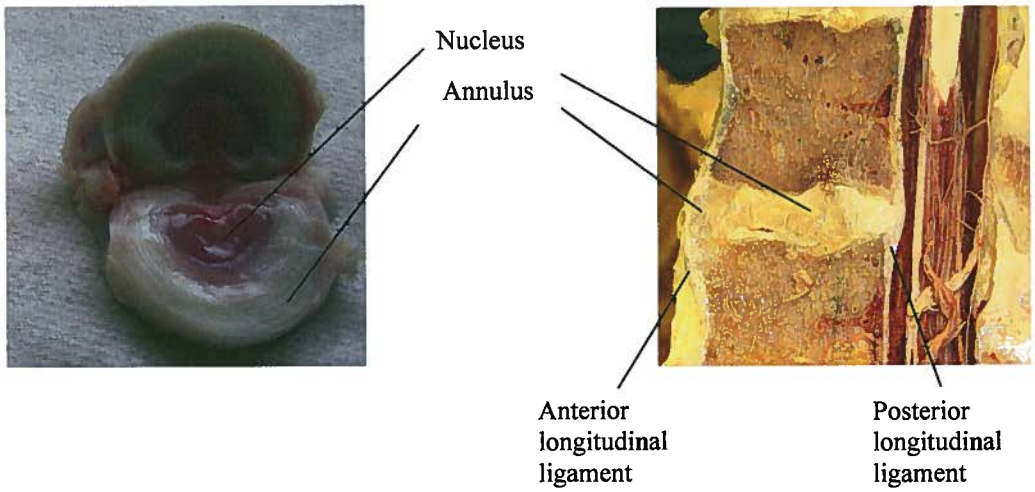

Figure 2.3: Axial and sagittal in-vitro view of the intervertebral disc

2.1.5.1. *Biology of the Intervertebral Disc*

The nucleus pulposus, which is formed from the notochord in the embryonic stage of development, contains oval and chondrocyte-like cells, which primarily synthesize type II collagen. The nucleus is therefore made up of mostly collagen II fibrils, mixed in a proteoglycan rich matrix (Figure 2.4)[147]. Proteoglycans are negatively charged molecules which allow the storage of water, and are therefore important in the load bearing properties of the disc. They consist of a protein backbone, with glycosaminoglycan (carbohydrate polymers) side chains which impart the negative charge. The distribution of charges in the three dimensional structure of the glycosaminoglycans (GAG) can attract water molecules, thus contributing to the ability of the healthy disc to retain more water[168]. In the mature nucleus pulposus, the collagen fibrils are randomly oriented and are interspersed by the matrix. This proteoglycan rich area of the disc gives the nucleus fluid-like properties, and is responsible for the disc's ability to resist compressive forces and act as a viscoelastic structure[141,160,181].

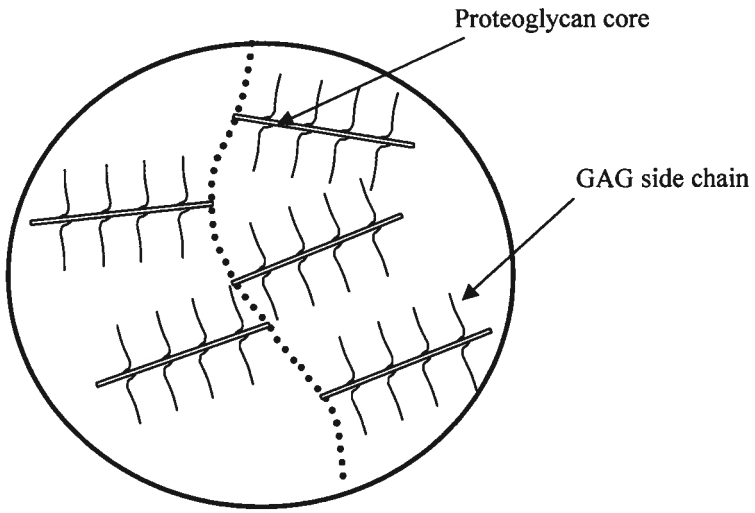

Figure 2.4: Illustration of the molecular makeup of the nucleus pulposus. The figure depicts a collagen fiber entrapping a number of proteoglycan molecules connected to a carbohydrate molecule (dashed line). The proteoglycan consist of a protein core (open line) substituted with glyosaminoglycan side chains (solid lines).

The annulus fibrosus is formed from the mesenchymal tissue during the embryonic stage of development. The cells in this region are more fibro-blast like, and produce both type I and type II collagen. The annulus is a more structured region of the disc, containing up to 25 lamellae of collagen fibrils, all arranged parallel to one another. The lamellae traverse the adjacent vertebrae at approximately 60 degrees to the axis of the spine. In adjacent lamellae, however, the fibrils alternate in their traversing orientation which greatly contributes to this region's ability to resist tensile forces, such as those created by the bulging nucleus in load bearing[151].

The cartilage endplate changes extensively throughout development. In its mature stages, it consists of a bony rim at the periphery, with the center being made of primarily hyaline cartilage. Because the disc is avascular, diffusion through the endplates is a significant

method of nutrient transmission to the disc itself, and pathology here can lead to disc degeneration as will be discussed in section 2.4.2.2.

2.1.5.2. Age Related Changes in the Intervertebral Disc

The structure of the IVD is quite different between the developing and mature states and is important in the degenerative process. Figure 2.5 shows the general trends in the structure which will be discussed.

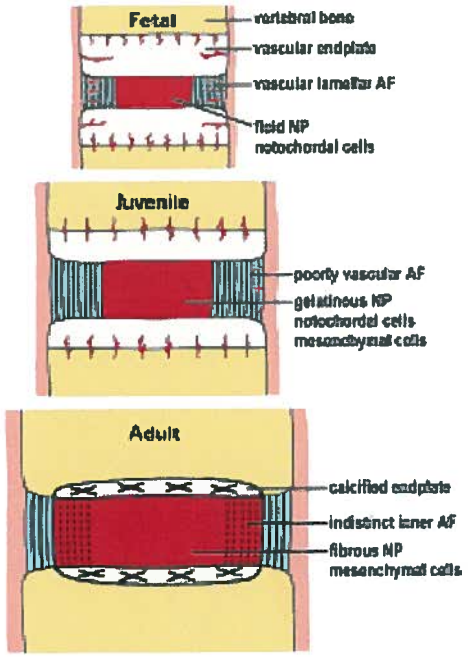

Figure 2.5: Age Changes in the intervertebral disc[151]. Printed with permission from the publisher.

In the embryonic or fetal disc, there is a clear distinction between the nucleus pulposus and annulus fibrosus structures. Superior and inferior to the disc, mesenchymal cells slowly take the place of notochordal cells to form the endplates, which occupy most of the intervertebral space in early life. In this early stage, the endplate is penetrated by vascular channels as well, as seen in Figure 2.5.

Through the juvenile stages, the endplates decrease in width, and the number of vascular channels supplying them decreases. By the age of 4-6, the vascular channels will mostly have disappeared; from this point on, nutrients such as oxygen and glucose no longer have the vascular system to reach the disc, and therefore diffuse through the endplate itself to reach the inner areas of the disc. During this stage, notochordal cells in the nucleus are slowly replaced by the chondrocyte-like mesenchymal cells. By approximately age 10, notochordal cells are essentially absent in the disc. This transition increases the amount of collagen fibrils in the nucleus, causing it to become harder, and more similar in structure to the inner annulus.

By adulthood, the endplates have become calcified and have shrunk such that they only cover the nucleus and the inner annulus. The nucleus and inner annulus are indistinct, with both having similar proteoglycan content. Throughout this process, the proteoglycan and water content in the nucleus have continually decreased as chondrocytes cannot synthesize the molecules at the same rate they are broken down. The more solid annulus may being to experience higher compressive loads as the nucleus dehydrates, and it will be more prone to cracking or damage[147,151].

2.2. Load Bearing of the Lumbar Spine

The lumbar spine bears the most weight of any unfused spinal level due to its caudal position in the body. The bony and soft tissue structures of the lumbar spine have therefore evolved to resist large deforming forces while still allowing physiologic

movement. A brief discussion of spinal anatomy as it pertains to biomechanics is helpful to identify possible pathologic issues associated with anatomical changes.

2.2.1. Configuration of the Lumbar Spine

The shape of the spine varies from kyphotic (convex curve toward posterior direction) in the thoracic spine to lordotic (concave toward the posterior direction) in the lumbar spine (Figure 2.6). The resulting biomechanical effect of an axial load on the spine can partly be explained by the spine's shape. We will demonstrate with an axial load created by the weight of the head (Figure 2.6). There is a relatively large ventral moment arm from the axial load axis to the internal axis of rotation (IAR) - the axis about which a single vertebra will rotate about if acted upon by a bending moment – in the thoracic spine. This results in a bending moment in the thoracic spine, which results in compressive stress in the ventral portion of the disc and distractive stress in the dorsal portion of the disc. The axial load axis is close to the IARs of the lumbar vertebrae, so less flexion results, and a more uniform compression is seen across the vertebral body and intervertebral disc. Based on this loading scenario, the lumbar spine will experience more burst or compression factors compared to the thoracic region.

The configuration of the spine can also result in the transfer of large loads to the lumbar region during everyday activities. Nachemson found that lumbar loads can reach approximately 300% of body weight when standing with a 20 kg object, even though only 60% of the body's weight is actually present above the lumbar spine; while sitting, loads of approximately 250% body weight are seen at the L3 level[121]. The large loads

seen at the lumbar spine may help explain why degeneration is so common in the lower lumbar levels.

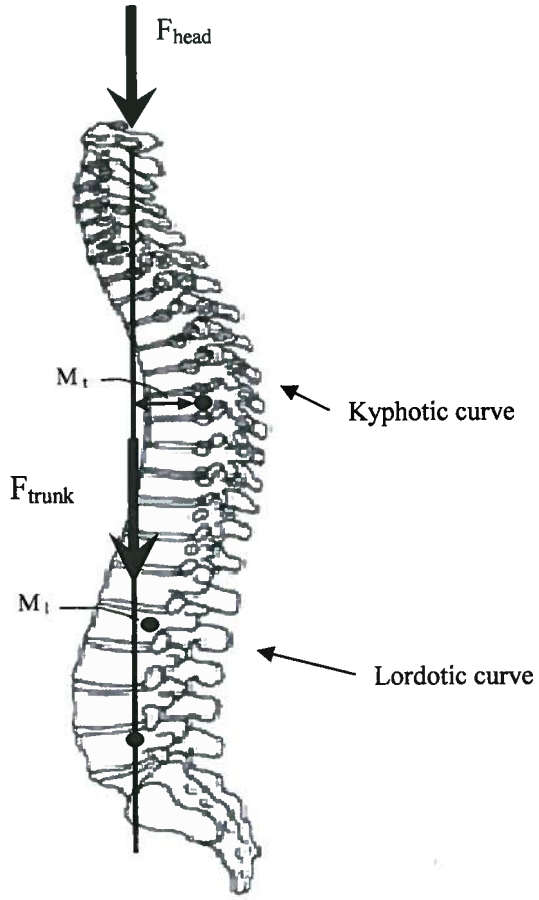

Figure 2.6: The kyphotic shape of the thoracic spine and lordosis of the lumbar spine. The moment arm from an axial load axis to the thoracic (M_t) and lumbar (M_l) approximate IAR are shown and the difference in length can easily be seen. External forces acting on the spine include the weight of the head and trunk, while muscles will generate internal forces (not shown) at each spinal level.

2.2.2. Intervertebral Discs

Transfer of loads between vertebral levels occurs through the intervertebral disc and the facet joints, with the disc supporting approximately 80% of the load, depending on the

position of the spine[122]. The large compressive loads seen in the lumbar spine are mainly supported by the hydrated nucleus pulposus, which provides high hydrostatic pressures for support. The outer annulus acts like a tensile skin to restrain the bulging nucleus[5].

2.2.3. Vertebral Bodies

The vertebral bodies of the lumbar spine are both wider and deeper than the cervical and thoracic levels, and this size increase correlates with increased strength[21].

2.2.4. Facet Joints

The orientation of the facet joints varies between levels and the orientation helps to explain the kinematics seen in each spinal section. The lumbar facet joints are oriented primarily in a sagittal direction in the lumbar spine, providing resistance to axial rotation while allowing some flexion and anterior-posterior, and superior-inferior translation. Conversely, in the cervical spine, facet joints tend to have a more coronal orientation which resists anterior-posterior translation at lower flexion angles[6,172]. By resisting deforming forces, the facets influence the type of movement seen at each spinal level and transmit some load.

2.3. Lower Back Pain

2.3.1. Epidemiology

Lower back pain is one of the most common disorders in society today, affecting between 70-85% of the general population at some point during their lives[8]. In the USA, back pain is the second most frequent reason for doctor visitations, the fifth ranking cause for

hospital admissions, and the third ranking cause for surgical procedures[65,164]. In terms of Workers' Compensation, lower back pain is also the most common and expensive cause of disability related to work, with an estimated annual cost of $11.7 billion for lower back pain compensation in the United States[120]. Patients experiencing chronic lower back pain (consistent pain over a period greater than 3 months), use health services more often than most other patient groups[65]. Lower back pain can interfere with the most common daily activities such as walking stairs or standing from a chair. In people under the age of 45, it is the most common cause of activity limitation, and therefore is a great concern to an individual's overall quality of life[8].

2.3.2. Etiology

The etiology of lower back pain is multifactorial, and diagnosing a single cause for the pain is impossible in the majority of cases. Many factors can play an important role in the symptomatic patient; most notably muscular pain, psychosocial factors, facet joint disease or intervertebral disc degeneration.

2.3.3. Muscular Pain

Muscular pain is one main research foci in the lower back pain field. Studies examine such variables as static and dynamic muscle strength and muscle activation during loading scenarios in symptomatic and asymptomatic subjects[58,109,143]. Muscle imbalances or weakness may cause pain by placing increased loads on other back structures (i.e. lumbar vertebrae, IVD).

In general, muscle research has inherent difficulties because, as stated by Stokes et al, "Due to the large number of muscles which act during trunk loading scenarios, and the possible variability in these patterns between individuals and tasks, it is impossible to find a direct relationship between a task and spinal loading"[162]. Monitoring one set of muscles in lower back pain studies may not be sufficient for determining all underlying contributors of the pain. This theme reoccurs in the lower back pain research field, as it is difficult to fully attribute the pain to a single factor or tissue type.

2.3.4. Psychosocial Factors

Psychological and social factors have been shown to be associated with lower back pain. Boos et al found that psychosocial factors such as occupational anxiety and depression were often correlated with lower back pain[26]. Carragee et al found that patients with chronic non-lumbar pain showed a higher incidence of lumbar back pain[39], and another study by the same group showed individuals with previous incidences of lower back pain were more likely to have lower back pain in the future[40]. It is important to consider that in many of these cases, it is difficult to determine whether psychological factors have contributed to lower back pain, or if psychological factors have arisen because of the lower back pain.

Another interesting concept discussed by Deyo et al[46], is the psychological effect of clinical imaging on patients. In a recent randomized trial, disability scores were lower and pain was more consistent at 3 months in a group who were given radiographic

imaging diagnosis compared to those who were not (control group)[90]. The psychological factors present in lower back pain cases make diagnosis of the actual cause of symptoms more difficult than a simple clinical test or imaging diagnosis.

2.3.5. Facet Joint Disease

Spinal nerve segments innervate the facet joints, and controversy exists over facet joint damage causing radiculopathy (nerve root irritation) and pain in the lumbar spine[42]. A study by Kuslich et al showed that stimulation of the facet joint capsule rarely caused pain in patients undergoing spinal surgery for disc herniations and/or spinal stenosis[96]. However, the same study found pressure applied at the point where the superior articular facet joint comes into contact with the posterior aspect of the disc could have caused lower back pain in many of their 193 patients. Although the capsule itself may not be involved in lower back pain etiology, contact between the bony structures and the disc may cause irritation and subsequent pain[96]. Other possible mechanisms by which the facet causes lumbar pain are direct compression of nerves due to facet hypertrophy or osteophyte formation (as in osteoarthritis). Superior-inferior subluxation of the joint due to disc height loss (as seen in disc degeneration) can reduce the size of the spinal canal again causing root compression and possibly pain[81].

2.3.6. Intervertebral Disc Related Pain

Ever since Mixter and Barr associated sciatica - pain in the lower back and legs due to compression of the sciatic nerve – with a prolapse or herniation of the lumbar

intervertebral disc in 1934, lower back pain caused by intervertebral disc pathology, and specifically disc degeneration, has been a major area of study in the lower back pain field[116]. The field of research has since expanded to looking at the progression, causes, and diagnosis of disc degeneration, what aspects of degeneration cause lower back pain, and treatments for disc degeneration including conventional therapy, surgical treatment, or, more recently, cell, gene, and hormone therapy. The next section will provide a more complete explanation of intervertebral disc degeneration.

2.4. Intervertebral Disc Degeneration (IDD)

Deterioration of spinal structures is an inevitable consequence of aging. Developmental, biomechanical, or other factors can accelerate the rate of degeneration, though, causing pathologies before they are expected. Although a standard definition of disc degeneration is not agreed upon[34], it is generally considered the accelerated process of disc tissue degeneration previously described in the section 2.1.5.2[5,14,73,118,151]. Such a definition only gives an idea as to what characterizes degeneration, and says nothing about the underlying causes. Distinguishing disc degeneration from physiologic processes such as aging and healing has been difficult. Controversy often arises when determining whether degeneration has been caused by disease processes or normal changes to the disc, and research therefore aims to provide a definition of degeneration which will satisfy researchers and clinicians alike[5].

Intervertebral disc degeneration is a common clinical finding, with the lumbar spine and lower cervical spine showing the most severe signs of the disease. The lumbar spine is the most common site for the disease[99].

2.4.1. Signs of Disc Degeneration and Lower Back Pain

The cellular changes present in degeneration follow the same pattern seen in normal disc aging. These changes can lead to structural alterations of the disc, which are consistent signs of disc degeneration[5]. These include tissue tearing, disc prolapse, and endplate alterations. Although the mechanism of disc related (i.e. discogenic) low back pain is not well understood, theories about the role of degenerative changes as the cause have been made.

2.4.1.1. Annular Tearing

As the disc ages and degeneration occurs, the nucleus becomes smaller and decompressed, which transfers more load to the annulus[4] and generally alters disc and spine mechanics[84,114,115,149,167,181]. Because of these load changes, and other factors present in degeneration, there is a greater occurrence of tearing in the annulus fibrosus[29,67]. Three types of tears are generally seen in the annulus: Circumferential (or delaminations), peripheral rim, and radial fissures. Vascularised granulation tissue can fill these tears as the disc attempts to heal, and the nerve fibers associated with the new tissue are thought to be a cause of lower back pain[53,135]. Tears are often detected on MRI

images because of the imaging modality's ability to image soft tissue and the internal morphology of the disc[52,77,88,174] (Figure 2.7).

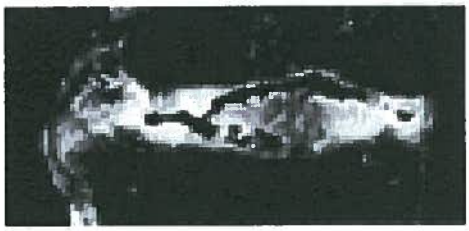

Figure 2.7: Morphologic image showing annular tears[165]. The dark lines throughout the disc indicate tearing of the tissue. Reprinted with permission of the publisher.

2.4.1.2. Disc Bulging and Herniations

Disc bulging and herniation are other signs of degeneration, and are seen when either the annulus (bulging) or nucleus (herniation) enters into the spinal canal. In bulging, the annulus is pushed into the spinal canal, for example by excessive nucleus movement due to abnormal loading. In more severe cases herniation occurs in which the nucleus material can migrate through radial fissures in the annulus and enter directly into the canal[5,81]. A loss of disc height often accompanies such changes, with the disc acting like a "flat tire"[33]. Disc height narrowing is a common sign of disc degeneration and can be seen on radiographs, CT and MRI. Herniations and bulging have the potential to contribute to spinal stenosis, a narrowing of the spinal canal[161,163]. Spinal cord and nerve root compression can occur with stenosis, possibly resulting in lower back and/or leg pain. Another theory states that in a herniation, the nucleus material chemically irritates the nerve roots when it comes in contact with them, resulting in an inflammatory response and pain[25,112,131].

2.4.1.3. Endplate changes

Endplate changes are yet another structural alteration common in the degenerated disc. Endplates are the weak link in the compressive resistance of the spine, and tend to accumulate trabecular microdamage as one ages[173]. It has been shown that fatigue damage to the endplates can occur at loads well within the normal ranges of everyday spinal loading[64], and that even slight mechanical damage to the endplate can affect internal stress distributions in the disc[1,2] . It is possible for damaged endplate to deform more when under load, potentially forcing the nuclear material toward the annulus or allowing some nucleus to pass through it. Both scenarios will result in load transference to the annulus, and therefore increases the possibility of the annulus bulging inward into the nucleus, or outward into the spinal canal[2,156]. The nucleus can also protrude through the endplate fractures into the adjacent vertebrae, a pathology known as Shmorl's nodes.

2.4.2. Causes of Intervertebral Disc Degeneration

Certain specific influences are thought to impact the rate and degree of disc degeneration, and can account for the variability in degenerative signs seen amongst individuals. The influences can be broken into genetic, nutritional, and biomechanical factors.

2.4.2.1. Genetic Influences

In the last 20 years, studies have found strong evidence that genetic inheritance is the highest risk factor in developing disc degeneration[15,105,153]. These studies have used twin populations to determine what influences explain disc degeneration, studying such factors

as genetics, loading due to employment-related activities, or smoking. In general, it has been found that approximately 50-70% of the variability in disc degeneration between twins can be explained by familial aggregation, and genetics seems to be the most significant factor[153].

2.4.2.2. *Diffusion and Nutritional Influences*

The intervertebral disc requires a nutrient and oxygen supply, as well as waste removal (i.e. lactic acid) system to maintain its health. In the growing disc, these supply and removal processes occur through the vascular system which extends into the endplates and peripheral annulus. As aging occurs and vasculature recedes from the endplates, diffusion across the endplates and periphery of the annulus becomes the main process by which nutrients and waste are transported in and out of the disc; endplate diffusion is the primary route. Anything that compromises the diffusion process and threatens to lower nutrient supply in the disc, such as decreased blood flow [95], or endplate changes[142] may encourage degeneration, although controversy exists[69].

Studies have used MRI imaging after in-vivo intravenous injections of contrast agent to study the diffusion pattern of nutrients into the disc[7,124,125,128,137,142,148]. The contrast agent is used to mimic nutrient flow; as it flows into the disc, signal intensity changes are seen on MRI images, and the changes are used to identify diffusion patterns into the disc. Degenerated discs have consistently shown altered diffusion patterns from healthy discs[128,142], with more localized diffusion changes being associated with degeneration[142].

A decreased or altered nutritional supply to the disc can lead to cell death and matrix degradation, and consequently disc degeneration[170].

2.4.2.3. *Mechanical Influences on Disc Degeneration*

Disc health is influenced by its mechanical environment, and particularly the cyclic loading magnitudes and frequencies the disc experiences. Both an extended static compressive load and a lack of loading can result in a change in proteoglycan and collagen content[70,71,162] and general cell death[101]. Hutton et al have found, for example, that there is a strong correlation between high tensile or compressive static force, as well as time the force is applied over, and decreases in proteoglycan content[70,71]. Discs likely require an intermittent compressive loading environment to maintain health and improve disc metabolism, but the results depend on frequency and magnitude of loading[133,157,177]. Constant exposures to vibrations or excessive loads, for example from work related machinery, constant heavy lifting, obesity, and excessive physical activity have been suspected causes of degeneration[48,57], but there is controversy because studies have found mixed results[38,72,140,144,150].

Mechanical disc degeneration may also be accelerated because of changes in the biochemical content of the disc. Studies which have correlated GAG depletion with mechanical properties of the disc have found a number of changes in the disc's mechanical response after biochemical degeneration. Such research has employed a chemical called Chondroitinase ABC (ChABC), which cleaves the bond between GAG and its proteoglycan core, allowing the GAG to be expelled from the disc[31,102,155,182].

ChABC has been consistently shown to degrade GAG in the intervetebral disc[51,56,89], and therefore can be used to mimic GAG depletion seen in early disc degeneration, as explained in section 2.1.5.2. This technique allows researchers to isolate GAG changes from other degenerative characteristics. The results of such research, which generally aims to simulate early disc degeneration, indicate there is a decreased spinal motion segment stiffness and increased range of motion in ChABC injected discs[31,102,155]. With GAG loss, there is less negative electrostatic repulsion and less water retention in the nucleus, and the decrease in internal pressure may lead to such changes in mechanical responses. Further studies which focus on more severe disc degeneration have found an increased compressive stiffness commonly follows the early degenerative mechanical changes[73,87,122,129,182]. This relative increase in stiffness with degeneration is likely due to the continued decrease in water content and increased load bearing of the more solid collagen fibers

In summary, the mechanical environment of the intervertebral disc can affect its rate of degeneration, and degenerative biochemical and morphologic changes can alter the mechanical response of the disc. Therefore, as unfavourable mechanical environments affect the collagen and GAG content of the disc, the degenerative changes may expose the disc to further altered stress and strain, promoting the continued degenerative cascade[31,84,113,167].

2.4.3. Diagnostic Imaging of Disc Degeneration and Low Back Pain

Disc degeneration is often considered a major cause of low back pain, and with the advances in medical imaging in recent years, attempted detection of disc degeneration in patients with LBP has become commonplace. Radiographs have been the gold standard for some time, but MRI's ability to image soft tissue has made it a widely-used diagnostic standard recently. The major problem to address in the field, however, is the large number of disc degenerative signs seen in asymptomatic individuals in all imaging modalities. Conversely, first time episodes of lower back pain have not been shown to correlate with new MRI findings[39]. An important goal in current research is to find degenerative signs that consistently correlate well with lower back pain, but, except for extreme and severe degenerative signs, this has eluded the research community.

2.4.3.1. Radiography

Radiographs were the original gold standard for diagnosis of degeneration, and with their low cost and availability, they are still the most common spinal imaging test[79,179]. Radiographs are useful for assessing spine alignment, diffuse sclerosis, osteophyte growth, and disc height, which are the most important signs of disc degeneration not seen directly on the disc tissue itself[79]. These signs are generally not present in early degeneration, though, limiting radiography's ability to detect early stages. Discography, in which a contrast dye is injected directly into a potentially-pathologic disc, can help identify disc herniations on radiographs and CT. Provocative discography also uses an injection to invoke discogenic pain similar to the clinical symptoms experienced by the patient in order to confirm the source of the pain, and single out the pathologic

disc(s)[41,77,100]. Investigators have recommended the discontinuation of certain types of radiographs because their limited ability to provide clinically adequate findings and the excess radiation exposure[146,158]

Although many radiographic grading scales for disc degeneration have been used, they suffer from a high interobserver variability or no measure of it at all, questionable validity, or a subjective analysis thus increasing observer variability [55,98,106,159]. New scales have been suggested recently by Wilke et al[179] and Benneker et al[19] which address these issues, but the inability of radiographs to detect early degeneration and the radiation output are still its biggest liability.

2.4.3.2. Computed Tomography (CT)

CT has the advantage over radiographs in that it can create multi-slice, high resolution, cross-sectional images of spinal anatomy, and can image some soft tissue. However, it is more expensive and subjects the patient to higher radiation levels than radiography.

CT can accurately detect disc herniations and subsequent nerve root impingement, and is comparable to MRI in its ability to do so[78,166]. CT is unable to image the internal morphology of the disc, though, so it is used primarily to detect changes in the outer shape of the disc, as is present in disc bulging[52]. The use of contrast agent with CT can improve the contrast of different tissues. In CT myelograms, which are used to visualize nerve roots and the spinal canal, the contrast is injected into the lower back. This is not favourable because of its invasiveness[166].

2.4.3.3. Magnetic Resonance Imaging (MRI)

MRI has several advantages over CT and radiographs for spinal imaging, the primary one being the soft tissue contrast that is produced. Different tissues, such as the annulus and nucleus pulposus, can be clearly distinguished so the internal morphology of discs can be viewed. Images can easily be taken in any plane, and MRI offers better visualization of the contents of the spinal canal, endplates, and vertebral marrow than other imaging modalities. There is no ionizing radiation exposure to the patient either[79]. The major drawback of MRI is the high machine maintenance and operating costs which often translates to fewer clinical scanners and long wait lists for patients who need a scan. MRI is the focus of this thesis, so a more detailed explanation of the principles behind it and its use in detecting degeneration is relevant here.

2.4.4. MRI and Intervertebral Disc Degeneration

2.4.4.1. MRI Basics

MRI images are created by using magnetic field and a radiofrequency pulse. Protons, like those found in body tissues, have their own small magnetic field. When they are placed in another stronger magnetic field, the protons' nuclei want to realign themselves with that stronger magnetic force. The MRI bore has a strong magnetic field called B_o, aligned through the center of the bore, parallel to the head to foot direction of a patient in the scanner. When tissue is exposed to this field, tissue protons realign themselves in the B_o field direction; approximately the same number of nuclei align themselves with the field as against it, with the aligned state being slightly favoured because it is a lower energy

state. The net magnetization from the protons therefore points in the same direction as B_o (Red arrow inFigure 2.8A).

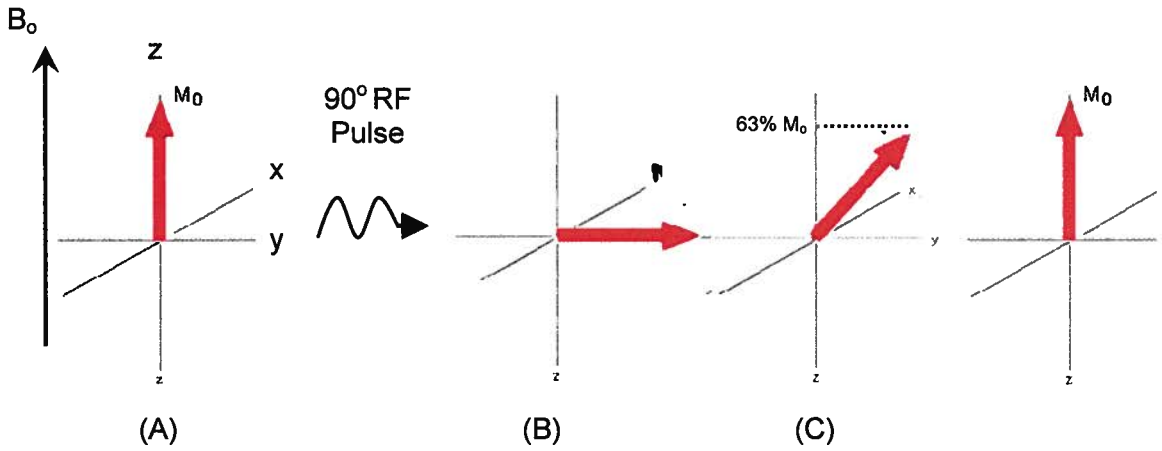

Figure 2.8: Explanation of T1 relaxation times in MRI. The arrow represents the direction of the net magnetization.

When a radiofrequency pulse of a specific frequency is applied to the system, lower energy state protons jump to a higher state. This causes the net proton magnetization vector to rotate away from B_o by an angle (the flip angle) proportional to the length of time the pulse is applied. With a long enough pulse, the proton magnetization aligns itself perpendicular to B_o, in the x-y plane, as shown by the red arrow inFigure 2.8B. The MR scanner can detect the magnetization vector when it is not aligned with Bo, with the strongest signal being measured when the vector is 90° to the main field. Once this RF pulse is removed, the protons want to realign with Bo, and begin to rotate back toward the main field (Figure 2.8C), and eventually do return to their original state (Figure 2.8D). The time to return from the 90° pulse to the main field is governed by an MRI parameter known as the T1 relaxation time. It is the relaxation of the protons in the longitudinal direction which is parallel to B_o. T1 time is only dictated by the mobility of

the protons in the material being imaged, and the field strength of the magnet (higher field strengths measure higher T1 times).

When comparing T1 times of different tissues, a sequence known as an inversion recovery sequence is often used. Before the 90^{o} pulse is applied as explained above, a 180^{o} pulse is used to flip the magnetization vector into the –z direction. By applying the 90^{o} pulse at a specific time after the inversion pulse (a time known as the inversion time, TI), the signal of specific tissues can be suppressed in order to highlight other tissues. The TI used to suppress a tissue signal is based on that tissue's T1 time.

When protons are rotated into the x-y axis, as in Figure 2.8, the net transverse magnetization vector tends to rotate about the z-axis (axis of B_o). The transverse magnetization is made up of all the proton's magnetic fields. Initially, all the protons are spinning about the z-axis in phase with each other. As they spin in the x-y plane, though, they each experience a slightly different magnetic field from each other and surrounding tissue which causes some protons to speed up their spin and some to slow down. The proton's spins therefore dephase; the longer the elapsed time, the greater the phase difference. The net transverse magnetization weakens as the spins dephase and the rate of transverse magnetization decay is governed by another time constant called T2.

T1 and T2 processes occur at the same time and are purely based on tissue type and the strength of B_o, with T2 times generally being much shorter than T1. Determining these two parameters can help distinguish different tissue types. For example, fat has a shorter T1 time and T2 time than water. A T1 weighted image will be used to better image fat

(shorter T1 means brighter on T1 weighted image), while a T2 weighted image can better image tissue water content (longer T2 means brighter on T2 weighted image). One more image sequence called a proton density weighted image minimizes T1 and T2 effects, and focuses purely on the number of protons in a given tissue. High density areas will appear brighter on the images than low density areas.

In order to calculate T1 and T2, two or more images of the same tissue need to be taken. Each image needs to contain a slightly different value of a given parameter, for example flip angle or inversion time. A curve is then fit to the signal intensity versus variable parameter data. This curve will be governed by an equation containing T1 and/or T2, and using an iterative process, we can determine the equation and therefore determine the T1 and/or T2 times. More details on this method will be given in section 4.1.3.

2.4.4.2. MRI of Disc Degeneration

MRI's versatility allows for the imaging of many different signs of degeneration including disc water content, annular tearing, endplate damage, disc herniation, nerve root impingement, and vertebral body changes. Researchers often suggest the use of MRI, or the combined use of MRI and radiographs for the most complete assessment of degeneration[19,106,166]. Before MRI was widely used as a grading modality, Thompson et al[165] developed a 5 level morphologic grading system for ex-vivo disc degeneration. This was based on gross morphological disc signs such as annulus/nucleus separation, annular tearing, and nucleus colour (Table 2.1; Figure 2.9, left side). Photographs were taken of

dissected spines and grades were assigned based on characteristics seen in Table 2.1. As an in-vitro scale, the Thompson grades are widely accepted and are still commonly used in studies[19,29,73,84,117,167]. As MRI developed, the use of the modality to assess disc degeneration in-vivo became widespread. Grading scales have been developed, which use MRI signal intensity differences and gross morphologic signs to assign a degenerative grade level to each disc[19,62,139]. The Pfirrmann[139] scale is a regularly used grading system which relies on T2 weighted images to determine degenerative grade (Table 2.2; Figure 2.9 right side). It is one of the most reliable scales created to date.

Table 2.1: Thompson's morphologic classification of disc degeneration[165]

Grade	*Nucleus*	*Annulus*	*End-plate*	*Vertebral body*
I	Bulging Gel	Discrete fibrous lamellas	Hyaline, uniformly thick	Margins rounded
II	White fibrous tissue peripherally	Mucinous material between lamellas	Thickness irregular	Margins pointed
III	Consolidated fibrous tissue	Extensive mucinous infiltration; loss of annular-nuclear demarcation	Focal defects in cartilage	Early chondrophytes of osteophytes at margins
IV	Horizontal clefts parallel to end plate	Focal disruptions	Fibrocartilage extending from subchondral bone: irregularity and focal sclerosis in subchondral bone	Ostephytes less than 2 mm
V	Clefts extend through nucleus and annulus		Diffuse scelorsis	Osteophytes greate than 2mm

Table 2.2: Pfirrmann's MRI classification of disc degeneration[139]

Grade	Structure	Distinction of Nucleus and Anulus	Signal Intensity	Height of Intervertebral Disc
I	Homogeneous, bright white	Clear	Hyperintense, isointense to cerebrospinal fluid	Normal
II	Inhomogeneous with or without horizontal bands	Clear	Hyperintense, isointense to cerebrospinal fluid	Normal
III	Inhomogeneous, gray	Unclear	Intermediate	Normal to slightly decreased
IV	Inhomogeneous, gray to black	Lost	Intermediate to hypointense	Normal to moderately decreased
V	Inhomogeneous, black	Lost	Hypointense	Collapsed disc space

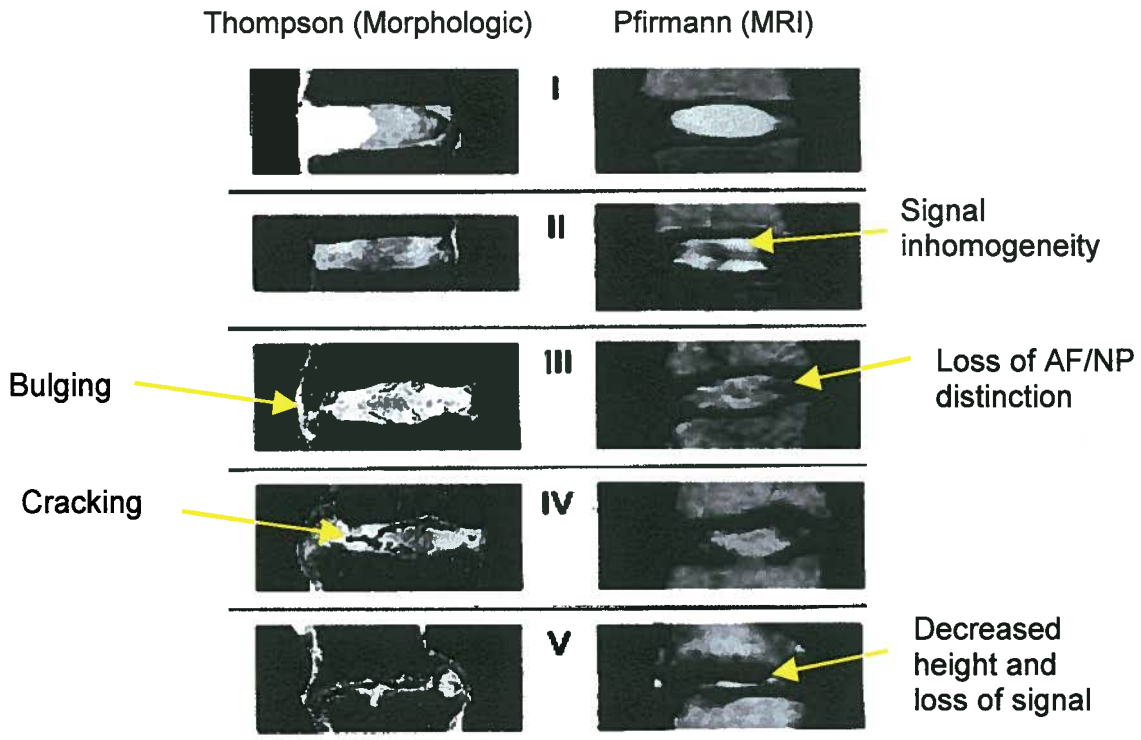

Figure 2.9: Image characteristics for Thompson (left) and Pfirrmann (right) scales for disc degeneration. The Thompson scale uses morphological images while Pfirrmann relies on MRI images. Adapted from Thompson et al,[165] and Pfirrmann et al[139]. Printed with permission from the publisher.

Concerns with the existing scales have been expressed in the literature. These degeneration assessments are based on subjective variables which are open to personal interpretation. Subjectivity can lead to poor reproducibility when the same image is graded by two or more different observers[106]. Interobserver reliability has been found to be substantial to excellent in both morphologic[165], and MRI scales[29,139]. Another concern with such scales is the inability of integer-based grading to discriminate between early stages of degeneration, in which there have been no gross morphological changes[104,106]. Further, clinical images are generally taken when a patient comes in with symptoms, and there are no prior images to compare them with to assess which morphologic signs, if any, were present before back pain began. Carragee et al showed this by comparing MR

images before and after lower back pain began and found that there was no correlation with the onset of back pain and new MRI degenerative signs[39]. It is unclear what MR degenerative scale signs lead to lower back pain. A particular concern is that the same morphologic characteristics are often present in symptomatic and asymptomatic patients, so these scales do not usually tell us the source of the pain [39].

Based on these concerns, researchers have suggested using quantitative MRI scales to provide a more continuous scale able to detect early non-morphologic degenerative changes. As Boos et al write "Since magnetic resonance imaging (MRI) is influenced by the molecular level organization of biological systems[30], MRI can go beyond providing only an anatomic appraisal. In contrast to common qualitative MRI, the calculation of T1 and T2 relaxation times...could allow an observer independent and quantitative analysis of the images"[28]. Studies have focused on proton density, and T1 and T2 times of disc tissue to assess the condition of the intervertebral disc[9,11,19,27,28,43,127,128,136,138,174]. Perry et al assessed the use of T2 relaxation times to provide a continuous measure of disc degeneration, finding that there were changes associated with T2 times in degenerate discs (although more studies are needed to asses the range of T2 values in normal and degenerated discs)[138]. Boos et al have made many contributions to the lumbar spine quantitative MRI field focusing on use of MRI to assess the water content and biochemical makeup of the disc[24,25,27,28]. Their studies have found, for example, that there are differences in T1 and T2 times between normal and high grade degenerated and herniated discs[25,28], and that T1 and T2 can be used to detect both temporal and degenerative disc water content changes[27]. Benneker et al compared morphologic

changes seen in biochemical and MRI analysis. They found that T2 correlated significantly with both water and proteoglycan content, although water and proteoglycan content did not differ significantly between different levels of T2 changes (an additional factor may be contributing to T2 changes)[19]. Such quantitative MRI parameters have thus far been unable to diagnose early degeneration. A technique known as T1ρ imaging has proved more sensitive to early changes than previous measures, though. T1ρ uses what is known as a spin-lock MRI sequence which is sensitive to low frequency reactions in tissue (i.e. physiochemical reactions between water and extracellular matrix molecules)[82]. It has been found to correlate with Pfirrmann disc degenerative grades in-vitro and in-vivo, and proteoglycan content in-vitro[11,82,126]; however, T1ρ may be influenced by other matrix constituents such as collagen, water, and the degree of crosslinking in collagen, so it does not necessarily narrow down the source of degeneration.

The quantitative MRI studies show there is promise in the creation of a continuous, quantitative scale for disc degeneration. The quantified parameters, though, are influenced by too many factors to directly quantify biochemical content or to single out individual characteristics of degeneration. One technique, called delayed gadolinium enhanced magnetic resonance imaging of cartilage (dGEMRIC), has been developed for this reason. Its purpose is to indirectly measure glycosaminoglycan content in cartilage using only MRI and specialized software.

The dGEMRIC protocol involves the injection of gadolinium based contrast agent, $Gd(DTPA)^{2-}$, into the vascular system of a patient. Both this agent and the commonly

used non-ionic gadoteridol contrast agent (i.e. used in diffusion studies outlined in 2.4.4.2) are both gadolinium based, but the biochemical structure of $Gd(DTPA)^{2-}$ imparts a negative charge to the agent. Because of this negative charge, $Gd(DTPA)^{2-}$ diffuses into cartilage regions in which the negatively charged glycosaminoglycan (GAG) molecule is depleted, a feature of cartilage degeneration. The contrast agent lowers the T1 times of the tissue based on its concentration in an area. With validated MRI sequences for quantifying T1, detailed maps of cartilage health can be created by outputting T1 maps of the area. The protocol has most extensively been used in the knee and hip [13,36,154,180], and a recent paper has done in-vivo work in the intervertebral disc of patients undergoing spine surgery for disc herniation[171].

An MRI method to directly determine biochemical or water content is an asset to the study of in-vivo lumbar spine health and mechanics. It may even help provide more insight into the link between degeneration and lower back pain.

2.4.4.3. MRI Degenerative Signs and Lower Back Pain

An overriding concern in spinal imaging is that degenerative changes seen on x-ray, CT, or MRI are rarely good indicators of lower back pain symptoms. The uncertainty about what causes the pain arises, in part, because many asymptomatic patients have degenerative signs. This is especially noticeable on MRI because of its ability to image more degenerative signs than the other modalities. Many asymptomatic patients' MRI scans have been found to have herniated discs, decreased disc height, reduced signal intensity, high intensity zone (bright signal assumed to be represent tears in the

annulus[10]), as well as other degenerative characteristics[23,25,26,39-41,63,77,80,92]. Boden et al[23] found that in asymptomatic individuals (67 subjects, average age 42 yrs), 33% had abnormal MRI scans, while Jansen et al[80] found that 64% of asymptomatic patients (98 subjects, average age 42 yrs) had abnormalities. Carragee et al have produced a number of studies investigating lower back pain with MRI, and have found no convincing evidence of LBP association with MRI disc abnormalities; rather, they find that psychosocial and work related factors are better predictors of pain[39,40]. Aside from severe degenerative signs, especially those which cause neural compromise and nerve root impingement, there is little clinical correlation of pain to MRI abnormalities[16,26,77,100]. It is difficult to know what needs to be treated in lower back pain patients when the source of the pain is unknown.

2.4.4.4. Treatment for Disc Degeneration and Low Back Pain

Before images are taken in a patient presenting with lower back pain, the physician will generally prescribe a treatment which does not necessarily target any specific cause of the pain. Most low back pain is self-limiting and acute. During this time, pain reduction and restoration/continuation of patient function is the goal of treatments until the back pain episode is over. Such conservative treatment includes the use of oral non-steroidal anti-inflammatory drugs or muscle relaxants[20,47], physiotherapy, chiropractic manipulation, and heat, ice, or electrical stimulus exposure. Studies have shown that conservative management can reduce the size of disc herniations and help resolve sciatica [32,37,107,152], but there is not always a correlation between the reduction and clinical symptoms.

If intensive conservative treatment does not alleviate lower back pain symptoms, surgical intervention may be undertaken. Spinal fusion, in which the vertebrae surrounding the pathologic disc(s) are immobilized, is the most common surgical repair for disc degeneration with back pain. Other options include a discetomy, in which the extruded portion of a herniated intervertebral disc is removed, or a lumbar decompression to relieve stenosis, which includes a laminectomy to relieve pressure on the spinal cord. Surgical intervention in low back pain patients is generally only considered after they have suffered pain and functional impairment for 6-12 months while undergoing an extensive conservative treatment plan with no cessation of the pain. An 'ideal' candidate for surgery will have a single level degenerated disc (as diagnosed on MRI and radiographs) and will have shown concordant discographic pain (pain similar to that experienced clinically) with provocative discography[97]. Although surgery can have reliable outcomes in patients with MRI degenerative signs and positive discography tests[54,59,123], these signs do not always correctly predict who will benefit from surgery[132]. In recent years, total disc replacement has become an option for disc degeneration treatment. It has shown some long term success in properly selected patients[45,50,61,184], but more studies need to be undertaken to prove its benefit over conventional surgery, and for what patient groups and spinal level it is most effective for.

Recent advances in biotechnology combined with our better understanding of the biological mechanisms present in disc degeneration have led to innovative disc repair methods utilizing gene[176], cell[145], or growth factor[134,183] therapy. The main goal of these therapies is to reduce the degradation and/or increase production of proteoglycans in the

disc through biological means. Because in-vivo cellular analysis is not currently possible, animal models are often employed in these studies; animals are sacrificed after the therapy period and biological analysis can be performed on the excised discs. An in-vivo technique to quantify cellular health may help the development of these less invasive therapies, with the ability to determine the effects of such therapies at different time steps in the same subject. That ability will also eventually allow for the in-vivo study of biological repair in humans.

2.5. Summary

1. The intervertebral disc is a primary compressive load bearing structure of the spine. The well hydrated healthy nucleus is able to resist compressive forces while the outer annulus helps prevent disc bulging. As the disc ages, the decrease in proteoglycan content and increase in collagen in the nucleus results in a loss of hydration of the disc, and a change in the load bearing characteristics of the disc.
2. Disc degeneration is often thought to be a leading cause of lower back pain, a condition which afflicts the majority of the population at some point in their lives. Genetics seems to be the most important cause of disc degeneration, but nutritional deficiency due to diffusion changes, and an abnormal mechanical environment will also contribute to the degenerative cascade.
3. Degeneration can be characterized by a number of gross morphologic signs, including annular tearing, disc bulging or herniation (possibly resulting in spinal stenosis), and endplate changes. Glycosaminoglycan loss is a consistent sign of all grades of disc degeneration, but in-vivo biochemical measurements are currently not available.
4. Magnetic resonance imaging has become integral in the assessment of disc degeneration because of its ability to image soft tissue at high resolution. However, in most cases, MRI is not able to identify the source of lower back pain. The difficulty in correlating disc degeneration with lower back pain is in the large number of degenerative signs seen in asymptomatic patients, and the lack of signs in symptomatic patients. Advances in quantitative MRI imaging have allowed the quantitative assessment of glycosaminoglycan health in the knee and hip; the development of such a sequence in the intervertebral disc may give us more insight

into causes of lower back pain, as well as a method to assess the effects of regenerative therapies in the disc.

3. Specimen Preparation and Dynamic MRI Study

The dGEMRIC protocol, which we are adapting for the intervertebral disc, relies on complete diffusion of contrast agent into the specimen to be imaged. We have the same requirement for ACMRI of the disc. In-vivo, the contrast agent is brought to the endplate via the venous system, and then diffuses into the disc through the endplates and the annulus periphery. In our in-vitro study, the discs were to be soaked in the contrast agent and diffusion through the endplate and annulus periphery still had to occur. It was therefore important to develop a preparation method which would encourage full penetration of the contrast agent into the disc in a short time; long periods of disc exposure to liquid may result in disc degeneration[22]. A preparation method which would allow for imaging of multiple discs at once would also reduce the time needed in the MR.

The objective of the first research study was to answer the following research question: In order to create an in-vitro model for testing the feasibility of ACMRI in the intervertebral disc, what is the best anatomical preparation method to ensure equilibrium contrast agent diffusion occurs into the in-vitro disc in a reasonable amount of time during undisturbed soaking? A preparation method which would allow multiple discs to be imaged at once was a secondary goal, but was not essential to the study.

Ethical approval for this and all subsequent studies was obtained through the University of British Columbia Clinical Research Ethics Board and the Vancouver Coastal Health Authority Clinical Trials Administration Board. Please refer to Appendix A for all ethical

approval forms. All MRI imaging performed was approved by the UBC High Field MRI center. MRI protocol forms can be found in Appendix A.

3.1. Materials and Methods

Three preparation methods were used in this study. The first involved imaging a single disc from a fully intact lumbar spine, while the other two methods involved imaging single discs which had been separated from the spine. In total, 5 discs from 4 different lumbar porcine spines were used, and diffusion times for each were determined. It was an iterative process in which each sequential preparation method was developed based on the results of the tests before it.

Full intact porcine spine specimens (average age 5.5 months, young adult, unknown gender) were obtained from the UBC Injury Biomechanics Laboratory. The lumbar spine was immediately isolated from the full intact spine; a diamond saw was used to cut midway through the last thoracic vertebra, and to cut through the sacrum after the most caudal lumbar disc. After lumbar spine isolation, specimens were immediately frozen until use.

Spine specimens were thawed in air overnight at 3-4° C prior to the day of use. All soft tissue was then removed from the spine in order to expose as much of the disc periphery as possible. The following three preparation methods were then used:

1. Full spine 1: Two full intact lumbar spines were used for imaging. Some soft tissue was removed to expose the peripheral annulus of the discs, but no other dissection was performed. Imaging took place on the L5-6 disc, as this is the largest disc and we would therefore expect diffusion to take the longest (i.e. compared to smaller discs). A total of 2 discs (one from each of 2 spines) were imaged in this way.
2. Single disc 1: A diamond saw was used to cut through each vertebra as close to the L5-6 disc as possible on the superior and inferior sides (Figure 3.1). The goal was to cut as close to the endplate as possible so that the contrast agent could easily reach and diffuse through the endplate (i.e. without the vascular channel flow which is present in-vivo). One disc was prepared this way.
3. Single disc 2: Preparation step 2 was followed, and a diamond bit drill burr was used to remove excess superior and inferior bone covering the disc (Figure 3.1). Approximately 2-3 mm of bone was removed in this fashion. One L5-6 disc and one L4-5 disc were prepared in this way.

All specimens were washed thoroughly with phosphate buffered saline solution after preparation to remove any foreign material.

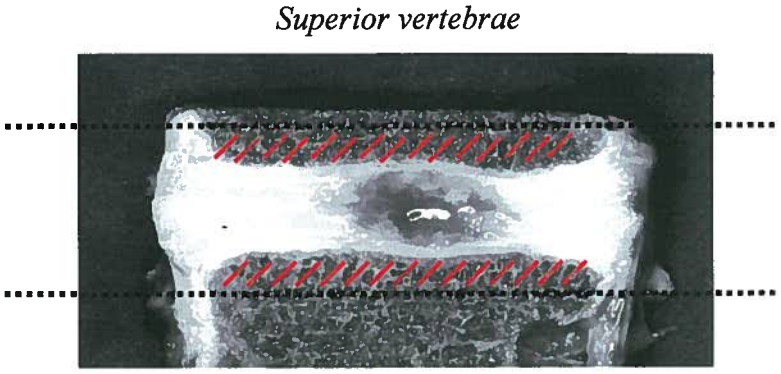

Figure 3.1: Approximate position of cutting planes (dotted lines) used to separate the intervertebral disc from the vertebral body. Specimen preparation method 2 was complete after cutting along these planes, while the remaining bone (red hatching) was removed with a diamond burr in specimen preparation method 3.

After preparation, specimens were placed in a solution of phosphate buffered saline (0.01 M phosphate buffer, 0.0027 M KCL, 0.137 M NaCl, Sigma Aldrich, Canada) and 0.2 mM $Gd(DTPA)^{2-}$ contrast agent (Magnvist, Berlex Canada), the equivalent of a double dose of contrast agent when injected intravenously in clinical settings. The specimens had to be stabilized in the bath for imaging. For preparation method 1, the intact spines were potted with Tru-stone pink dental stone (Heraeus Kulzer, NY, USA) on the superior and inferior ends and the potting allowed the spines to remain motionless in the bath. In preparation methods 2 and 3, the discs sank in the bath, but were secured to the side of the bath container with a waterproof silicon based adhesive. The spines or discs were then placed in a 3.0T Phillips Intera MRI (UBC High Field MRI Center, UBC, Vancouver). A semi-dynamic MRI sequence was then used to visualize contrast agent diffusion into the discs in each of the above preparation scenarios; two discs were imaged using preparation method 1 (one disc from each of 2 spines), 1 disc was imaged using preparation methods 2, and 2 discs were imaged using preparation method 3. The MR sequence was a T1 weighted – FFE (gradient echo) 3D sequence. The parameters for

each test are listed in Table 3.1. There are differences in the MR parameters between the four sequences used. These represent a sequence development process performed by a co-author (Bukhard Maedler, UBC Physics) to improve image quality, and this was specimen dependent. Images were obtained over a 10 hour period at multiple times after being placed in the bath: Immediately after submersion, after 5, 10, 15, 25, 35, 45, and 55 minutes, then at every 15 minute interval until 10 hours was reached.

Table 3.1: MR parameters for T1W_FFE_3D dynamic imaging.

	Prep method 1, 1st image	Prep method 1, 2nd image	Prep method 2, 1st image	Prep method 3, both images
FOV (mm x mm)	120 x 120	140x140	100x100	100x100
Resolution (mm)	0.5x0.5	0.5x0.5	0.4x0.4	0.4x0.4
TR/TE(ms)	25/4.5	10/4.7	21.5/5.8	21.5/4.8
Matrix Size	256x256	256x256	256x256	256x256
# Slices	20	20	18	22
Slice thickness (mm)	2	2	2	2
Flip Angle (deg)	50	70	70	70
Individual Scan Times (sec)	167	128	161	170

In a T1 weighted imaging sequence, contrast agent increases signal intensity of the images. Therefore as more contrast agent enters a given area of the disc, the signal becomes brighter. We measured signal intensity for each image at each MRI image time point, and equilibrium diffusion was assumed to occur when the signal intensity steady state occurred in the center of the nucleus pulposus. On T2-weighted images we obtained before the dynamic imaging sequence, the nucleus was easily distinguishable from the annulus due to its high water content, so the center of the nucleus was manually defined in custom Phillips software during the MRI. If no enhancement was seen in the central nucleus, we manually defined a new region of interest based on where the deepest point of enhancement occurred.

3.2. Results

In preparation method 1, the spine was left fully intact and bathed in contrast agent. There was little enhancement beyond the edges of the intervertebral discs over the 10 hour period. Due to this, we manually measured signal intensity versus time in the peripheral region of the annulus as well as the central nucleus. There was a 315% signal intensity enhancement of the peripheral anterior annulus (Figure 3.2), but no enhancement of the central nucleus pulposus (Figure 3.2, graph). No steady state enhancement was reached in any region of the disc. After viewing the results of preparation method 1, we decided that sagittal images would allow us to better visualize the diffusion paths into the disc; we assumed diffusion would occur mostly through the endplate and progress to the nucleus, so a sagittal image would allow us to see this progression on one slice through the anatomical center of the disc. The remainder of the dynamic images was therefore taken in the sagittal plane.

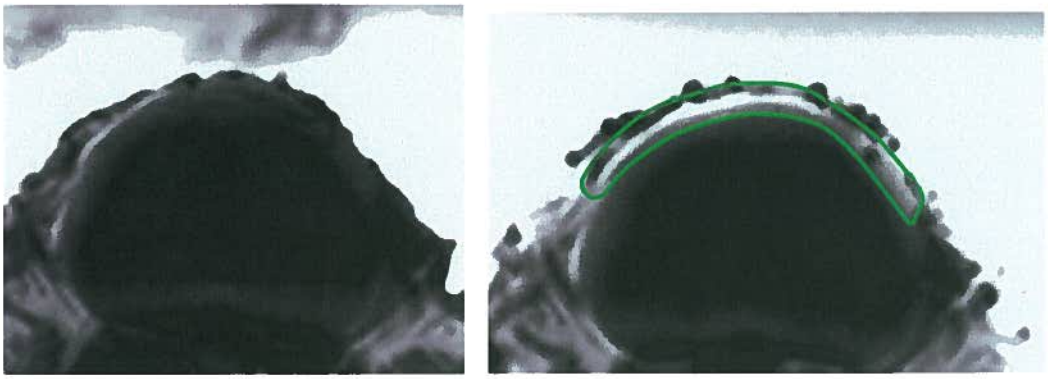

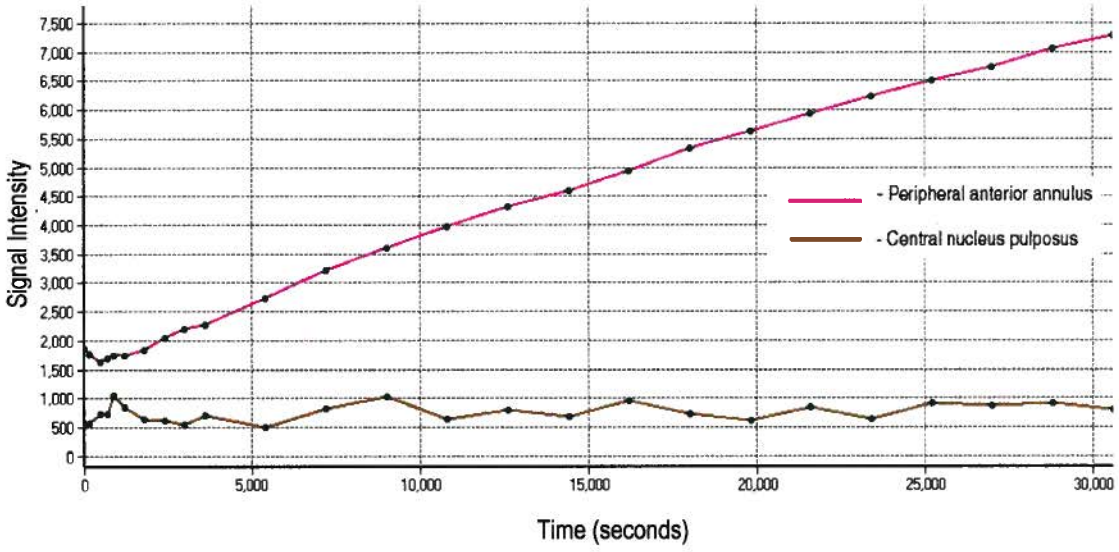

Figure 3.2: Above: Axial image slice of specimen prepared by method 1 before (left) and after 10 hours (right) of bathing in contrast agent. There was enhancement of the peripheral anterior annulus as shown in the outlined region in the post-contrast image. There has been no adjustment of the window/level settings. Below: The graph shows the signal intensity changes over time of the peripheral anterior annulus and central nucleus pulposus. After 9-10 hours, the enhancement was still increasing at the edge of the disc. There was no enhancement of the nucleus region; the variations in the graph can be attributed to random noise in the image.

Imaging specimens prepared using method 2 resulted in the same diffusion patterns as method 1 above, although contrast agent seemed to penetrate further into the disc (Figure 3.3). There was approximately a 500% enhancement of the peripheral regions of the disc, and no enhancement deeper into the disc.

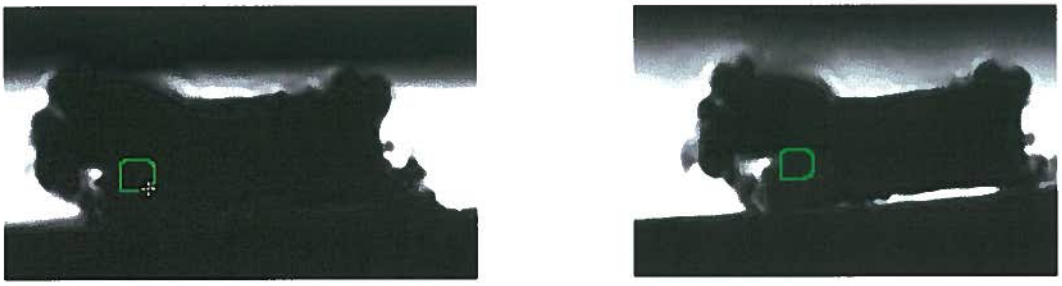

Figure 3.3: Contrast enhancement of disc prepared by method 2 before (left) and after 10 hours of soaking in a contrast agent bath. There was deeper penetration of the contrast agent into the disc compared to method 1, but still no nucleus enhancement was seen.

For method 3, 2 discs were imaged. Unfortunately, metal traces present in the first disc caused large artifacts in the first set of images, so we could not quantify enhancement for that disc. For the second disc, the metal traces were not present, and we saw enhancement in all regions over the 10 hour period. All areas of the post-contrast disc appeared markedly brighter when compared with the pre-contrast image (Figure 3.4). A 750% signal intensity increase occurred in the central nucleus pulposus. The signal intensity versus time graph is approaching a linear horizontal line (Figure 3.4) indicating enhancement was at almost steady-state equilibrium at the end of the imaging period (Figure 3.4, graph). Due to time restrictions, we could not continue the scan to full steady state.

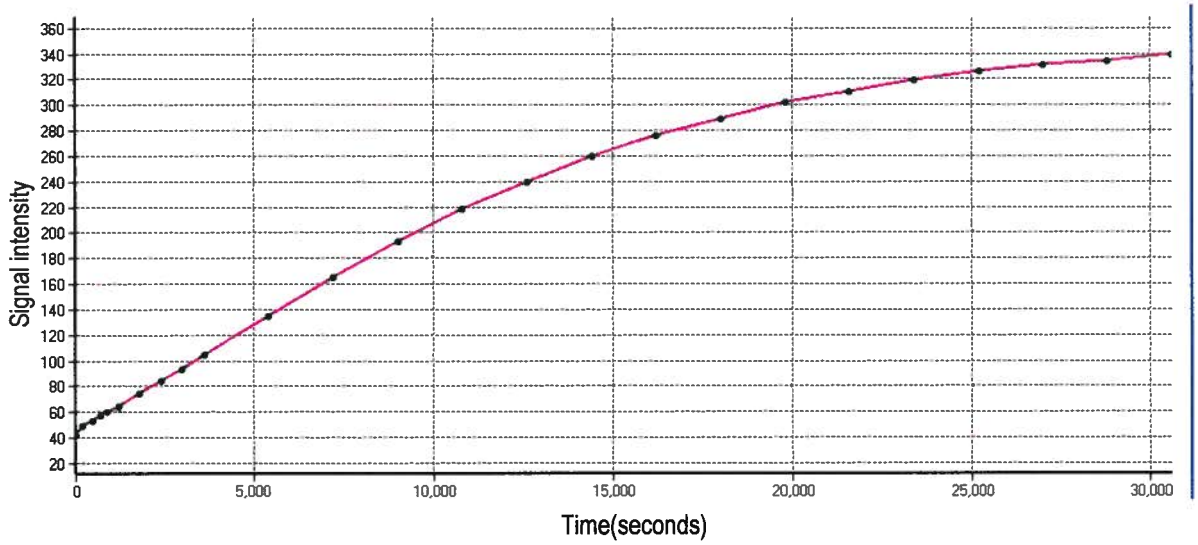

Figure 3.4: Enhancement of a specimen prepared by method 3. Above: Sagittal images of pre-contrast (left) and post-contrast disc slices after 10 hours (right). The entire disc enhanced over the imaging period. No adjustments have been made to the window/level settings. Below: Enhancement of the nucleus pulposus. Toward the end of the imaging time, the enhancement curve was almost horizontal indicating an almost steady state equilibrium enhancement.

3.3. Discussion

The objective of the dynamic imaging study was to determine a specimen preparation method that would ensure maximum contrast agent diffusion into the disc. Three preparation methods were used, and contrast agent enhancement of the specimens was determined with MR imaging over a 10 hour period. Isolation of the disc from the spine followed by manual removal of excess bone covering the annulus and endplate was required to allow diffusion of contrast agent fully into the disc, within a reasonable amount of time.

3.3.1. Analysis of Results

The improved diffusion characteristics of preparation method 3 can be explained with reference to the in-vivo nutrient and waste transport process. In-vivo, nutrients are transported to the periphery of the endplate, and to a lesser extent the peripheral annulus, by the vascular system in the surrounding vertebrae. They then diffuse through these two regions to reach the internal areas of the intervertebral disc. In our study, the cadaveric specimens no longer had blood flow to provide fluid transportation, so we relied on purely diffusion to bring the contrast agent to the disc. In preparation methods 1 and 2, the surrounding vertebrae were a barrier between the contrast agent and the endplate. Peripheral annulus diffusion was therefore the easiest path available for contrast agent movement, which explains why enhancement in the peripheral regions was all that was seen. Further, in preparation method 1, no posterior diffusion was seen, likely because the posterior elements of the spine and the spinal cord acted as diffusion barriers. Although some controversy exists[69,108], studies suggest that the endplate is the principal route of

diffusion to the disc in-vivo[34,124,125,128,142], which would explain why contrast enhancement did not penetrate farther into the disc in the first 2 preparation methods. Once the endplate was directly exposed in the third preparation method, the contrast agent could more easily reach the center of the disc without having to find a path through the bone to the endplate.

Although we saw contrast enhancement throughout the disc in preparation method 3, we did not reach full equilibrium enhancement of the central nucleus (which would be indicated by a steady state signal intensity over various time points). Unfortunately, we could not image past the 10 hour mark due to time restrictions on the MRI scanner. It is evident from Figure 3.4 that the signal intensity rate of change is relatively small at the end of the imaging period, indicating that the equilibrium state is almost reached. This will be further discussed in the limitations section.

In our application, we relied on contrast agent diffusion into the disc without the aid of any other processes. In-vivo, fluid flow into and out of the disc is encouraged by cyclic mechanical loading[117,133,157,169,177] seen during daily activities. The state of blood vessels feeding the disc also affects nutrient transport[94,95], so blood pressure may be another factor which encourages diffusion. The lack of such processes in our study may partially explain the long diffusion times we measured, as compared to the shorter times seen in-vivo (1-6 hours, section 3.3.2).

The use of preparation method 3 for the remainder of the studies described in this thesis meant that only one disc could be imaged at a time. More MRI time would be needed, as

opposed to the ideal situation of multiple spinal levels being imaged at once. However, imaging one disc at a time allowed us to use a small field of view, and therefore increase resolution. Our goal in the upcoming studies was to indirectly image the biochemical makeup of the disc, specifically the glycosaminoglycan (GAG) disc distribution. Although imaging individual GAG molecules is well beyond the capabilities of MR, a smaller imaging resolution will allow us to distinguish more local GAG distribution differences.

3.3.2. Synthesis – A Comparison to the Literature

While measuring diffusions times of contrast agent into the intervertebral disc, we also gained insight into the diffusion patterns of fluid into the disc. Previously completed in-vitro studies used radioactive or fluorescent tracers to quantify diffusion properties of the disc. An early study, for example, determined that diffusion rates of radioactively marked glucose were similar through both the annulus and the endplate, and both were therefore important in fluid uptake of the disc[108]. Since then, it has become generally accepted that the endplate is the primary route of diffusion[130,142]. Similarly, in our study, we saw diffusion through both the annulus and endplate; some diffusion through the annulus periphery was evident before the endplate was exposed (preparation methods 1 and 2), and endplate exposure greatly sped up the diffusion process (preparation method 3).

Our calculated diffusion times are comparable to the literature in this field. There are a number of in-vitro and in-vivo diffusion protocols that have been used with fluids of various charges, molecular sizes, and concentrations, as well as intervertebral discs with

various sizes and at different degenerative levels[3,7,74-76,124,125,137,142,148,169,171]. Diffusion times into the central nucleus pulposus times have ranged from 4-30 hours in in-vitro studies, and 1-6 hours in in-vivo studies.

A variety of factors can help explain the differences in diffusion times between our study, and previously completed research. The first factor is the charge of the fluid used. Because of the negative fixed charged density of the intervertebral disc, anionic fluids (as we used) diffuse slower than uncharged or positively charged fluids[3,75]; they are repelled by the negative charges present in the disc. Contrast agents consisting of larger solutes will also take longer to diffuse than lower molecular weight fluids[137,148,169]. The $Gd(DTPA)^{2-}$ used in our study has a molecular weight of approximately 1000 u, which is comparatively bigger than bodily solutes (i.e. glucose weight = 180 u, oxygen weight = 16 u). An in-vitro study which used compounds with molecular weight ranging from 4000-20000 u found diffusion occurred through the endplate between 18-30 hours[148]. The 10 hours taken by our contrast agent, a lighter fluid than the range in that study, is comparable with those findings. Higher concentrations of fluid will also diffuse faster into the disc as shown in an in-vivo rabbit study using non-ionic contrast agent[76]. When the investigators in that research used the same concentration as in our model, they found equilibrium diffusion into the central nucleus took approximately 2 hours. Higher concentrations tended to diffuse faster.

Our in-vitro diffusion times are generally longer than those seen in the in-vivo literature. The fastest time for in-vivo equilibrium penetration of non-ionic contrast occurred

between 60-120 minutes in the rabbit intervertebral disc[74-76]. As the rabbit disc is smaller than pig or human discs, contrast agent will not have as far to travel to reach the central disc tissue, so a faster diffusion time is expected. In human studies, the fastest diffusion time (to equilibrium concentrations) reported is approximately 3.5 hours[171] with anionic contrast agent, while one of the most complete and detailed diffusion studies using non-ionic contrast in the human disc found equilibrium concentration in the central nucleus at approximately 6 hours after contrast injection[142]. Both studies, as well as another in-vivo human study[128], also found measurable diffusion in the central nucleus after approximately 10-20 minutes after injection. All of these results are shorter than what we measured in our study. As previously mentioned in 3.3.1, cyclic loading in-vivo will encourage diffusion into the disc, and no loading was applied to the discs in our study; they were undisturbed while soaking in the contrast agent.

In general, our diffusion times fall into the range seen in the literature. Unfortunately, because of the range of preparation methods, solutes/contrast agents used, specimen type, and objectives of the diffusion studies previously performed, it is hard to directly compare our study with the others. Our inability to determine contrast agent diffusion times in an in-vitro setting from the literature was the reason this study had to be undertaken.

3.3.3. Strengths and Limitations

The main strength of this work is that we have developed a protocol to image diffusion of the in-vitro intervertebral disc over extended time periods. To our knowledge, in-vitro dynamic MRI of contrast agent diffusion into the intervertebral disc has not been performed over this length of time. We have eliminated diffusion variability which may be caused by surrounding blood vessel or bone properties, so this may be an important tool to study the effect of endplate health on nutrition into the disc. Further, the diffusion increase after exposing the endplate has not been shown previously in this way, and our results lend some support to the idea that endplate diffusion is the primary source of disc nutrient supply. Further studies will have to be undertaken to confirm this. For our purposes, the dynamic study provided us with essential data for the studies carried out in the following sections.

The main limitation in this study is the low number of specimens tested with each preparation method. If one method did not work over the 10 hour period, we proceeded to the next preparation method. Once the satisfactory result was found, no further testing was done. The length of time needed in the scanner was the primary reason for the small sample size. It was difficult and expensive to book the MRI and the technicians over that time, so testing was kept to a minimum. It was therefore assumed that future specimens would show the same diffusion characteristics as the final dynamic testing specimen. The one property which may cause variations in diffusion patterns in-vitro is the relative size of the discs. We saw in the study in section 4 that, although the lower level discs tend to be slightly larger, there was little variation in the size of lumbar discs in the porcine spine

in general. We did use the lower lumbar discs for the dynamic MR study just in case disc size added variability, though. We expected the longest diffusion times would occur in a larger disc, so we measured this as a worst case scenario to be applied to our future specimens. We would expect no biochemical differences between the lumbar spine discs which would alter the diffusion patterns either. Another limitation which follows from this discussion is the fact we did not see complete equilibrium, as defined by a constant signal intensity over several time points. In the study described in section 4, we relied on the diffusion times determined by our dynamic study. Because we did not fully reach the equilibrium point, we decided to leave the discs soaking an extra two hours in the consequent research (12 hours total). If we extrapolate the data see in figure Figure 3.4, equilibrium diffusion appears to occur between 11 and 12 hours. In the data we obtained in section 4, there did not appear to be signal differences throughout the nucleus after contrast uptake which suggests that equilibrium enhancement was reached after the additional 2 hours. Further, as we obtained more disc preparation practice, we improved our ability to completely expose the endplate. The increased exposure may have encouraged contrast agent uptake, thus speeding up the time necessary to reach equilibrium diffusion.

The final limitation is that in these tests, diffusion occurred only because of concentration gradients between the contrast agent bath and the disc interior. Cyclic compressive cycles would likely speed up the diffusion process. Designing an MRI compatible cyclic loading device which would function over a 10 hour period without supervision was a difficult

task, and we decided against it. Diffusion occurred in a reasonable time without such a device, so it was found to be unnecessary.

3.4. Conclusion

Dynamic MRI was used to assess the best disc preparation method to enhance contrast agent diffusion into the central region of the disc. Separating the disc from the surrounding vertebrae, and exposing the endplate with a burr was the most satisfactory method for this purpose. An almost steady-state enhancement was reached in 10 hours with this preparation technique. The endplate is the primary region of nutrient and waste diffusion in-vivo, so direct exposure of the endplate to the contrast agent bath was expected to enhance contrast agent uptake. The diffusion times determined were within the range of previous studies which have used a variety of research protocols. Performing this study was essential to answering the next research question, which will be focusing on contrast uptake in healthy and degenerated discs.

4. Anionic Contrast Magnetic Resonance Imaging (ACMRI) of the Intervertebral Disc: A Comparison of Healthy and GAG-degenerated Discs

The objective of this study was to determine whether T1 mapping after equilibration of anionic contrast agent is sensitive to glycosaminoglycan differences in the intervertebral disc. This was an in-vitro study.

4.1. Materials and Methods

Every specimen in this study was first prepared as dictated by the results of the study in section 3. In short, discs were isolated from the surrounding vertebrae, and a burr was used to remove the remaining bone. Our results from that study showed that this preparation method ensured diffusion of anionic contrast agent in the annulus and nucleus pulposus.

4.1.1. Healthy and Degenerated Specimen Preparation and Imaging

Twenty-four lumbar discs from 6 porcine spines were imaged. Spine specimens were obtained with help from the UBC Injury Biomechanics Laboratory from an abattoir (Britco Pork Ltd., Langley, BC) immediately after the pigs were sacrificed. The age of each specimen was 5-6 months, which corresponds to a young adult pig. Upon obtaining spine specimens, discs were randomly classified into three groups (Table 4.1). A method of artificial GAG degeneration, which will be explained, was used in two groups, while the third acted as a control.

Table 4.1: Specimen group assignments. Twenty four discs were separated into three equal groups. Groups differ based on if/when GAG degradation was peformed.

	Before contrast	After Contrast	Group name
Group 1 (control) n=8	Healthy	Healthy	HH
Group 2 n=8	Healthy	Degen	HD
Group 3 n=8	Degen	Degen	DD

Soft tissue was removed from the spines immediately after obtaining them, and discs were separated from the vertebrae with a diamond saw. The discs were then frozen at -20°C. Discs were thawed 12 hours prior to imaging. In general, 2 discs were used per imaging session, and each session consisted of one scan per disc on two consecutive days; the first day (pre-contrast imaging) and the second day (post-contrast imaging, after the discs were soaked in anionic contrast agent)

4.1.1.1. GAG Degeneration and Histologic Validation

The porcine discs obtained were from young, healthy animals, so a method of artificial GAG degeneration was necessary. A chemonucleolytic agent, Chondroitinase-ABC (ChABC), was used to model GAG degradation in the disc. The chemical has been found to degrade GAG in animal intervertebral discs[31,51,56,89,155], by breaking the chemical bonds between the GAG molecule and the core proteoglycan it is attached to (explained further in section 2.4.2.3). In-vivo, the unattached GAG is free to diffuse out of the disc with the wastes that constantly exit the disc. In this in-vitro model, free GAG would diffuse into the surrounding bath due to the concentration gradient between the inner disc (high GAG) and the outer disc (no GAG). The ChABC was prepared as 5 units per 100 µl of PBS and 100 µl Bovine Serum Albumin (BSA) to create a 0.025 U/ µl solution. This

concentration is in the range of previous studies, and has been shown to create GAG degradation equivalent to that seen in early physiologic degeneration[31,51,155,182]. Fifty microliters of the ChABC solution was then injected antero-laterally with a 25-gauge needle into the nucleus pulposus. The disc was then placed in a PBS solution for 12 hours, as suggested by Hiyama and Okada[68] to allow for enzymatic GAG degradation by ChABC.

In order to confirm that the ChABC was acting to degrade GAG in the discs, after all tests were performed, healthy and GAG-degenerated discs were prepared for histologic analysis. In order to preserve the state of the specimens, the discs were immediately placed in formalin following the last round of imaging. After at least 48 hours in formalin, the discs were exposed for 6 days to a series of alcohols. They acted to dehydrate the disc (without effecting the disc tissue), which was necessary to prepare the disc for the cutting process. After that, the discs were decalcified to remove excess bone which may impede the cutting process. The discs were then embedded in paraffin wax for two days, which allows a microtome to easily cut slices of the disc able to be viewed under a microscope. Axial disc sections with a thickness of 5 μm were cut through the entire disc. Following cutting, disc slices (encompassing an entire axial cross section of the disc) from the middle of the specimen were stained using an alcian blue stain, at pH 2.5. Alcian blue is used to highlight sulphated GAG in tissue which was what we were concerned with. A qualitative assessment was performed to determine if GAG degradation in the disc occurred.

4.1.2. Research and MRI Protocol

The research protocol for each group involved two imaging sessions, but there were differences in treatments of each group (Figure 4.1). All discs were initially prepared in the same way, and all were thawed for 12 hours before the first imaging session. The control group (group 1 – HH) was thawed, imaged on day 1 (pre-contrast image), soaked in a 0.2 mM solution of $Gd(DTPA)^{2-}$ contrast agent and phosphate buffered saline (PBS), and then imaged again on day 2 (post-contrast image). Group 2 (HD) was thawed, imaged on day 1, injected with ChABC and soaked in a contrast agent/PBS bath before the day 2 imaging session. Group 3 (DD) was degenerated before imaging day 1, then imaged once, soaked in contrast agent, and imaged again on day 2.

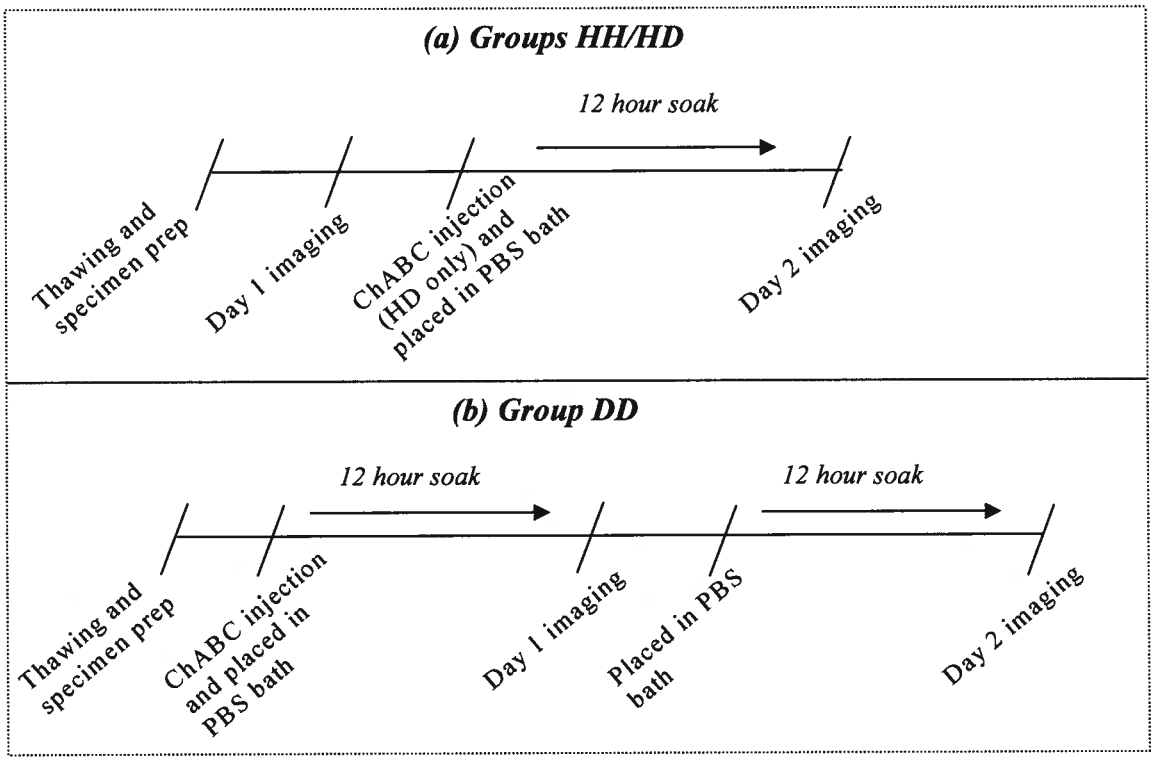

Figure 4.1: Research protocol timeline for HH/HD groups (above) and DD group (below). The only difference in the HH and HD groups is HD received a ChABC injection immediately before soaking in PBS for 12 hours.

To prepare the discs for imaging, silicon based adhesive was used to fasten the disc to the inside of a plastic container, in order to prevent movement during scanning. At 1 hour before imaging, a phosphate buffered saline solution was poured into the container with the disc; the solution was isotonic to blood to minimize degradation of the disc in the solution. The discs were then imaged, one at a time, with a 3D IR-TFE sequence on the 3.0T Phillips Intera MRI with a two element surface loop coil (Flex-S) and the following parameters: Twenty axial slices were obtained per disc with a 0.5mm isotropic resolution, 256x256 acquisition matrix (reconstructed to 512x512), TR/TE of 17/8.3 ms, FOV of 100x100 mm, inversion times of 85, 150, 300, 500, 750, 1500 and 2500 ms, and an imaging time of approximately 35 minutes/disc. When determining the position of the MR slices, the second slice was manually positioned so it was coincident with the flat inferior surface of the disc (Figure 4.2). The slices were therefore parallel to the inferior border of the disc, and this provided a method of reproducing the same slices during the post-imaging.

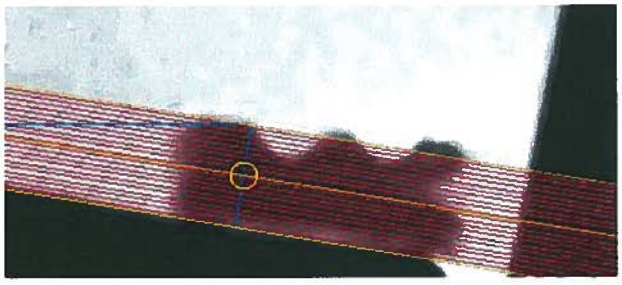

Figure 4.2: Slice selection for MRI of intervertebral disc. The first slice was aligned with the flat inferior edge (bottom of figure) of the specimen.

4.1.3. T1 Calculation

In anionic contrast agent MRI, cartilage T1 time is the quantitative measurement which acts as an indirect measure of glycosaminoglycan concentration as described in section 2.4.4.2. In our study, T1 times were calculated from inversion recovery (IR) MR images obtained using the 7 inversion times described in section 4.1.2. T1 colour maps of the disc were created to assist in the visualization of GAG concentrations.

To calculate T1, custom code developed in IGOR (WaveMetrics, Portland, OR) by collaborator Burkhard Mädler (UBC Physics) and altered by the primary author, was used. Original Phillips formats of the images (Par-Rec) were loaded into the software which then plotted signal intensity versus inversion recovery time for each pixel of each slice. The software then fit a curve through the points with the following equation, as was done in the dGEMRIC protocol described in section 2.4.4.2:

$$S(TI) = W_0 \left| 1 - W_2 e^{\left(-\frac{TI}{T1}\right)} + e^{\left(-\frac{TR}{T1}\right)} \right| \qquad \text{Equation 4.1}$$

where S(TI) is the signal intensity, TI is the inversion time, W_0 is the signal intensity as TI goes to infinity, W_2 is a fit factor which accounts for inhomogeneities in the MR magnetic field, and T1 is the spin-lattice relaxation time being calculated. An iterative fit process was used for each pixel of the image to determine the T1 values. Figure 4.3 shows a sample curve generated by this method.

After T1 was calculated for each pixel, the software was used to create a full T1 map of each slice. A colour map was used to represent a range of T1 values (Figure 4.4). This aids in the visualization of relative T1 values throughout the disc.

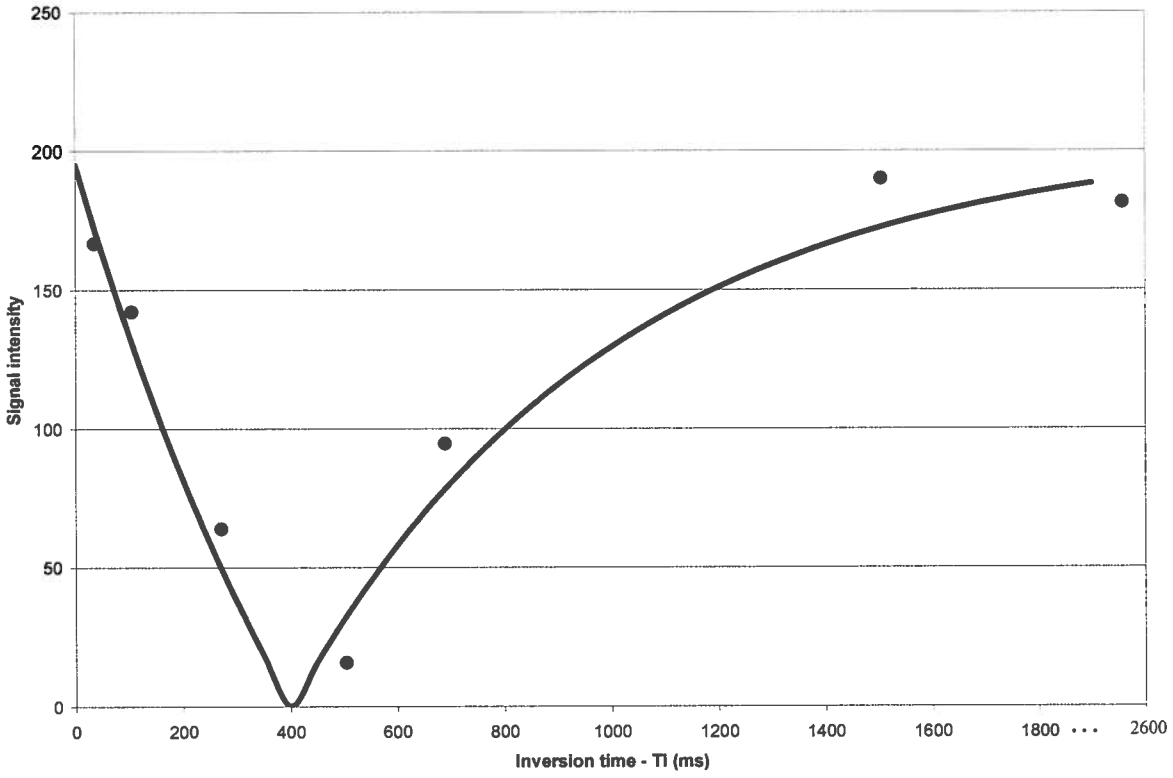

Figure 4.3: Typical inversion recovery curve plotted by equation 4.1 for a single pixel. The data points represent sample data used to plot the curve. This is used to determine the T1 of the pixel being analyzed, as T1 is a constant of the equation describing the curve. A similar curve is generated for each pixel in the image.

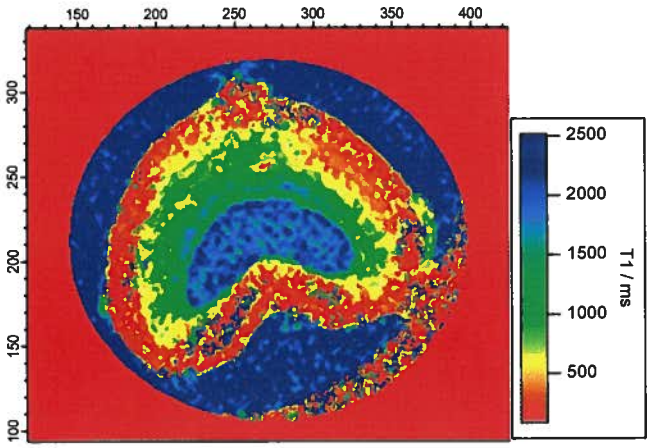

Figure 4.4: Sample T1 colour map of the intervertebral disc before contrast agent uptake. High T1 values represent areas of high water concentration, and lower T1 represents more solid, less hydrated regions.

4.1.4. Comparison of Healthy versus Degenerated Discs

Mean T1 before and after contrast agent exposure, and the change in T1 for each disc from pre- to post-contrast agent exposure was measured for a total of 120 slices (40/group) in two manually drawn regions of interest: The central nucleus pulposus and the anterior annulus fibrosus (Figure 4.5). Regions of interest were decided based on personal communications with an orthopaedic spine surgeon (Brian Kwon, UBC Orthopaedics). In early degeneration, GAG loss is most prevalent in the nucleus pulposus so it was our main area of interest. GAG concentration is relatively low in the anterior annulus, and we would not expect to see large changes with the injection of ChABC into the nucleus, so we wanted to confirm this hypothesis. The size of the ROI was kept constant between regions and specimens unless imaging artifacts prevented this. In these cases, the ROI size was kept as similar to the other specimens as possible, and the position was kept constant between pre- and post-contrast images. To place the ROI, the

centers of the regions were marked on the pre- and post-contrast images simultaneously, and a visual check was used to ensure the centers were in the same position. The ROI was then centered on this mark, and a visual check again confirmed the placement in both images was the same.

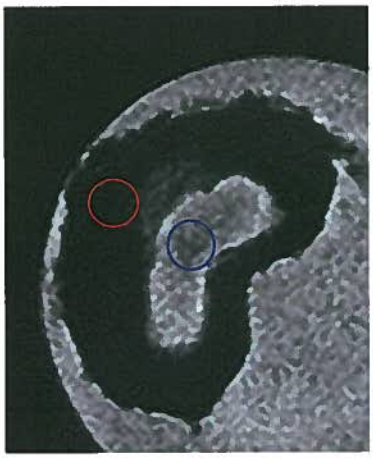

Figure 4.5: Regions of interest defined for T1 map measurements. The blue indicates the central nucleus region, the red indicates the anterior annulus region.

A 3x2 two way ANOVA was used to compare the group mean T1 magnitudes over all pixels in the ROIs in 5 central slices for each disc(Table 4.2). The 5 consecutive slices used in the analysis were manually determined by ensuring they provided enough nucleus and annulus area to create an ROI in each. The three null hypotheses being tested by the ANOVA were: There is no difference in the mean T1 times between groups, there is no difference in T1 times between imaging states (pre- and post-contrast), and there is no interaction between the groups and the imaging state (i.e. do differences between groups differ between imaging states). If significance was observed, a Tukey HSD post-hoc analysis was used to test for significance between the means of all cells in Table 4.2

Table 4.2: Set up for 3x 2 two-way ANOVA comparing T1 magnitudes.

	Before contrast	After contrast
Group 1-HH	T1	T1
Group 2-HD	T1	T1
Group 3-DD	T1	T1

A 3x1 ANOVA was used to test for differences in ΔT1 (pre contrast T1 – post contrast T1) between groups. The null hypothesis being tested was: There is no difference between the mean ΔT1 of specimens in the three groups. If significance was observed, a Tukey HSD post-hoc analysis was used to determine between group ΔT1 differences. Testing of ΔT1 correlations was performed because this value is independent of the variability in T1 times between discs, and only considers changes seen within the *same* disc. Further, it has been shown that ΔT1 may be better at distinguishing between discs of different degenerative grades when compared to post-contrast T1[128,171]. All significance levels were set at 0.05 (α=0.05).

4.2. Results

Sample pre- and post-contrast T1 maps from one specimen in each group are shown in Figure 4.6. As expected, the center of the nucleus has the highest T1, and T1 times continue to drop toward the annulus periphery. In the degenerated discs, an area of low T1 times surrounded by high T1 can be seen in the nucleus. This is a susceptibility artifact caused by an air bubble in the nucleus, which was injected with the ChABC. The artifact was apparent in most of the degenerated discs, but only encompassed a small area in most discs. This will be discussed further in section 4.3.

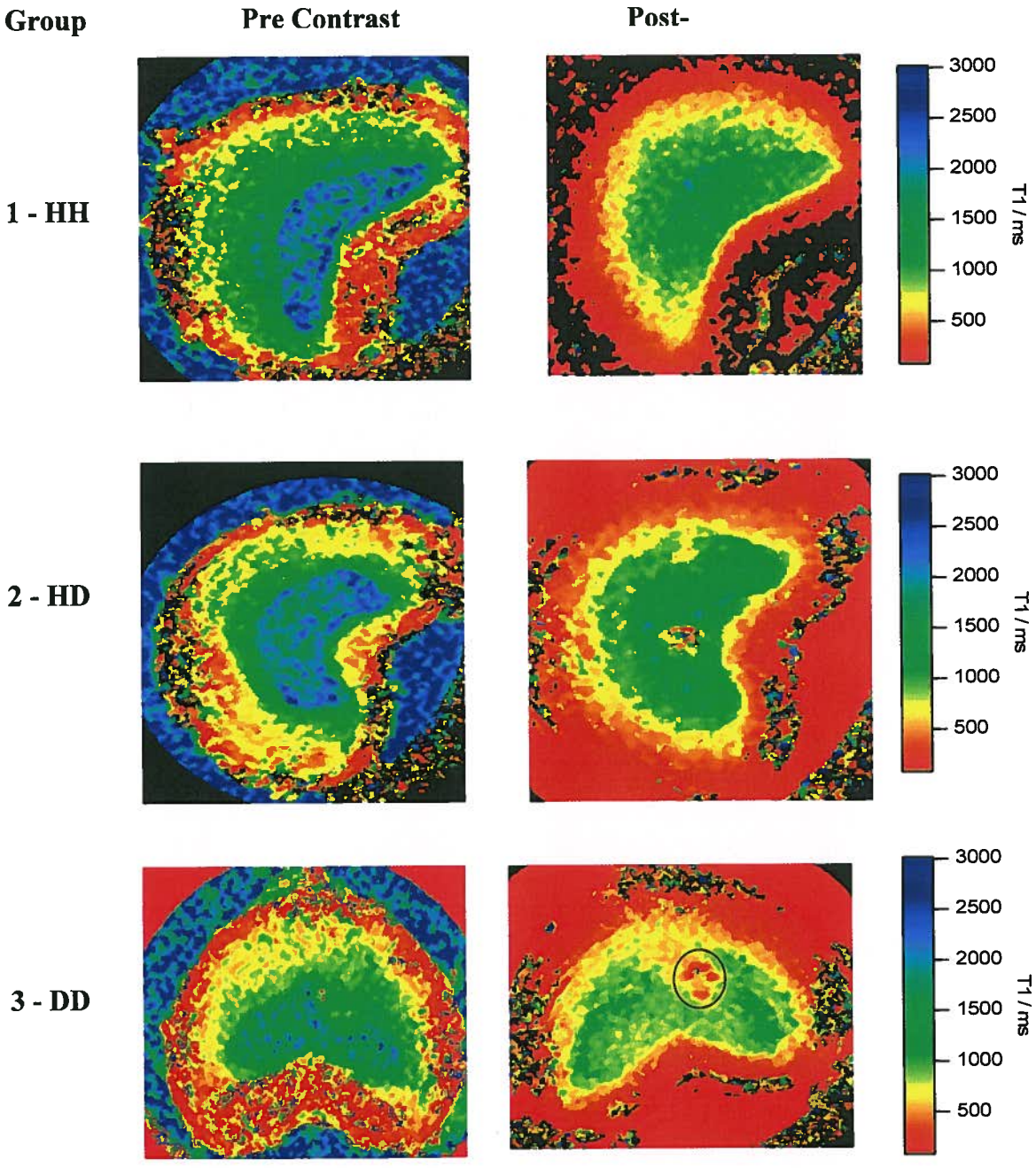

Figure 4.6: Sample T1 maps pre and post-contrast for one specimen in each group. In all cases, T1 continually decreases from the central nucleus to the peripheral annulus. The area of low T1 in the nucleus in degenerated discs is due to a susceptibility artifact created by a small air bubble injected with the ChABC (circled in group 3 post map). T1 times are similar in all pre-contrast images but are lower in the degenerated post contrast image when compared to the healthy post-contrast image.

4.2.1. Validation of GAG-degradation by ChABC

Histologic analysis of a healthy and a GAG-degenerated specimen confirmed that chondroitinase ABC did deplete GAG in the disc. There is an obvious difference in the staining results between healthy and ChABC injected (Figure 4.7).

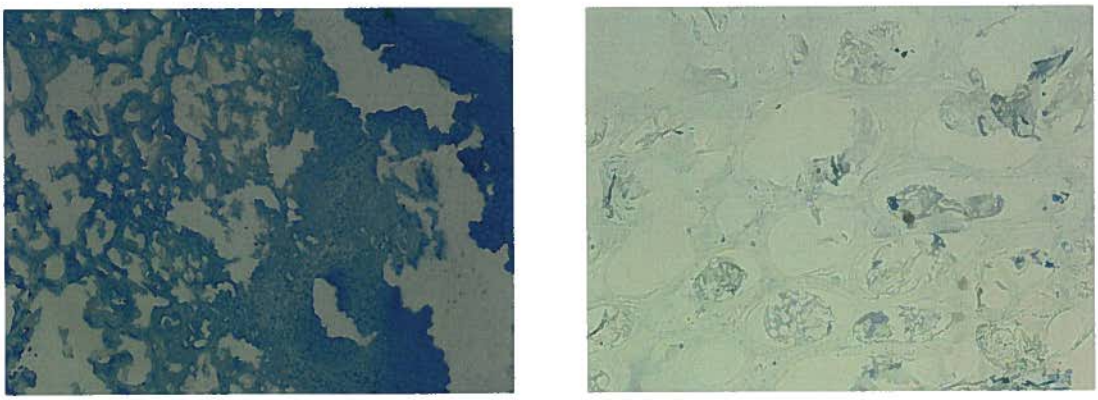

Figure 4.7: Alcian blue staining of intervertebral disc sections (5x magnification). LEFT: A nucleus pulposus of a healthy disc. There is an abundant amount of GAG, as shown by the high concentration of blue staining. RIGHT: Nucleus pulposus of a GAG degenerated disc. The lack of blue staining indicates a low GAG concentration.

4.2.2. Central Nucleus Pulposus ACMRI

Results for the T1 magnitudes in the central nucleus pulposus are seen in Table 4.3 and Figure 4.8. There was a significant interaction effect ($p=0.001$) so a Tukey HSD post-hoc test was performed. T1 times were significantly lower in each group's post-contrast images when compared to the pre-contrast times ($p<0.0001$ for all groups). Mean T1 times of the degenerated discs post-contrast were significantly lower than the healthy discs post-contrast ($p<0.01$, Figure 4.8); however, there was no significant difference between healthy and degenerated T1 times pre-contrast. Repeatability tests showed that mean T1 values from an ROI's defined at least a week apart were within 5% of each other.

The magnitudes of the $\Delta T1$ values for each group are shown in Figure 4.9. The values and standard deviations for group 1, 2, and 3, respectively, are 633 ± 176 ms, 858 ± 165ms, and 895 ± 295ms. The magnitude of both group 2 and group 3 $\Delta T1$ was significantly higher than group 1 $\Delta T1$ ($p<0.01$).

Table 4.3: Mean nucleus T1 times for 5 MR slices per specimen. The pre- and post-contrast agent T1 is shown for each specimen. The group mean T1 and standard deviation is show in bold at the bottom of each group

Group #	Specimen number	Spinal level	Pre-contrast T1 (ms)	Post-contrast T1 (ms)
1 (HH)	1	L2-3	2004	1379
1	2	L3-4	1988	1548
1	3	L5-6	1526	570
1	4	L6-7	2048	1199
1	5	L3-4	1880	1339
1	6	L4-5	1991	1461
1	7	L5-6	1798	1224
1	8	L2-3	1954	1405
			1908 (164)	**1283(260)**
2 (HD)	1	L3-4	1864	1300
2	2	L4-5	1657	729
2	3	L1-2	1941	1096
2	4	L3-4	1863	739
2	5	L2-3	1910	1056
2	6	L4-5	1927	1041
2	7	L1-2	1895	1182
2	8	L1-2	1793	841
			1855(126)	**1004(203)**
3 (DD)	1	L2-3	1848	1047
3	2	L4-5	1816	963
3	3	L5-6	1832	803
3	4	L3-4	1965	616
3	5	L5-6	1822	748
3	6	L2-3	2072	1512
3	7	L5-6	1910	1451
3	8	L3-4	1749	1113
			1880(136)	**1029(320)**

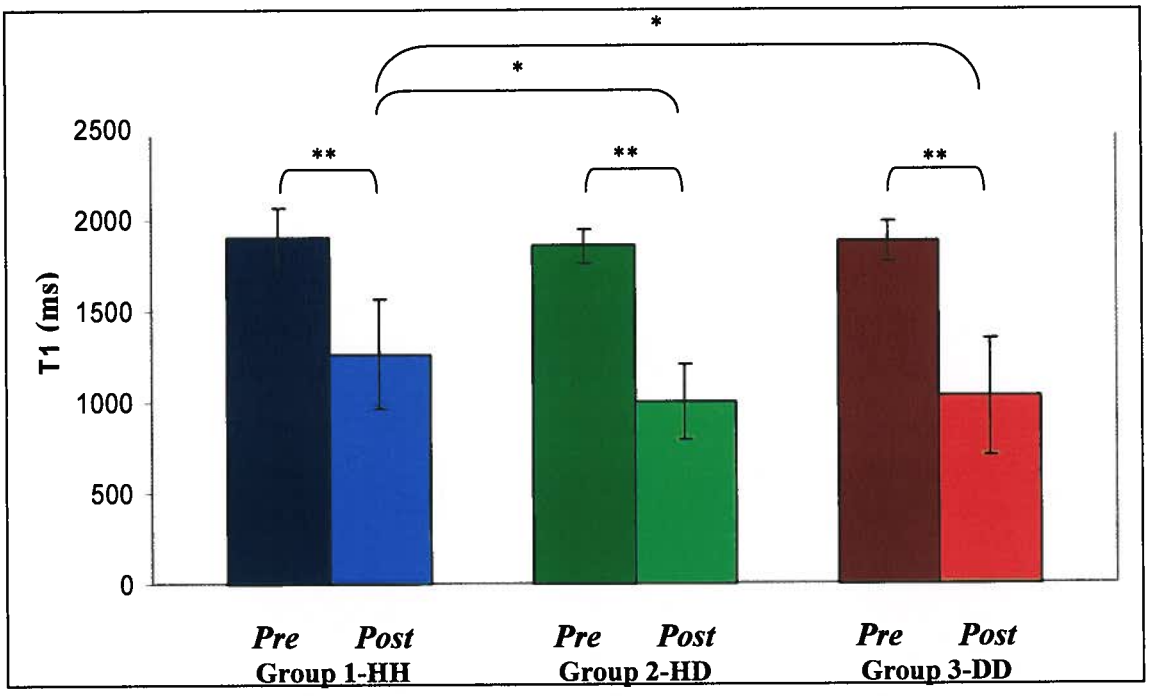

Figure 4.8: Mean anionic contrast agent MRI T1 times in the nucleus for pre- and post-contrast images. T1 was significantly lower in post-contrast images in all groups (p<0.001). Degenerated T1 times post-contrast were significantly lower than healthy T1 times post-contrast (* p<0.01). Error bars represent standard deviation.**

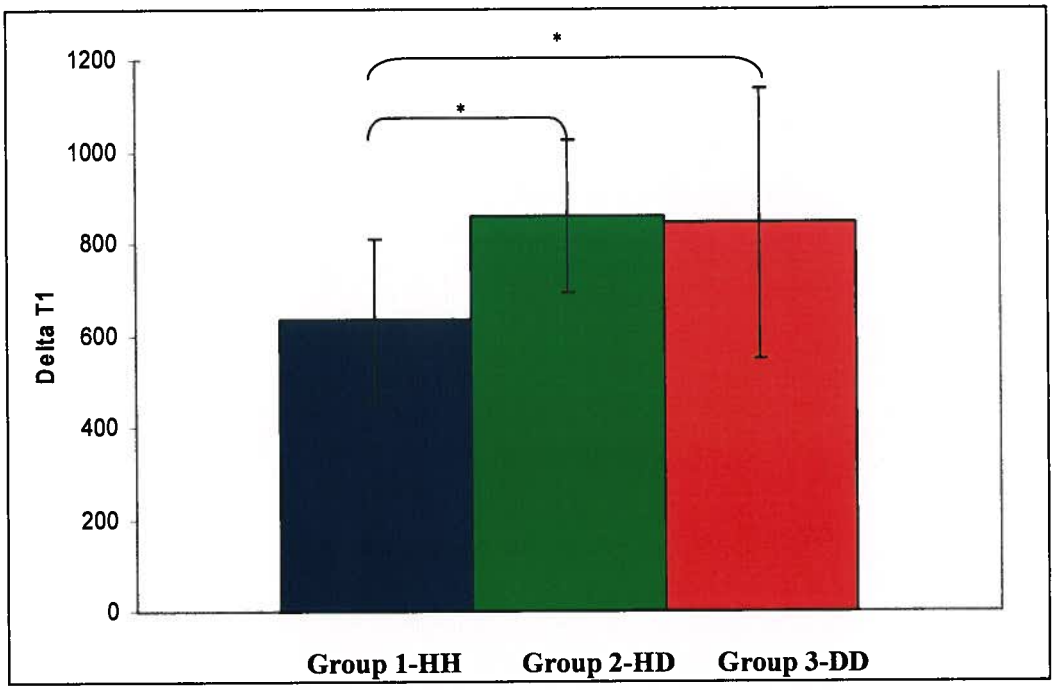

Figure 4.9: Mean magnitude of T1 time change in the nucleus pre- to post-contrast for the three specimen groups. The change in T1 was significantly greater in degenerated discs compared to healthy discs (*p<0.01). Error bars represent the standard deviations.

4.2.3. Anterior Annulus ACMRI

Results for the T1 magnitudes in the anterior annulus are seen in Table 4.4 and Figure 4.10. T1 times were significantly lower in each group's post-contrast images when compared to the pre-contrast times ($p<0.0001$ for all groups). For the number of specimens tested, we did not find any significant differences between healthy and degenerated discs' pre- and post-contrast T1 times.

The ΔT1 values for the annulus are seen in Figure 4.11. The values and standard deviations for group 1, 2, and 3, respectively, are 233 ± 104 ms, 272 ± 152ms, and 257 ± 122ms. For the number of specimens tested, there were no statistically significant differences in the mean ΔT1 between groups. A power analysis reveals that to detect significant differences in this data with a power of 0.8, 212 samples would be needed.

Table 4.4: Mean annulus T1 times for 5 MR slices per specimen. The pre- and post-contrast agent T1 is shown for each specimen. The group mean T1 and standard deviation is show in bold at the bottom of each group

Group #	Specimen number	Spinal level	Pre-contrast T1 (ms)	Post-contrast T1 (ms)
1 (HH)	1	L2-3	814	708
1	2	L3-4	608	393
1	3	L5-6	474	354
1	4	L6-7	708	432
1	5	L3-4	620	416
1	6	L4-5	640	297
1	7	L5-6	568	278
1	8	L2-3	702	492
			642 (101)	**421 (135)**
2 (HD)	1	L3-4	626	468
2	2	L4-5	554	299
2	3	L1-2	778	416
2	4	L3-4	936	566
2	5	L2-3	669	544
2	6	L4-5	449	308
2	7	L1-2	677	289
2	8	L1-2	803	407
			687 (152)	**412 (108)**
3 (DD)	1	L2-3	844	626
3	2	L4-5	738	584
3	3	L5-6	803	500
3	4	L3-4	618	250
3	5	L5-6	621	279
3	6	L2-3	660	470
3	7	L5-6	677	389
3	8	L3-4	636	460
			700 (86)	**445 (133)**

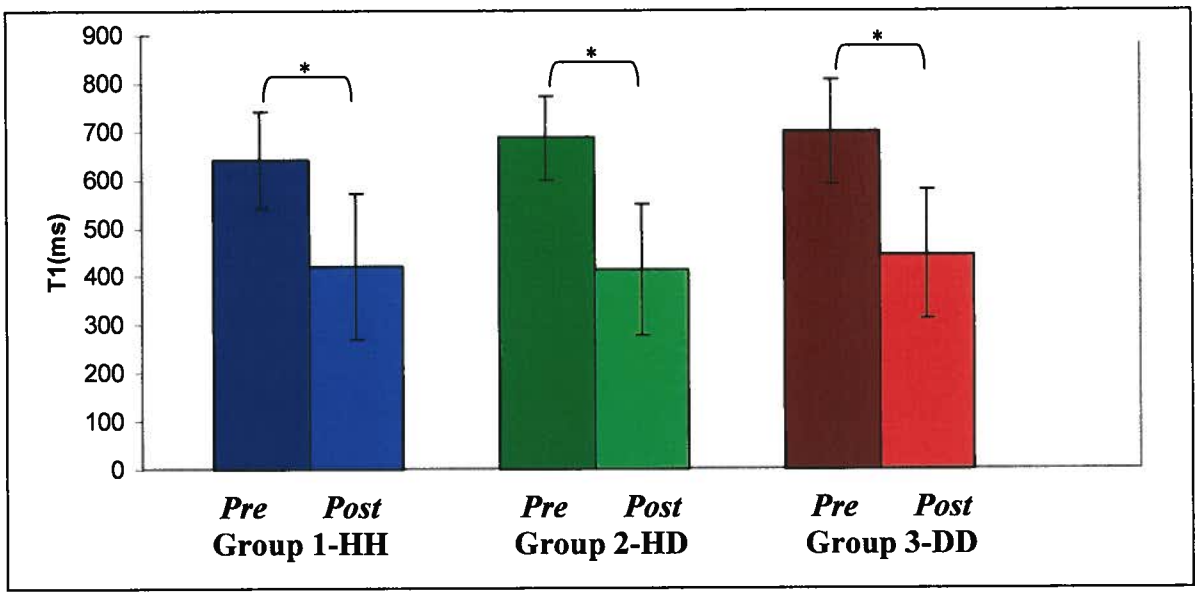

Figure 4.10: Mean ACMRI T1 times in the annulus for pre- and post-contrast images. There was as significant drop in T1 times pre- to post-contrast in all groups (*p<0.0001). Error bars represent standard deviation.

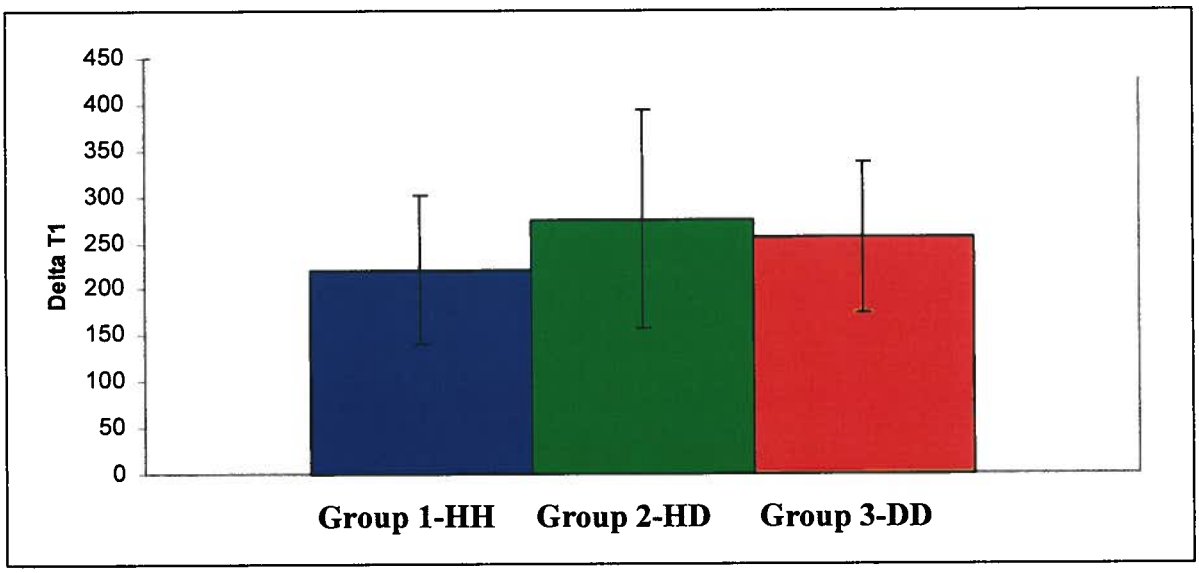

Figure 4.11: Mean annulus change in T1 times pre- to post-contrast in the three specimen groups. There were no significant differences between the groups. Error bars represent the standard deviation.

4.3. Discussion

We studied the feasibility of using anionic contrast agent MRI (ACMRI) as an indirect measure of glycosaminoglycan content in the intervertebral disc by comparing contrast uptake in healthy and GAG-degraded discs. By calculating two quantitative indices, T1 and ΔT1, we were able to determine that ACMRI is sensitive to GAG degeneration in the nucleus pulposus. This may be a tool which will provide a surrogate measure of GAG health in-vivo.

4.3.1. Analysis of Results

Our results are consistent with the hypothesis that anionic contrast agent accumulates in higher concentrations in areas of glycosaminoglycan depletion. A characteristic of clinical intervertebral disc degeneration is a loss of GAG, caused by the inability of the disc cells to synthesize GAG at the same rate it is broken down by tissue proteins (section 2.1.5.2). As GAG is broken down, it will be excised from the disc as waste products, and take with it its negative charge. The reduction in GAG will therefore leave pockets of relatively lower negative charge in the disc. Our injection of ChABC simulated this process; ChABC will break the bonds holding GAG to the core proteoglycan, thus allowing the negative charge to diffuse out of the disc. When a negatively charged contrast agent is introduced into this system, it will more easily diffuse into the degenerated areas because it encounters less electrostatic repulsion. Because T1 relaxation time of the tissue is lowered by an amount proportional to the concentration of contrast agent present, regions of GAG degeneration should have lower T1 times. This explains the drop in T1 times we measured in the nucleus. We did not, however, find

such results in the annulus ROI, and this may have to do with where the degrading enzyme was injected. The ChABC was injected into the nucleus, so it may not have diffused into the annulus and consequently did not degrade annulus GAG. If some of enzyme did reach the annulus, the GAG changes may have been too small to be detected with ACMRI. Further studies with increased ChABC concentrations and different injection sites may help test these hypotheses. In larger quantities, we would expect ChABC diffusion throughout the disc.

Our results give us confidence that the post-contrast T1 change was due to the effect of ChABC on GAG, and not due to the ChABC itself. We found no literature outlining the effects of the ChABC on MRI parameters. Consequently, we included group 3 in our study, in which ChABC was injected before the first image, in order to confirm that ChABC did not change T1 substantially. With the sample size we had, we saw no difference in the mean pre-contrast T1 times in healthy and degenerated discs. In other words, the ChABC did not significantly affect the T1 of the discs, so we are confident the T1 differences we observed post-contrast were due to the degenerative effect of the chemical. ChABC is uncharged, so we would not expect it to have a direct affect on the electrical charges in the disc.

The smooth decrease in T1 that we observed from the center of the disc to the annulus periphery is consistent with the water distribution patterns in the healthy disc. Water has a relatively high T1 time (approximately 2500ms from our study). In healthy discs, there is an abundance of water in the semi-fluid nucleus, and progressively less throughout the

more solid, collagen filled annulus. The T1 map reflects this expected water distribution. In the post-contrast disc, the same pattern is observed. Based solely on the fact there is a concentration gradient between the disc and the bath (i.e. high concentration of contrast in the bath, low concentration in the disc) we expected the contrast agent to diffuse into all regions of the discs. Fluid uptake is still higher in the nucleus than the annulus, so the high to low T1 pattern from the center of the disc to the periphery was still evident. However, the decreased ionic gradient (i.e. less negative charge) in the GAG-depleted discs allows higher concentrations of contrast to diffuse in. It is this difference in concentration and ionic gradients which result in more contrast agent uptake and the lower T1 times in the degenerated discs.

The approximately twofold increased standard deviation of mean T1 in the post-contrast nucleus compared to the pre-contrast discs may indicate a difference in contrast diffusion patterns between specimens. There may be factors which cause discs in the same study group to take in different amounts of contrast. Diffusion patterns may be altered by the size of the disc (function of the spinal level), the number of freeze-thaw cycles specimens have gone through, the storage time of specimens, previous loading environments, or the state of the endplate and peripheral tissue. For example, in group 3 (DD), there were two specimens (specimens 6 and 7 from Table 4.3) which had uncharacteristically high post-contrast T1 times in the nucleus. Both of these discs had been used in previous, non-destructive mechanical tests. It is possible that loading affected the status of the endplate or other disc properties in such a way as to restrict contrast diffusion. Further variation in T1 values may be due to spinal level. In group 1 (HH), the discs which had the highest

ΔT1 were from spinal levels L5-6 and L6-7 (specimens 3 and 4 from Table 4.3). Although not all specimens from lower levels showed this trend, it is possible that increased size of discs at lower spinal levels may affect the diffusion patterns.

4.3.2. Synthesis - A Comparison to the Literature

The pre-contrast T1 values that we measured are comparable to those found in previous studies when differences in research protocols are accounted for. Table 4.5 compares our T1 results with a summary of previous quantitative MRI work and the magnitudes of T1 times that have been found.

In general, our T1 magnitudes are higher than those seen previously in the literature, especially in the nucleus region of interest. This can be explained by the differences in research protocols. Higher magnet strengths will result in increased T1 times, and we have used a higher strength than any of the previous quantitative MR studies (3T measures T1 times approximately 1.2 times higher those for of a 1.5T[60]; no data available for lower magnet strength comparisons). We have used young intervertebral discs which have been shown to have higher T1 times than older specimens[25]. There are also differences in the regions that quantitative MR studies have measured. Some take mean T1 of whole discs[27,28] while others have focused on specific regions of interest[9,44,128,171]. With its high water content, the nucleus has a higher T1 than the annulus, so our use of the central nucleus region may explain, in part, our relatively high measurements. Our annulus T1 values are similar to other studies[9,171], though, as seen in Table 4.5, which

Table 4.5: Quantitative T1 intervertebral disc studies. The most relevant T1 times to compare to our study listed. No contrast agent was used unless stated in the notes.

Study	Species	In-vivo/ vitro	Scanner	Mean T1 ± st.dev and/or T1 range (ms)	Notes
Current Study	Porcine	In-vitro	3.0T	*Healthy nucleus* Pre-contrast: 1908±164 Post-contrast:1283±260 *Degen nucleus* Pre-contrast:1880±136 Post-contrast:1004±203	
Antoniou et al, 1998[9]	Human	In-vitro	1.5T	*Nucleus* Grade 2: 1240ms Grade 4: 960ms *Annulus* Grade 2: 515ms Grade 4: 615ms	
Boos et al, 1994[28]	Human	In-vivo	1.5T	Healthy: 1180±2007 *Range*: (752-1983) Degen: 984±180 *Range* (713-1572)	-No grading scale for healthy discs. -Degen discs were herniated discs.
Chiu et al, 2001[44]	Human	In-vivo	1.5T	Nucleus: 1179±233 Annulus: 887±126	-No difference in T1 between grades
Hickey et al, 1986[66]	Human	Both	0.26T	Normal: peak 1250ms Degen: peak 420 ms	-did not provide mean T1
Modic et al, 1984[119]	Human	Both	0.15T	*In-vivo* Normal: 820±120 Degen: 700±100 *In-vitro* Normal: 650±150 Degen: 550±100	-No grading scale for degen discs.
Niinimaki et al, 2007[128]	Human	In-vivo	1.5T	Pre-contrast: 780±120 Post-contrast:690±160	-non-ionic contrast agent -nucleus T1 only
Vaga et al, 2008[171]	Human	In-vivo	1 T	*Healthy nucleus:* Pre-contrast: 883±89 Post-contrast: 841±35 *Healthy anterior annulus* Pre-contrast: 491±94 Post-contrast: 428±112	-in-vivo, anionic contrast study -most relevant to thesis work -many regions imaged

may indicate a smaller variation of T1 is present in this region across discs of different ages and species. Water content would also increase mean T1 times from MR slices taken closer to the center of the disc compared to those taken more on the periphery. We have used 5 axial slices through the center of the disc for our T1 calculations. T1 measurements which are averaged through the whole disc would likely result in lower

mean values than our methods. Our research is the only quantitative MRI work to use porcine discs, and although the biology of the disc is similar between humans and pigs[17], it is likely that there is some T1 variability between different species.

In contrast to our findings, a number of studies which have assessed T1 relaxation times in discs without contrast agent have found lower mean T1 in degenerated discs[25,28,66,119,128]. This discrepancy is likely due to the fact that we focused on early degeneration characterized by only GAG degradation. Many of these studies are done in-vivo on advanced stage degenerated discs as measured on common grading scales (i.e. Pfirrmann scale). It is possible that a number of morphologic and biochemical changes (i.e. collagen decrease, annulus cracking, nerve ingrowth, etc.) affected these discs and therefore the T1 times. In their research, investigators often confirm this hypothesis by discussing the likely correlation between T1 and advanced grade degenerative disc characteristics. In the studies which have examined disc degeneration over the full spectrum of Thompson[9] or Pfirrmann[44,128] grading scale levels, there have been no correlations between T1 times and early degenerative grades. This confirms our pre-contrast T1 findings in which we found no differences between healthy (group 1 and 2) and GAG-degenerated (group 3) discs' pre-contrast T1 magnitudes.

Our findings are quite different from the only study to have used in-vivo quantitative MRI in the presence of non-ionic contrast agent to detect disc degeneration[128], which we expected. These investigators compared T1 times before and 90 minutes after intravenous contrast agent injection. They found there were greater decreases in T1 times in higher

grades of degeneration (grades 4 and 5 compared to grades 2 and 3 as graded on the Pfirrmann scale), but there were no significant differences in T1 times between early grades (Figure 4.12). This suggests that non-ionic contrast agent uptake is not sensitive to GAG changes which characterize early degeneration, but it is sensitive to other degenerative changes. The authors postulated that changes in pre-contrast T1 across degenerative grades were related to the dessication of the disc. They attributed the greater post-contrast enhancement of the more degenerated discs to changes in the factors which control diffusion into the disc. Specifically, they cited neovascularization of the degenerated endplate and annulus as the likely cause of increased diffusion. Another important difference between these findings and our own is that our $\Delta T1$ values are at least three times larger than those reported for the in-vivo, non-ionic contrast agent study (Figure 4.12). The most likely reason is our use of a long soaking time in an in-vitro study. The investigators in the non-ionic contrast study did not measure diffusion times; based on uptake into articular cartilage in dGEMRIC studies, they allowed only 90 minutes for contrast to equilibrate into the disc. The studies reviewed in section 3.3.2 suggest that this is not long enough to allow equilibrium uptake to occur in-vivo. In our research, the long soaking time probably allowed more contrast agent to diffuse into the disc, hence the larger $\Delta T1$. In in-vivo diffusion work in general, non-ionic contrast agent has been the compound of choice because of its shorter uptake times when compared to electrically charged contrast agent[75].

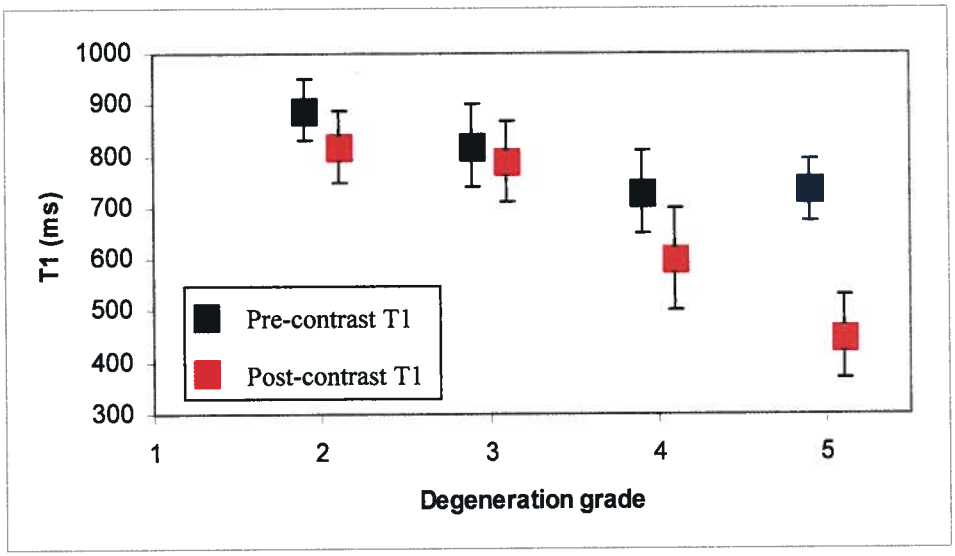

Figure 4.12: Intervertebral disc T1 results from a recent in-vivo study. Measured T1 times before and 90 minutes after non-ionic contrast agent injection vs. Pfirmmann degeneration grade are shown. T1 times decrease with increasing degenerative grade in both pre- and post-contrast measurements. Adapted from Niinimaki et al, 2006[128].

We are aware of only one study that has explored the possibility of using anionic contrast enhanced quantitative MRI[171]. This in-vivo study was performed on a 1T scanner and aimed to use ACMRI to obtain an index of molecular status of the intervertebral disc. After pre- and post-contrast in-vivo imaging, the investigators were able to obtain surgically excised regions of herniated discs to measure GAG content. They compared GAG concentration with T1 post-contrast, $\Delta T1$, and $\Delta R1$ ($1/T1_{postcontrast}$ -$1/T1_{precontrast}$). All but 3 of the herniated discs were Pfirrmann class 3 or higher with the majority being class 4. Consistent with our findings, these investigators found $\Delta T1$ was significantly greater in degenerated discs than healthy discs 3.5 hours after contrast agent injection. They also found there was a linear correlation between GAG content and $\Delta T1$ ($R=0.732$, $p<0.0001$)), indicating that $\Delta T1$ may be able to reflect the degree of disc degeneration. It is important to note that the tissue samples they excised were from herniated regions of

the discs and so the linear correlation reported may not necessarily reflect the entire health spectrum of disc tissue.

In contrast with our findings, this ACMRI study found ΔT1 values were approximately twice as high in the annulus as in the nucleus of healthy discs. They also found that degenerated post-contrast T1 values were only significantly lower than healthy disc values in the inner annulus, and not in the nucleus or peripheral annulus. These results are in direct contrast with ours, in which ΔT1 values were greater in the nucleus than the annulus (Figure 4.9 and Figure 4.11) and post-contrast T1 values were significantly greater in degenerated discs only in the nucleus and not the annulus (Figure 4.8 and Figure 4.10). A healthy nucleus is the most concentrated region of GAG in the disc, and nucleus GAG is severely degraded in high grade degeneration[9,147,151], so we would expect to see a significantly lower $T1_{post\text{-}contrast}$ in the nucleus of degenerated discs compared to healthy discs. In the study in question, it is possible that equilibrium diffusion did not occur throughout the discs, which would account for the low T1 changes in the nucleus. The authors did perform a pilot study to determine that 3.5 hours was sufficient time to reach peak enhancement in three patients, but they do not give details on that work. There is also no indication of how 'healthy' discs were chosen in their study, other than that they were from the same patients who had the herniations (average patient age was 33 ± 7yrs). It is possible that these controls were degenerated themselves, but the authors do not mention degenerative grades of these discs. Because there have been no previous ACMRI studies in the disc, it is difficult to pinpoint what differences in our work might be caused by the in-vitro versus in-vivo protocols, and what differences might be due to

other research protocol issues. The authors of the in-vivo study conclude that ΔT1 has potential as a quantitative indication of disc degeneration in-vivo. The authors stressed the need for pre- and post-contrast images, and not just reliance on T1 post-contrast measurements. This is consistent with our conclusions.

4.3.3. Strengths and Limitations

We have developed an MRI tool which appears to be sensitive to GAG degradation which is a feature of early intervertebral disc degeneration. We studied two indices as measures of degeneration: ΔT1 and the magnitude of T1 post-contrast. Our results suggest that both are effective in indirectly measuring GAG loss, although the use of ΔT1 in the disc has further support in the literature. With these indices, we can also consider creating a quantifiable, continuous scale of disc degeneration which might discriminate between the amount of early biochemical changes. More studies need to be done with discs of various degenerative grades to create such a scale. The main strength of the ACMRI measurements is they are free of observer variability, which has been reported to be a potential problem in subjective grading systems[91-93,106,139].

A strength of our approach is that we used a 3T MRI for our study, whereas the majority of quantitative MRI studies have used 1.5T or lower field strength. A higher strength magnet allows for higher resolution given similar imaging times. GAG concentrations vary locally throughout the disc, so a higher resolution allows us to see subtle changes in the disc biochemistry not visible on lower-resolution scans. This means we may be able

to better identify small regions of GAG degradation, and identify localized areas where GAG degeneration originates.

A further strength is that the use of ChABC in this in-vitro study ensured we only degenerated GAG molecules, so we are confident that the differences in T1 times are due to GAG changes. Other studies which used discs of various degenerative levels cannot conclude with certainty what exact changes quantitative MRI is measuring. A number of biochemical and morphological changes due to degeneration may affect MRI parameters, but we have singled out one specific property of disc degeneration. As we learn to single out other degenerative factors, we may gain a better understanding of degenerative etiology and the relation to lower back pain.

While this very specific model of degeneration is a strength, it also highlights a limitation of our study. GAG degradation alone may not be representative of clinical disc degeneration. Disc collagen changes, for example, may occur in early to mid-grade degeneration and we have not modeled that in our study. However, it is clear that GAG degradation does occur consistently in early degeneration, usually before other changes are present[151], and it is therefore a suitable target for a single characterization of early stages of degenerative disc disease.

Another limitation is our use of an in-vitro model because it is not clear that these methods will work in-vivo. There is constant fluid flow in and out of the disc in-vivo, which makes it difficult to ensure anionic contrast agent will reach its equilibrium

concentration throughout the disc, and remain there long enough to image. The in-vivo diffusion literature described in detail in section 3.3.2 and 4.3.2 gives strong evidence that uptake of contrast agent will occur in-vivo in a reasonable time. In dGEMRIC work, equilibrium contrast agent uptake into articular cartilage occurred over 90-120 minutes[36]. The one ACMRI in-vivo disc study described in section 4.3.2 provides the most encouraging evidence that equilibrium contrast agent uptake into the disc is feasible, although more in-vivo research will help confirm this. Previous dGEMRIC work has also suggested ways of enhancing contrast agent diffusion into articular cartilage[36], so applying such methods to ACMRI disc studies may improve in-vivo diffusion throughout the disc.

The fact we did not measure the effect of spinal level in our study is a limitation of our work. The unusually high post-contrast T1 from two discs of lower spinal level suggest there may be some effect of level on diffusion into the disc, which, if actually present, is likely a result of the increased size of the disc. However, we used a number of other specimens from lower levels which responded to the contrast treatment more consistently with discs from higher levels. In the section 3 study, we also used lower level discs to measure diffusion times, so we were confident equilibrium diffusion would occur even in the larger discs. In future studies, the use of discs from only the upper or lower lumbar levels will help alleviate this concern.

A limitation was also the effect of the injection of air bubbles which accompanied the ChABC. Most degenerated discs contained a tiny air bubble which created a sometimes

large susceptibility artifact on the MR images. Although we were able to measure T1 around these artifacts, they sometimes prohibited us from defining the ROI in the central nucleus as our research protocol prescribed. However, we were always able to measure a consistently-sized ROI close to the anatomical centre of the nucleus. Variations in T1 times throughout the nucleus were not large, so we are confident that an ROI slightly off center represents the same finding from the center. The artifact may have also covered some local GAG degeneration changes we would have liked to measure. In future studies, a smaller gauge needle, and larger volumes of injected fluid may help to reduce the appearance of air bubbles.

4.3.4. Future work

We should now aim to answer another research question which has arisen from our study: Do in-vitro ACMRI measurements correlate with the degree of GAG degeneration as simulated with injections of different concentrations of ChABC. If ACMRI is sensitive to changing levels of GAG, it will be an important step in the development of a continuous scale of degeneration. In-vivo, a similar study should be conducted correlating ACMRI indices with various degrees of degeneration graded on the Pfirrmann scale. Again, such a study will help create a new continuous scale. Sample data from such a study are shown in Figure 4.13.

The correlation between lower back pain and ACMRI indices should also be studied. ACMRI may identify new research directions to explore to find the underlying cause of the pain.

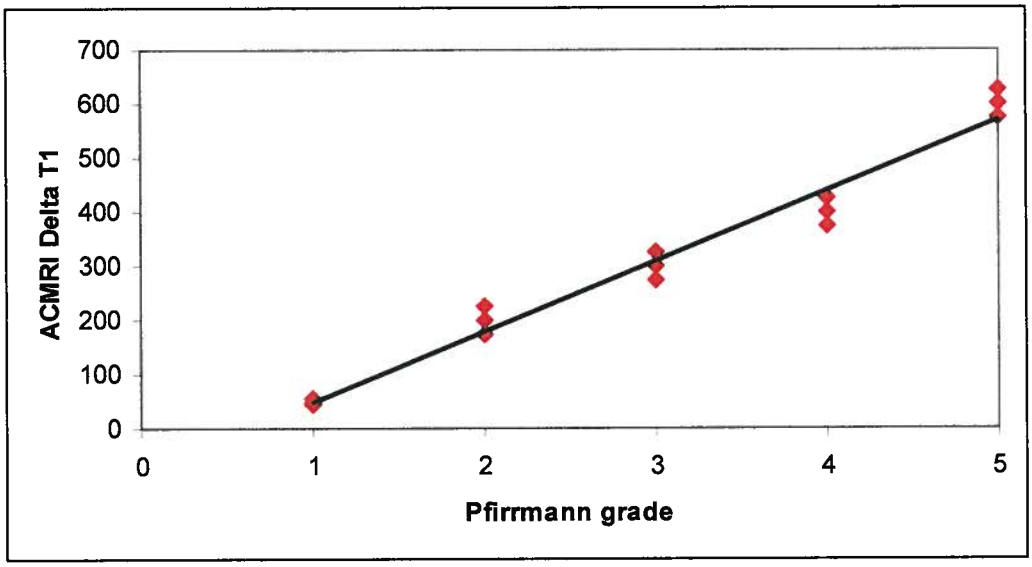

Figure 4.13: Hypothetical data from a study correlating ACMRI ΔT1 with Pfirrmann degeneration grade. The data points represent sample post-contrast T1times at each disc degenerative grade. A linear relationship as shown may be the basis for a continuous, quantifiable scale of disc degeneration.

Curing intervertebral disc degeneration may be the key to alleviating back pain in some individuals. An in-vivo, non-destructive measure of GAG health will be very useful in the development of disc regenerative therapy techniques aimed at preventing or reversing intervertebral disc degeneration[31]. Developing cell, gene, and growth hormone therapies often focus on regeneration of proteoglycans in the disc. There is no current method to measure gross GAG concentrations in-vivo so quantification relies on specimen sacrifice and destructive histological or biochemical measurement of GAG. With ACMRI, there is the potential to measure biochemical changes in the same animal over time, without the need to sacrifice.

4.4. Conclusions

An in-vitro, quantitative magnetic resonance imaging study was performed on porcine lumbar intervertebral discs. We found that T1 post-contrast and the change in T1 from

pre- to post-contrast images was significantly greater in the nucleus of GAG-degenerated disc compared to those from of healthy discs; ACMRI was able to distinguish between healthy and GAG-degenerated discs in our in-vitro work. We have begun to develop a tool which may be useful in the quantitative, continuous measurement of early intervertebral disc degeneration. Further in-vivo work may help identify the clinical value of such a tool, as well as the value of ACMRI in quantifying the effectiveness of disc regenerative therapy techniques.

5. Healthy and Degenerated Disc Mechanics and ACMRI Indices

As described in section 2, it is clear from the literature that mechanical function of the intervertebral disc is altered as GAG concentration changes, and that changes in the mechanical environment of the disc can affect GAG concentrations. Understanding the interaction between GAG and mechanics is important in understanding the progression of disc degeneration. We have shown the ability of ACMRI to act as an indirect measure of GAG concentration, so it will be valuable to this field. Combining ACMRI, a non-destructive GAG measurement, with mechanical testing of healthy and degenerated discs will allow us to gain new insight into mechanical degeneration of the intervertebral disc.

The objective of the research in this chapter was to create a mechanical testing protocol which will be used in a future study aimed at detecting differences in healthy and GAG-degenerated disc mechanical properties, and correlating them with ACMRI indices. Although the primary goal of this work was to create the protocol and test/improve the repeatability of it, we were also able to collect and analyze mechanical property data of healthy and GAG-degenerated discs. There are four sections to this chapter, which show the chronological progression of our work to design a protocol.

5.1. Protocol Development 1: Rigid Boundary Loading Repeatability

The eventual goal of our research was to compare the mechanical properties of healthy discs and those with GAG degeneration brought on by ChABC. ChABC requires 12 hours of soaking to work, so it was necessary to determine the mechanical effects of this soaking process without use of the enzyme. Therefore, the first objective of the research in this section was to assess the effect of soaking on the mechanical properties of the disc, and to identify other sources of variation; this required a two day repeatability study to be undertaken. The second objective was to identify loading-rig and load protocol improvements which could be made to improve repeatability and mechanical property measurements in future studies. We began our mechanical tests by performing compressive-tensile axial loading using a loading rig with two rigid boundary conditions.

Mechanical data for 3 healthy discs, each undergoing two mechanical tests, was obtained to assess repeatability. Three more GAG-degenerated discs were also tested to assess mechanical changes caused by degeneration. Although the results for all 6 discs will be shown here, the comparison between healthy and degenerated discs will not be discussed until section 5.3. The focus of section 5.1 is day-to-day repeatability of the rigid boundary loading protocol.

5.1.1. Materials and Methods for Protocol Development 1

Porcine lumbar spine specimens were obtained as described in chapters 3 and 4. Spines were immediately frozen until the day of testing. In this study, 3 functional units from 2 porcine lumbar spines were used for axial testing.

5.1.1.1. Specimen Preparation

Specimens were fully thawed for 12 hours before preparation took place. Functional spinal units (FSU) consisted of one lumbar disc and its superior and inferior vertebrae. Once separated from the intact spine, any remaining soft tissue on the unit was removed, except that all ligaments were left intact and facet joints were undisturbed. Specimens were then potted in dental stone to prepare them for mounting into the testing machine. A spirit level was used to ensure that the top and bottom surfaces of the potting material remained parallel, which was important in helping to ensure that pure compression was taking place during testing. We also attempted to visually align the balance point of the FSUs with the central axis of the potting material; axial loading through the balance point, which is approximately 1/3 of the distance from the posterior edge of the disc when the facet joints are intact, will minimize rotation of the FSU. We wanted loading to occur through the balance point of the disc in order to minimize any bending moments the FSU would experience during testing. Specimens were sprayed with phosphate buffered saline throughout the potting process to ensure that proper hydration was maintained.

5.1.1.2. *Axial Testing Protocol*

Each specimen was first mounted to the testing machine (Instron Dynamight™, MA, USA). Four ¼" bolts were used to secure a metal fitting to the top dental stone mold, and the fitting was then screwed into the load cell. Clamps were used to secure the inferior dental stone mold to the bottom plate of the Dynamight (Figure 5.1). With this setup (two rigid boundary conditions), the superior vertebra was free to move in an axial direction, while the inferior vertebra was secured to the base of the testing rig. The disc was able to experience both tensile and compressive loads. Some bending moments may have also been present, although we hoped to minimize these by aligning the central loading axis of the Instron with the balance point of the FSU. Bending moments were not measured.

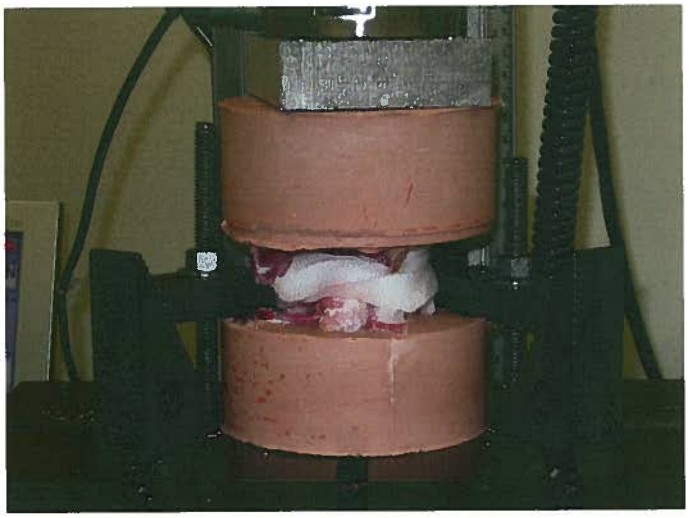

Figure 5.1: Axial mechanics testing setup. The inferior potting was rigidly fixed to the Instron, and the superior was rigidly attached to the load cell, but still free to move. The disc is wrapped in saline soaked gauss to maintain hyrdration.

Once secured we used a position controlled protocol as it does not require PID control, which is necessary when using force controlled testing. In pilot tests, we found PID control made it more difficult to create a repeatable loading protocol on the Dynamight.

In order to assess the repeatability of this protocol, each specimen underwent two tests on separate days. Between tests, discs were soaked in PBS for 12 hours. When research is eventually performed on GAG-degenerated discs, the 12 hour soaking period is necessary for the ChABC to take effect, so we wanted to see the effect of the soaking on mechanical properties from day-to-day.

The testing protocol consisted of 50 compressive-tensile cycles at a frequency of 1 Hz, and was repeated on the second day after soaking and/or degenerating. Data were collected at a frequency of 100 Hz. The 20^{th} cycle of the protocol was used to measure four axial properties of the intervertebral disc: Compressive, tensile, and neutral zone stiffness, and neutral zone displacement. Pilot testing allowed us to determine the maximum tensile and compressive positions the FSUs were able to withstand without tripping the pre-determined loading limits of the Instron. A detailed description of the testing and analysis protocol follows:

Testing protocol: Discs were first ramped up to their starting position at -0.4mm (negative indicates compressive position). After the ramp, a cyclic compressive-tensile cycle between -0.4 and 0.3mm was applied for 50 cycles at 1 Hz. The first 19 cycles are considered a preconditioning cycle to normalize the water content between discs[31,83-

[85,182], and the measurement of all axial properties was determined from the 20th cycle. Loading continued to the 50th cycle to ensure that preconditioning had occurred by the 20th cycle (as shown by the load vs. time curve).

Axial stiffness and displacement measurement: Each cycle of the loading protocol began at the full compression position so a cycle progressed from compressive unloading to tensile loading to tensile unloading to compressive loading. Tensile and compressive properties were measured from the respective loading regions of the curve. Figure 5.2 shows as typical curve for a cycle of the loading protocol.

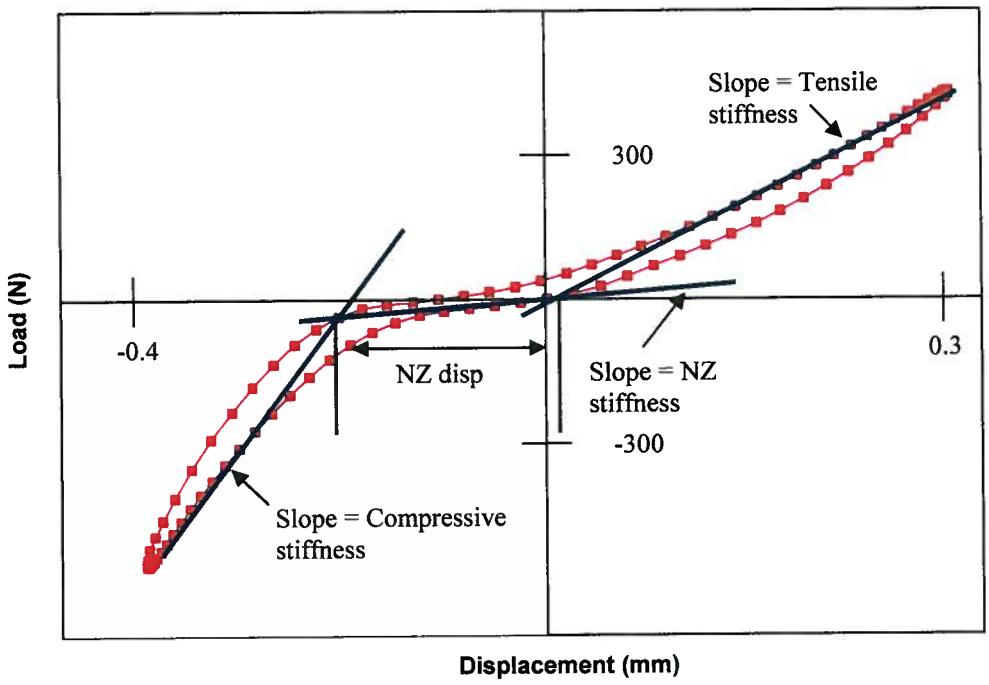

Figure 5.2: Sample force-displacement curve showing neutral zone (NZ) displacement and tensile, compressive, and NZ stiffness measurements. NZ displacement is defined as the distance between the two intersection points of the three stiffness slope lines.

The four measured axial properties were compressive stiffness, tensile stiffness, neutral zone stiffness, and neutral zone displacement, as can be seen in Figure 5.2. Because the disc has a non-linear force-displacement response, the stiffness is expected to differ throughout the loading cycle. To define stiffness for comparison between discs, it was also necessary to define a load level at which that stiffness would be calculated. The compressive and tensile stiffness were measured by calculating the slope of the linear regression about 3 points surrounding approximately -300N and 300N respectively; these values were chosen because, when disc geometry is considered, the compressive loads represent those seen every day in in-vivo standing positions, and are commonly reported in the literature[17,83,85,121]. If discs did not reach 300N in compression or tension, the closest load to those values were used on both test days.

The neutral zone (NZ) is the region between the elastic linear regions of tensile and compressive loading, where there is relatively high specimen movement at low loads. Neutral zone stiffness was measured by determining the point of minimum slope in the load-displacement curve and a linear regression was performed on the three closest data points to the minimum slope position. Neutral zone displacement was defined as previously described in the literature[31,182]: The distance between the two intersection points of the three stiffness slopes was used as the NZ displacement (Figure 5.2). Axial properties were calculated by a custom made Matlab program (Mathworks, MA, USA).
The loads FSUs experienced during testing ranged from -600N to 500N. When the geometry of the pig disc is accounted for (mean cross sectional area is 900 mm^2 [17]) these

loads create physiologic stresses experienced during human upright standing (0.5 – 1 MPa) and are within the range of stresses used in previous studies [4,31,35,73,111,141,167,175,177].

5.1.2. Results for Protocol Development 1

Every tested specimen showed a typical non-linear force displacement curve, with stiffness increasing at higher loads (Figure 5.3). Four axial properties were calculated from the force-displacement curves of each disc, for both days of testing. Specimen 1 was the only specimen to not reach 300 N in compression, so axial stiffness was measured about 200 N. The raw data for all specimens are shown in Figure 5.4 and Table 5.1. For this section, the focus will be on the healthy specimens' day-to-day repeatability.

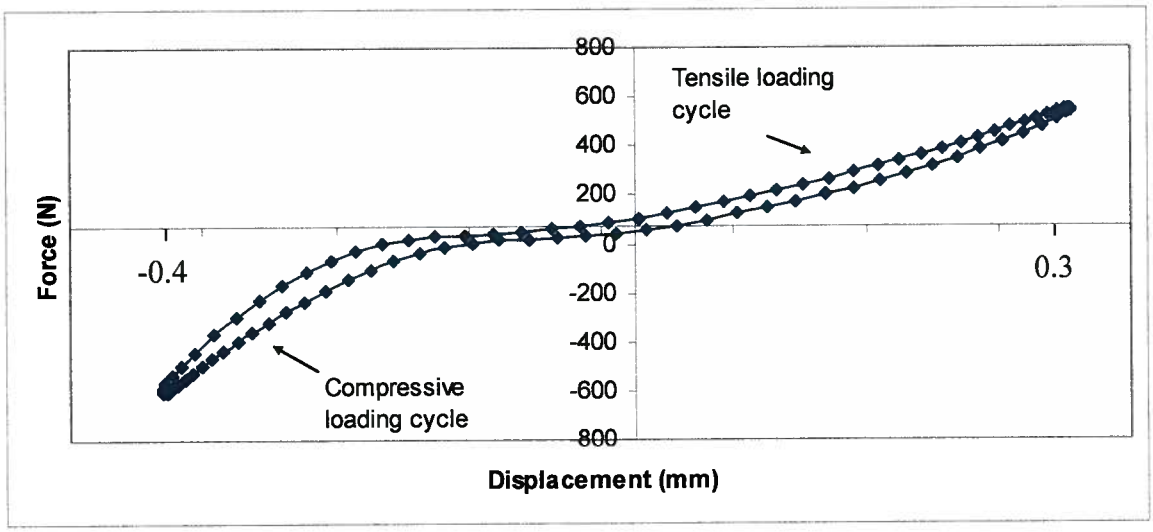

Figure 5.3: Typical Force-displacement curve observed during axial testing for a full cycle (maximum compression to maximum compression) of a healthy disc. The disc shows a non-linear response; stiffness increases as force increases. The upper most curve is the compressive unloading/tensile loading data while the lower-most curve represents the tensile unloading/compressive loading data.

Table 5.1: Raw data for axial property measurements, for all specimens on both test days. The healthy or degenerated specimen refers to the state of the disc in test 2. All discs were healthy for the first test day, so that they could act as their own controls.

Specimen		Comp Stiffness (N/mm)	Tens Stiffness (N/mm)	NZ Stiffness (N/mm)	NZ disp (mm)
Healthy 1	Test 1	1253	739	135	0.49
	Test 2	1130	816	127	0.49
Healthy 2	Test 1	1773	611	113	0.41
	Test 2	1576	580	219	0.34
Healthy 3	Test 1	2189	615	125	0.49
	Test 2	2147	670	154	0.43
Degen 1	Test 1	2107	699	105	0.52
	Test 2	1945	672	171	0.41
Degen 2	Test 1	1890	415	59	0.67
	Test 2	1288	535	44	0.67
Degen 3	Test 1	1869	760	73	0.44
	Test 2	1657	719	147	0.36

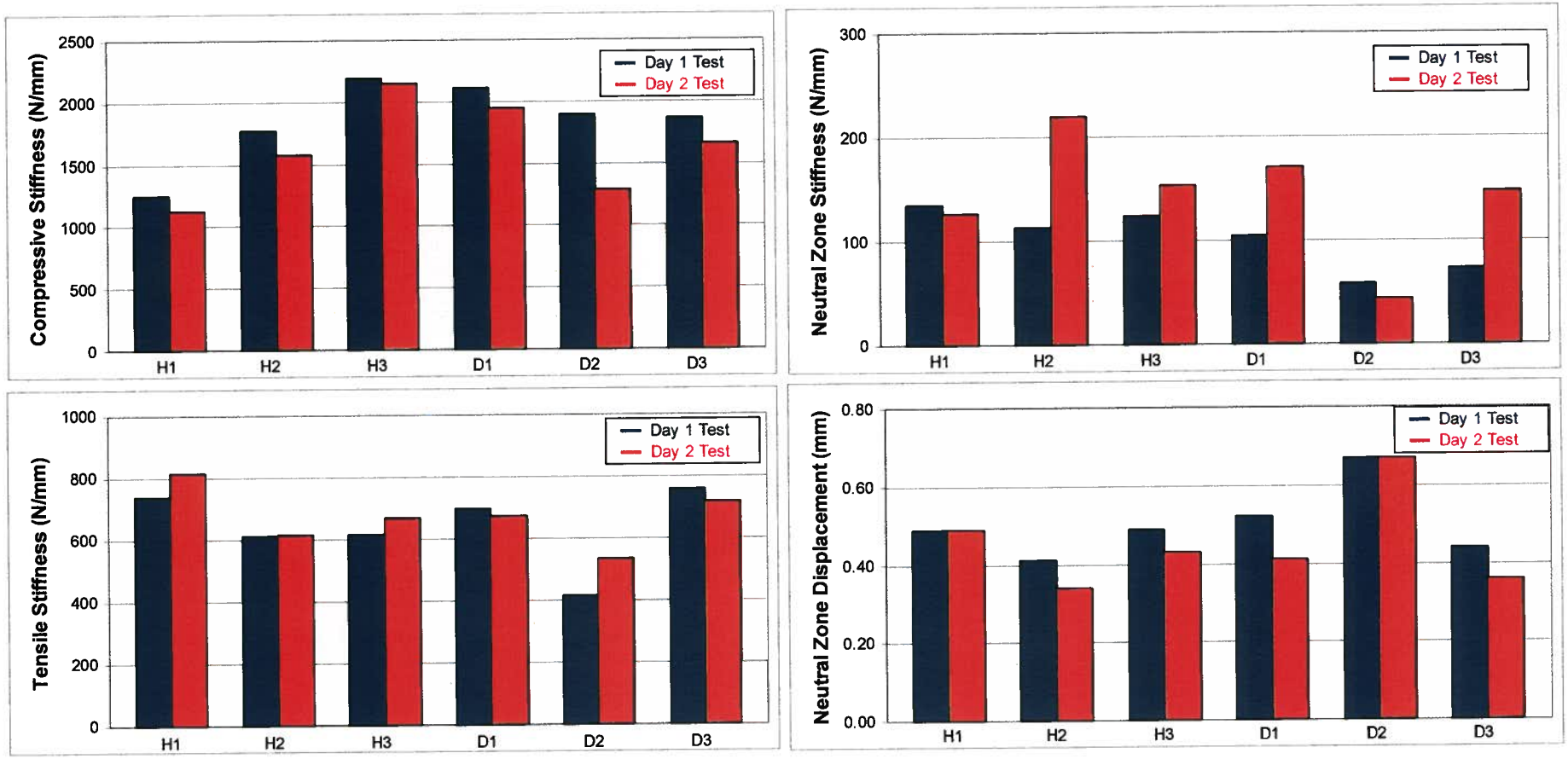

Figure 5.4: Raw data from mechanical testing analysis with each graph showing one of four axial properties for all 6 specimens tested. Each set of two bars represents measurements on a single specimen on two consecutive days. The specimens are identified as healthy or degenerated (H or D) with their respective specimen group number (i.e. H1 is healthy group, specimen 1). These designations match up with the specimen nomeclature in Table 5.1.

Comparison of day 1 and day 2 values for each specimen allowed us to assess the repeatability of this protocol. There was a consistent drop in compressive stiffness of each specimen from day 1 to day 2, averaging about 10% for all specimens. Tensile stiffness showed no direction of change (i.e. higher or lower values on day 2) from day to day, but day 2 values were within 5-10% of the values measured on day 1. The majority of specimens showed an increase in neutral zone stiffness, with day 2 values being as much as 95% higher than corresponding day 1 values (specimen H2). There was little repeatability in these measurements. Neutral zone displacement either showed no change between days (specimen H1), or dropped approximately 15% as shown in specimens H2 and H3.

Comparisons of property magnitudes between healthy and degenerated specimens will be addressed in section 5.3.

5.1.3. Discussion for Protocol Development 1

5.1.3.1. Day-to-Day Repeatability

The first objective of this study was to identify sources of variation in our loading protocol, with the focus on the effects of soaking. In general, mechanical properties of the disc changed between days, possibly due to a combination of experimental variability, and the soaking process. The latter was likely the most significant factor. The drop in compressive stiffness may indicate material softening due to soaking. The long exposure to fluid may have affected the soft tissue of the disc as well as the bones of the vertebrae

and facet joints, with the cumulative effect lowering the compressive stiffness. The stiffness drop may also indicate that some degeneration is occurring due to the soaking process. As previously described in section 2.4.2.3, early degeneration may decrease compressive stiffness of the disc. We do not know for certain whether soaking caused any degeneration in our protocol.

Neutral zone stiffness was the least repeatable measurement, which is exemplified by the large range of changes in the property from day-to-day. The changes may be explained by the mechanical response of the disc in the neutral zone, as this is the region in which the disc is hyper-mobile. This laxity may account for the large differences we observed between tests; tissue movement is less constrained here than when it is in tension or compression, so it is more difficult to get a repeatable response. It is also possible that a large amount of water uptake during the soaking process increased the neutral zone stiffness in some discs. It will be more difficult to deform the nucleus at low loads if there is more fluid (i.e. increased intradiscal pressure), so stiffness would increase. This would also explain the reduction in neutral zone displacement seen in some specimens. If the nucleus is harder to deform at low loads, there will be less movement between the tensile and compressive regions of the disc.

Experimental and specimen variability likely accounted for some of the mechanical response changes we saw between tests, such as the inconsistent pattern of change in tensile stiffness (some specimens showed an increase from day 1 to day 2, others a decrease). The orientation of the collagen in the disc may have been altered due to

mechanical testing and the soaking process, which may have resulted in small changes in mechanical response. If testing itself caused property changes, it may indicate that longer soaking or resting times are necessary to fully restore mechanical properties. Although the loading rig specimen placement could be another source of variation, it is unlikely that this affected the axial property measurements. The rig could only be connected to the specimen and the load cell in one position, so we expected an identical position of the specimen on both days.

Finally, the sensitivity of the axial properties to the manner in which they are calculated may have affected our repeatability. Using a 3 point linear regression to measure stiffness means it will be sensitive to a variation in any of the 3 points. Property changes between days could have been caused by noise affecting one those 3 points on one day, but not the other. Calculating mechanical properties with other techniques may give more reliable data, and was therefore the focus of section 5.2.

5.1.3.2. Strengths and Limitations of Loading Rig and Protocol 1

The second objective of this study was to improve upon the loading protocol and rig we have developed. Identifying the major strengths and weaknesses of the test allowed us to do that.

The major strength of this loading protocol, and the major reason we have designed it this way, is that each disc is able to act as its own healthy control. This is especially important

as intervertebral discs (and biologic tissue in general) tend to show variability in mechanical properties. The variability may mask inter-specimen differences. However, *changes* in mechanical properties from a healthy state to a degenerated state are independent of the magnitudes of such properties. Identifying such changes may allow us to better identify the effects of degeneration on disc mechanics. Our research protocol allows for such an analysis; for example, we can test a healthy disc, then artificially degenerate it (i.e. by ChABC), and test it again to measure the change in compressive stiffness which accompanies the degenerative process.

Another major strength of this loading protocol is the repeatability of specimen placement between days. As mentioned in the previous section, specimen positioning should be identical in both tests as there was only a single method of load rig and specimen connection to the load cell. This helped ensure that the axis of loading was the same during repeated tests, which is necessary for getting repeatable results. We are therefore confident that positioning did not introduce any significant variability to our measurements.

A third strength of this setup is it allows the application of both compressive and tensile loads, which in turn allows us to measure neutral zone mechanics. The disc's primary role in the body is to bear compressive forces, so compressive stiffness is a vital property to measure. Understanding neutral zone mechanics during axial loading, though, may give us additional insight into the degenerative process. We can measure such mechanics here.

The major limitation of our loading protocol is the two rigid boundary conditions in the testing setup (i.e. specimen connected rigidly to load cell and base of the Instron). This meant the disc was able to experience bending moments during the axial loading protocol. Although we were trying to measure axial properties, they may have been influenced by moment changes, and may therefore not represent true axial properties. We did aim to minimize these moments with careful alignment during specimen preparation and mounting, though.

Another limitation is the presence of posterior elements on the discs. As mentioned in section 2.2, the facet joints do bear some compressive loads. Any damage or change to these during the testing or soaking process may affect the mechanics of the disc, and may therefore account for some of the differences we saw in properties between test days. Damage may have been caused by the relatively high loading frequency (1 Hz) experienced by the specimen, and the high tensile forces the facet joints experienced. The contribution of the facets to load bearing is minor compared to that of the disc, so we assumed their effect on mechanical properties was small.

5.1.4. Next steps for Mechanical Testing Protocol Development

To further improve our mechanical testing protocol, the following recommendations arose from the research described in this section:

1. Determine the sensitivity of axial properties to how they are calculated. This helped remove one source of variation in the data.

2. Perform a preliminary study to identify axial property differences between healthy and GAG-depleted discs. This helped us determine whether or not mechanical changes due to GAG-depletion outweighted the mechanical changes caused by soaking and experimental variability (i.e. changes studies in this section); we had to ensure that degenerative changes were not masked by other sources of variability. This also provided data which was used to assess sample sizes necessary for future work.
3. Determine repeatability of the loading protocol with and without soaking. We had to measure repeatability without soaking in order to determine if the mechanical property changes were caused by the testing procedure itself. This allowed us to better understand the contribution of soaking to measurement variability.
4. Remove the posterior elements of the FSUs. This may have helped improve repeatability, as facet joint damage or changes will no longer contribute to mechanical response.

These recommendations were addressed in the subsequent sections.

5.2. Calculation Repeatability

The stiffness measurements from the force-displacement curves of the specimens may be sensitive to how the measurements are determined from the curves (i.e. linear regression versus fitting a tangent to the curve). In order to quantify this effect, measurements of axial properties of the specimens tested in section 5.1 were performed using four different methods.

5.2.1. Materials and Methods for Calculation Repeatability

Four methods were used to calculate the four axial properties we focused on. The first three methods involved calculating the slope from the linear regression about 300 N, using 3, 5, or 7 data points surrounding that load value. The fourth method involved first fitting a 5^{th} order polynomial to the data, as previously described by Boxberger et al[31]. A custom Matlab program was then created to determine the slope of the tangent to the curve at the same point the linear regression was performed about in the first 3 methods. The slopes of the compressive, neutral zone and tensile regions of the data were then recalculated with all four of these methods. To study the sensitivity of NZ displacement to the four calculation methods, NZ displacement was also calculated and compared using the regression lines of 3, 5, and 7 point regression and the tangent-fit lines.

5.2.2. Results for Calculation Repeatability

The values of each mechanical property calculated by four different methods are shown in Table 5.2. For each set of 4 calculations, the largest and smallest values of the axial

property are identified in the table, and the range of values for each set of 4 calculations is shown in Table 5.3. For example, for specimen 1, test 1, the highest compressive stiffness (1254 N/mm-indicated by blue in Table 5.2) was calculated by the 3 point linear regression method and the lowest was calculated by the tangent-fit method (1194 N/mm-indicated by red). The range of this value is the former minus the latter (1254-1195=60 N/mm). This was performed for each axial property and the results displayed in Table 5.3.

The results of calculating the compressive and tensile stiffness, and neutral zone displacement four different ways did not result in large differences. In general, the value of a given axial property was within 7% of the value of that property calculated by another of the four methods (i.e. for specimen 1 test 1, compressive stiffness calculated by 3 point regression was within 7% of compressive stiffness calculated by tangent fit method). The mean ranges for compressive stiffness, tensile stiffness, and neutral zone displacement (81 N/mm, 53 N/mm, and 0.01 mm, respectively) are consistently less than 10% of the average value of the property. The neutral zone stiffness, however, has the largest mean range of any of the measurements (104 N/mm, Table 5.3). The 3 point linear regression generally gives the lowest measure of NZ displacement, while the tangent-fit method gives the highest.

Table 5.2: Values of axial properties calculated by four different methods. Comp, tens, and NZ indicate compressive, tensile and neutral zone stiffness, respectively, all in N/mm. NZ disp is in mm. The 3, 5, and 7 points refer to the linear regression methods using that number of data points. The % change is between test 1 and test 2 for a given calculation method. Blue values indicate the largest magnitude of the property for each specimen, and red indicates the lowest values. Ranges calculated from these values can be seen in Table 5.3

Specimen	H1			H2			H3		
	test 1	test 2	%change	test 1	test 2	%change	test 1	test 2	%change
Comp (3points)	1254	1130	-10%	1773	1575	-11%	2188	2146	-2%
Comp (5 points)	1226	1117	-9%	1757	1563	-11%	2181	2115	-3%
Comp (7points)	1203	1083	-10%	1725	1538	-11%	2151	2096	-3%
Tangent-fit	1194	1073	-10%	1785	1568	-12%	2079	2049	-1%
Tens (3)	738	816	10%	611	580	-5%	615	670	9%
Tens (5)	729	791	8%	614	580	-6%	612	671	10%
Tens (7)	721	783	9%	611	578	-5%	636	681	7%
Tangent-fit	664	737	11%	545	613	12%	586	735	25%
NZ (3)	135	127	-6%	113	219	93%	125	154	23%
NZ (5)	155	147	-6%	138	253	84%	130	169	30%
NZ (7)	190	171	-10%	174	245	41%	138	187	36%
Tangent-fit	205	148	-28%	254	289	14%	161	274	70%
Nz disp (3)	0.49	0.49	0%	0.40	0.34	-15%	0.48	0.42	-13%
Nz disp (5)	0.49	0.49	0%	0.41	0.35	-15%	0.48	0.43	-10%
Nz disp (7)	0.49	0.49	0%	0.41	0.33	-20%	0.49	0.43	-13%
Nz disp tangent	0.49	0.48	-2%	0.40	0.34	-15%	0.48	0.44	-8%

Specimen	D1			D2			D3		
	test 1	test 2	%change	test 1	test 2	%change	test 1	test 2	%change
Comp (3points)	2101	1945	-7%	1625	1170	-28%	1868	1656	-11%
Comp (5 points)	2103	1942	-8%	1617	1161	-28%	1837	1633	-11%
Comp (7points)	2021	1908	-6%	1584	1144	-28%	1806	1606	-11%
Tangent-fit	2072	1972	-5%	1652	1217	-26%	1914	1638	-14%
Tens (3)	699	672	-4%	415	535	29%	760	719	-5%
Tens (5)	685	668	-2%	386	531	38%	756	714	-6%
Tenst(7)	687	663	-4%	389	527	35%	753	709	-6%
Tangent-fit	643	658	2%	358	512	43%	763	749	-2%
NZ (3)	105	171	64%	59	44	-26%	73	147	101%
NZ (5)	135	191	42%	63	63	0%	102	169	65%
NZ (7)	181	218	20%	67	85	27%	100	203	102%
Tangent-fit	259	257	-1%	86	120	40%	247	120	-51%
Nz disp (3)	0.49	0.41	-16%	0.69	0.64	-7%	0.45	0.35	-22%
Nz disp (5)	0.51	0.41	-20%	0.68	0.65	-4%	0.44	0.35	-20%
Nz disp (7)	0.52	0.41	-21%	0.67	0.67	-1%	0.44	0.36	-19%
Nz disp tangent	0.51	0.40	-22%	0.69	0.68	-1%	0.44	0.35	-20%

Table 5.3: The range of each axial property measured by four methods for test 1.

	Specimens						
	H1	H2	H3	D1	D2	D3	Mean
Comp stiffness range (N/mm)	60	60	109	81	68	108	**81**
Tens stiffness range (N/mm)	74	69	50	56	57	10	**53**
NZ stiffness range (N/mm)	70	141	36	154	27	174	**100**
NZ disp range (mm)	0.00	0.01	0.01	0.03	0.02	0.01	**0.01**

The largest variation between calculation methods was seen in the neutral zone stiffness measurements, especially when comparing the tangent-fit to the other three methods. It was evident looking at the data that the polynomial did not fit as well with the data points in the neutral zone region as it did in the tensile and compressive regions. A 6^{th} order polynomial was therefore also fit to the data to try to improve the measurements (Figure 5.5). In most cases, a better fit was achieved and the neutral zone stiffness was closer to the values calculated by the regression methods (Table 5.4).

Table 5.4: Neutral zone stiffness (N/mm) calculated by the tangent fit method. Two curves were fit to the data: A 5th and 6th order polynomial. The NZ stiffness calculated from these were compared with the stiffness calculated by regression analysis. The 6th order polynomial fit resulted in values closer to those of the regression.

	Specimen					
	H1	H2	H3	D1	D2	D3
Tangent-fit 5th order poly	260	247	86	254	161	205
Tangent-fit 6th order poly	219	111	84	180	114	197
3 point Regression	135	113	125	105	59	73

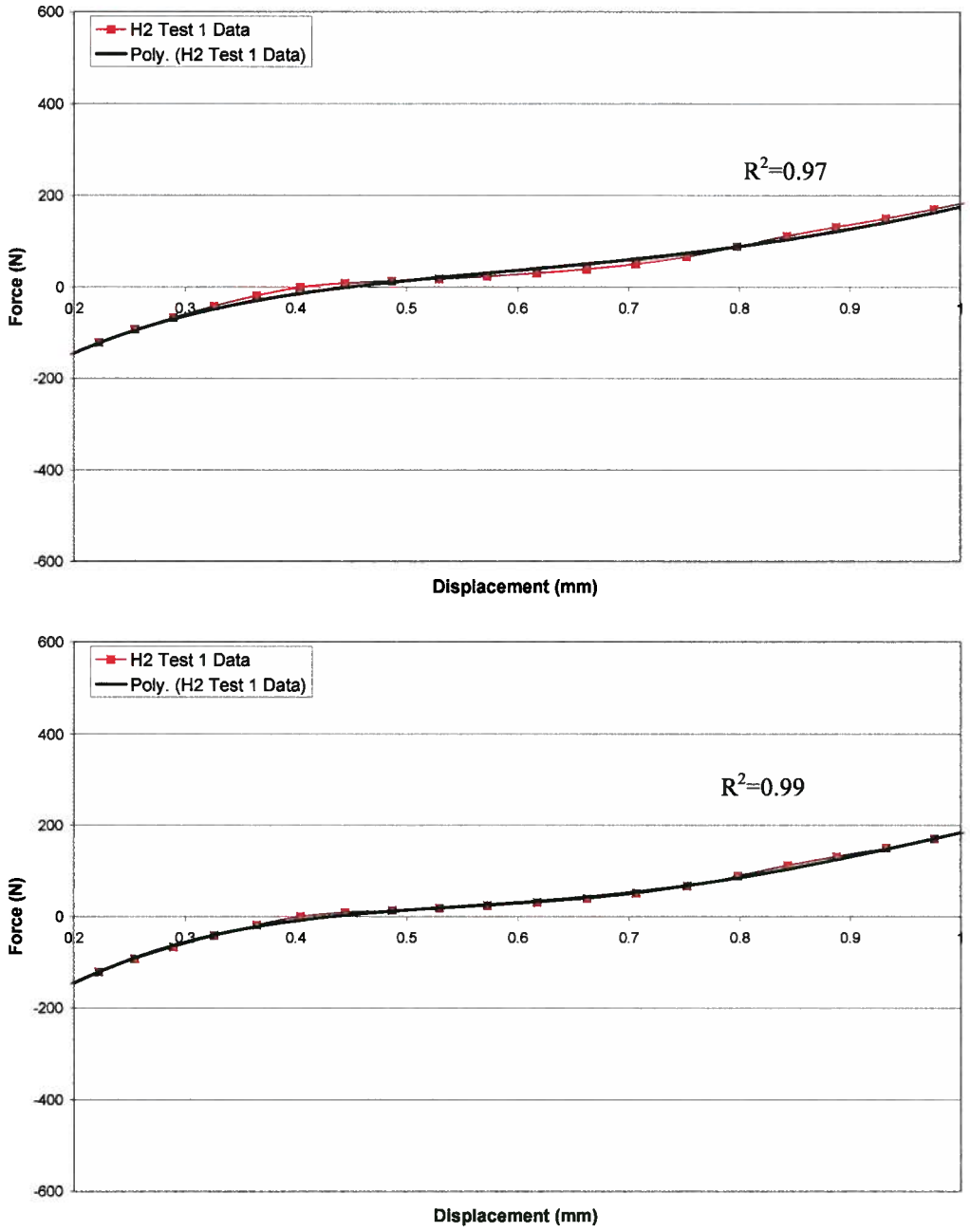

Figure 5.5: Magnified view of the neutral zone region of specimen H2 with a polynomial curve fit to the data. Above: 5th order polynomial fit. Below: 6th order polynomial which shows a slightly better fit.

5.2.3. Discussion for Calculation Repeatability

For all properties except neutral zone stiffness, the method of calculating the axial properties did not appear to change the results of our research. The compressive and tensile stiffness measurements showed little variation when calculated by the 3, 5, or 7 point regression analysis or the tangent-fit method. This is likely due to the fact that in the compressive and tensile regions of the load-displacement curves, there is a relatively linear region around loads seen during physiologic motion in-vivo (i.e. around 300N in our porcine model). Performing linear regression about any number of points in the linear region would result in a similar slope. However, the neutral zone stiffness measurements were more sensitive to the calculation method, with the tangent-fit method generally giving higher stiffness and the 3 point regression generally giving the lowest. The load-displacement curve shows that in most specimens, there is more variation in the neutral zone load-displacement data compared to that in the tensile or compressive regions. The variation in the data points helps explain the wide range of NZ stiffness values we calculated using four different methods. The difference in slopes of linear regression lines found using a small number of data points is sensitive to a deviation in the pattern of those points. The tangent fit method measures the tangent slope of a curve of best fit to a number of neutral zone data points. This will be less sensitive to deviation of one or two data points.

5.2.4. Recommendations for Property Calculations

To calculate compressive and tensile stiffness, and neutral zone displacement, we recommend the use of the 7 point linear regression method. Although the differences in the four methods are minor, using a larger number of points will help reduce the effect of random noise in the data, if present. We suggest the use of the 6^{th} order polynomial tangent-fit method to calculate NZ stiffness, as the curve will average the randomness of the data points which seems to be prevalent in the neutral zone region.

5.3. Healthy and GAG-degenerated Disc Mechanics and ACMRI Indices

Preliminary mechanical property data was obtained to compare axial mechanics of healthy and GAG-degenerated discs, using the loading protocol outlined in section 5.1. Performing this research helped identify protocol changes which needed to be made before a full study was undertaken. The data was used to determine if our ChABC injection caused enough GAG depletion to change mechanical properties to a greater extent than changes brought upon by soaking and experimental variability. With this data, we were also able to perform a power analysis to determine a sample size necessary for future studies. It should be noted that mechanical data for all healthy and degenerated discs to be discussed in this section was previously presented in section 5.1.

We also performed ACMRI imaging of each specimen and compared the indices with the mechanical properties. This was done to show how ACMRI indices, which act as an indirect measure of GAG concentration, can be used in future mechanical studies.

Comparisons of healthy and degenerated disc mechanics are prevalent in the literature. Therefore, unlike the other sections of chapter 5, a detailed literature comparison with our work is discussed in this section as well.

5.3.1. Materials and Methods for Healthy and GAG-degenerated Disc Mechanics and ACMRI Indices

The loading protocol has been previously explained in the protocol development 1, section 5.1, and will be summarized here. A total of six functional spinal units were tested for this analysis. Three were designated to remain "healthy" and three were designated to be "degenerated". This nomenclature refers to the state of the disc on the second day of the two day mechanical testing protocol, as all discs were tested in their healthy state for day 1. We then assessed compressive, tensile, and neutral zone stiffness, and neutral zone displacement in the specimens. Testing occurred over a two day period as previously explained (Figure 5.6), with the only difference between the two specimen groups being the injection of ChABC following the first mechanical test in the degenerated group

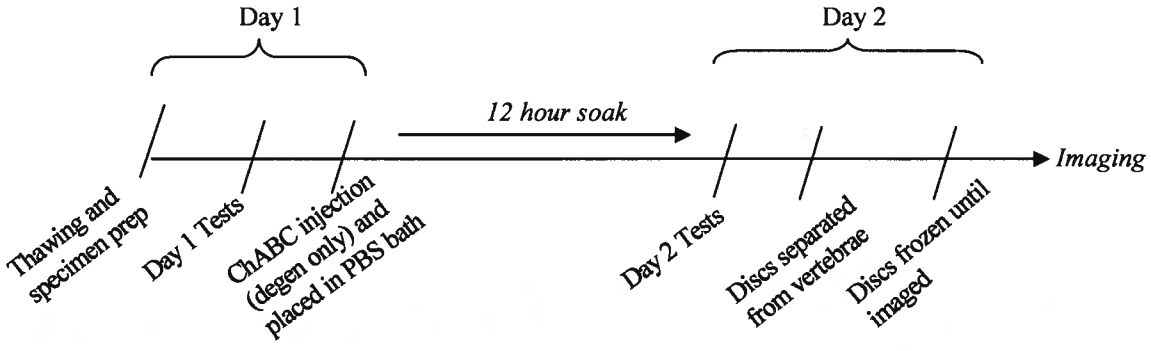

Figure 5.6: Timeline schematic for mechanical testing protocol. After the first test (day 1 tests) healthy discs were immediately placed in PBS to soak, while degenerated discs were injected with ChABC and immediately placed in PBS.

All FSUs were first tested immediately after thawing and potting. All discs were considered healthy for day 1, as no treatment was applied to them prior to the first mechanical test. Discs in the degenerated category were injected with ChABC following

the first day of testing, and soaked in PBS for 12 hours. All healthy discs were soaked in PBS for the same length of time to negate any differences caused by the soaking process. All discs were then tested again after the soaking process.

After the second mechanical test, discs were prepared for ACMRI imaging. As outlined in section 3.1, discs were separated from the vertebrae and excess bone was removed. Discs were imaged over two days with the protocol discussed in chapter 4. T1 calculations were performed and used as indirect measures of glycosaminoglycan content.

We decided to inspect the data of each individual specimen to identify differences between healthy and degenerated discs; both comparisons of property magnitudes and property changes between test days (i.e. day 1 to day 2 changes in healthy specimens compared to changes in degenerated specimens) were considered. Axial properties were then compared to both $\Delta T1$ and T1 post-contrast to identify correlations between mechanics and ACMRI indices. Based on the small sample size we used for this pilot study, we did not expect to find statistical significance. We instead reported the raw data from the tests and qualitatively discussed any trends that were seen.

5.3.2. Results for Healthy and GAG-degenerated Disc Mechanics and ACMRI Indices

Raw data for axial properties of all specimens was previously shown in Figure 5.4 and Table 5.1. Figure 5.7 shows a sample force displacement curve for specimen D3, in which the 'healthy' curve and the GAG-degenerated curve overlap is displayed. The

compressive stiffness measurement and the relative drop between days is also shown on in Figure 5.7.

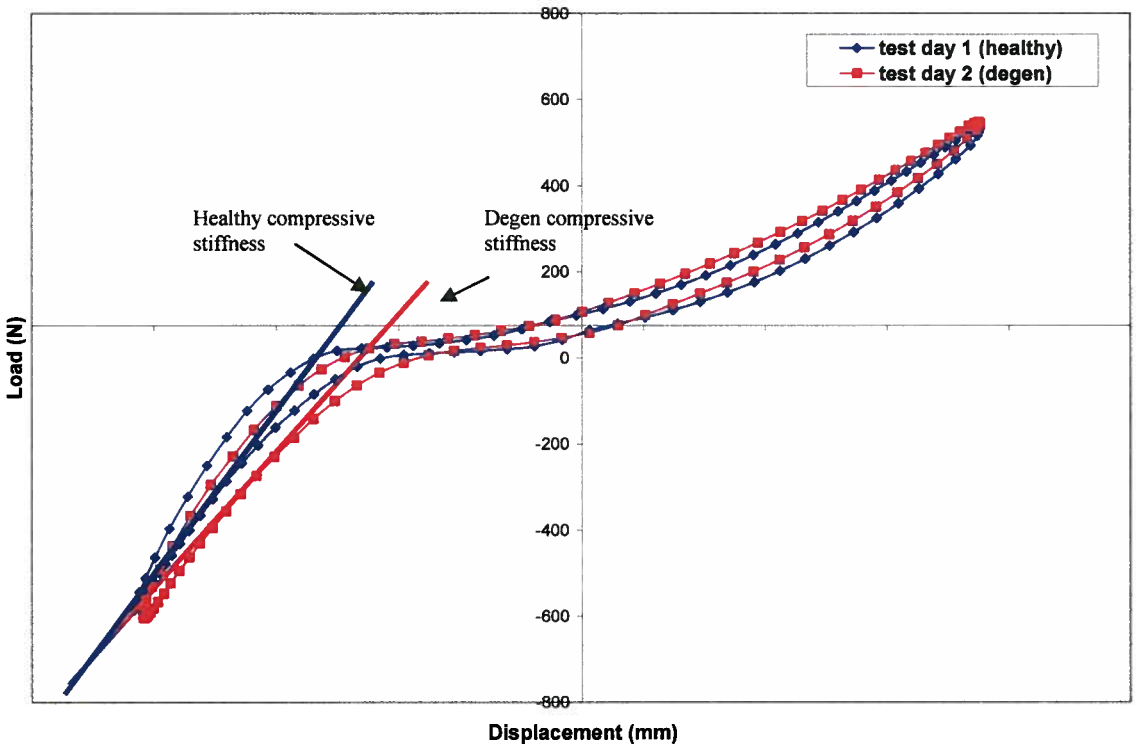

Figure 5.7: Force-displacement curve for specimen D3, which is 'healthy' for test 1 (blue) and GAG degenerated for day 2 (red). The slope of the degenerated compression curve is less at -300N compression than the healthy curve, as indicated by the slopes of the straight lines shown.

No noticeable differences were seen between the magnitudes of any of the four mechanical properties of healthy and degenerated discs, but there are some minor trends in the changes in properties between test days. In degenerated discs, compressive stiffness appeared to drop more from day 1 to day 2 (drops of 156, 455, and 212 N/mm) compared to healthy disc changes (drops of 124, 197, and 43 N/mm), although all discs' compressive stiffness dropped between tests (example in Figure 5.7). Degenerated specimen 2 had the largest change of all discs (drop of 455 N/mm). The relatively lower

compressive stiffness of the H1 specimen is consistent with the fact we had to measure the property at a lower load, as H1 did not reach 300N in compression. Two of the degenerated discs showed a minor decrease in tensile stiffness between tests, while all healthy discs showed an increase or no change. These differences here were all small. There was no consistent pattern in neutral zone stiffness, although a relatively large increase was seen in the specimen H2. Neutral zone displacement decreased or remained the same in all tests, with no obvious difference between healthy and degenerated specimens.

There were no noticeable trends seen when comparing axial properties to ACMRI indices. Compressive and tensile stiffness versus post-contrast T1 graphs are shown as examples from this analysis (Figure 5.8, Figure 5.9). Post-contrast T1 is generally lower for degenerated specimens as expected, although there is one outlier with a higher post-contrast T1 than the healthy specimens.

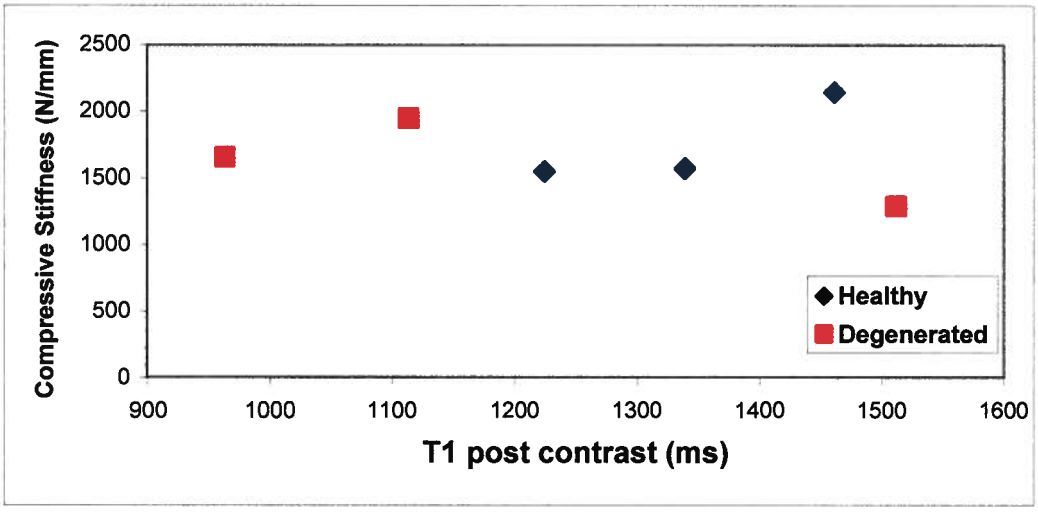

Figure 5.8: Test 2 compressive stiffness vs. post-contrast T1 of healthy and degenerated discs. Degenerated discs have lower post contrast T1 as shown in chapter 4 (one outlier in this data), but there is no correlation between stiffness and post-contrast T1.

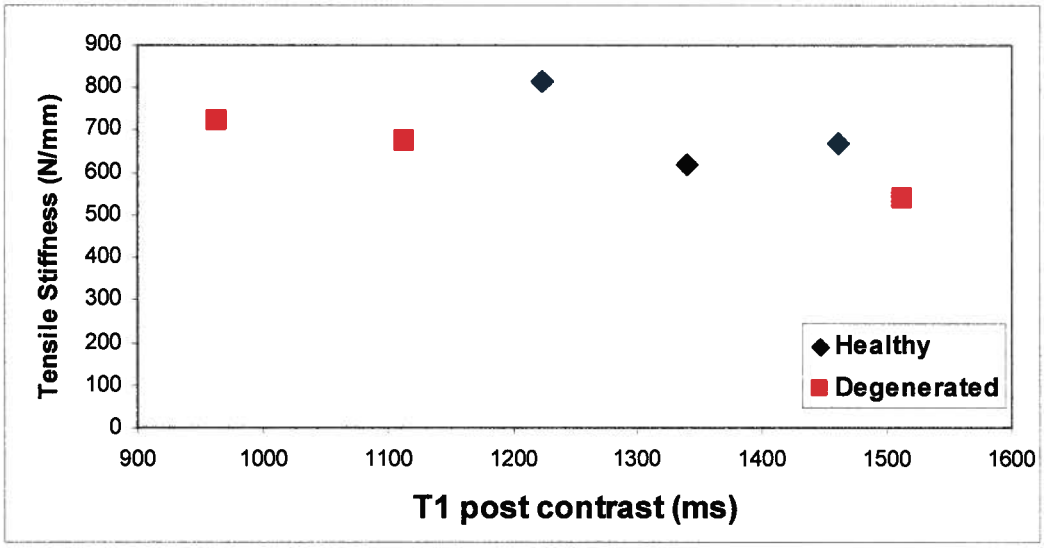

Figure 5.9: Test 2 tensile stiffness vs. T1 post-contrast of healthy and degenerated discs. There is no correlation between tensile stiffness and post-contrast T1

Based on the standard deviation of compressive stiffness in healthy discs from our initial data (s.d. = 340 N/mm), a power analysis reveals that to find a significant difference

($p \leq 0.05$) in compressive stiffness of 400 N between healthy and degenerated discs, with a power of 0.8, 15 specimens per group will be needed.

5.3.3. Discussion for Healthy and GAG-degenerated Disc Mechanics and ACMRI Indices

We compared the mechanical properties of healthy and GAG-degraded intervertebral discs in order to determine methods to improve our mechanical research protocol. We did not see differences in the magnitudes of axial properties between healthy and degenerated discs, although the compressive stiffness dropped more from day 1 to day 2, on average, in degenerated discs compared to healthy specimens. In general, when comparing healthy and degenerated discs, it was difficult to see differences in mechanical properties from day 1 to day 2, and this may indicate that soaking and experimental variability was masking changes brought on by GAG degeneration. A higher concentration of ChABC (i.e. more GAG depletion) may emphasize these differences more, and should be considered in future studies. We also acquired enough data to predict sample size for a larger study.

Weak negative trends were seen comparing compressive and tensile stiffness to post-contrast T1, but no significant correlations were found between ACMRI indices and any of the axial properties. Again, more GAG degradation may results in stronger correlations.

5.3.3.1. *Analysis of Results*

The larger drop in compressive stiffness in the degenerated specimen 2, and the relatively larger mean drop of all degenerated specimens compared to healthy specimens, may confirm that we are in the early stages of GAG-degeneration. In-vivo, the initial stages of disc degeneration are characterized by GAG and water loss. With these changes, the nucleus becomes more easily deformable and an initial decrease in stiffness occurs[31,102,155], and this is what we measured. The reduced stiffness in GAG-degenerated models may indicate that stiffness is affected significantly by electrical charge changes. In the healthy disc, there is a large negative fixed charge density in the nucleus because of the high GAG concentrations. The repulsive forces that develop because of the negative charge density may impart some stiffness to the disc, and as GAG depletes and negative charge densities drop, the decreased repulsion may lower stiffness.

As degeneration progresses, the compressive loads which are usually resisted by the fluid filled nucleus begin to transfer to the stiffer annulus, and an increased compressive stiffness of the disc is therefore associated with advanced degenerative stages[73,87,122,129,182]. We did not observe this phenomenon in our GAG-degenerated specimens because of the differences in physiologic disc degeneration and our GAG-depleted model. We have only modeled GAG changes in the disc and not collagen or general morphologic changes which occur in physiologic degeneration. It may be that the full spectrum of degenerative changes is necessary for that stiffness increase.

The annulus is the primary tensile load bearing structure of the disc, so we would expect a change in the tensile stiffness of the disc if there was a change in the annular properties. In chapter 4, we reported that there was no difference in annulus post-contrast T1 times between healthy and degenerated discs, implying there was no change in annular GAG concentration brought on by the ChABC injection. The absence of biochemical changes may explain the lack of differences between the tensile stiffness of healthy and degenerated discs that we saw in our 6 specimens. The small changes we saw in tensile stiffness are likely due to experimental variability between test days.

In general, we did not see obvious large differences between neutral zone stiffness and displacement in healthy and degenerated discs even though we would expect to. In GAG-degenerated discs, we would expect to see larger neutral zone displacements and decreased stiffness because of intradiscal pressure differences. During neutral zone mechanics (low loads), the nucleus likely resists loads directly. As disc loads increase, the pressure developed by the nuclear fluid will eventually build enough to distribute loads radially to the annulus. With reduced fluid content due to GAG loss, there is decreased intradiscal pressure and there may therefore be more deformation of the nucleus before annulus fibers are engaged and loaded. This phenomenon would be expected to increase neutral zone displacement and decrease neutral zone stiffness in the degenerated disc. The neutral zone displacement in all our discs decreased or remained the same after GAG-degeneration, while neutral zone stiffness tended to increase. In general, we saw the opposite of what we expected, or no differences at all. As previously explained in section 5.1.3, it is feasible that the long soaking time resulted in too much

nuclear fluid uptake for the disc to expel during the 19 cycles before the axial property measurements were made. The general increase in neutral zone stiffness and decrease in neutral zone displacement we saw from test 1 to test 2 would support this because a higher fluid concentrations would increase intradiscal pressure and result in these trends.

We observed property changes in both healthy and GAG-degenerated discs over the two test days. In general, the percent changes in tensile, compressive, and neutral zone stiffness between days were relatively small (generally <10%), though, and it was difficult to separate healthy and GAG-degenerated discs based on these differences. We need to enhance the mechanical changes in degenerated specimens, and increasing the concentration or volume of ChABC injected may help do this. A recent study showed a percent change of approximately 40% in the compressive stiffness of discs after treatment with ChABC in concentrations 5x higher than what we used here[182]. If we are to see mechanical changes caused by ChABC injection in future studies, and not have them masked by changes caused by other sources of variability, we will likely have to increase the concentration of the enzyme we use to similar levels.

In our current research, we also compared disc mechanics with ACMRI indices. Because ACMRI post-contrast T1 is a surrogate measure of GAG concentration, we would expect to see the same correlations between GAG concentration and mechanical properties as we would between post-contrast T1 and mechanical properties. In other words, lower post-contrast T1 should be associated with degenerative mechanical changes such as increased compressive stiffness, and lower neutral zone stiffness. We did not see such trends,

although there was a very weak negative correlation between post-contrast T1 and compressive stiffness. Specimen variability in T1 times and axial properties likely account for the minor differences we saw in our comparisons, so it is difficult to discern any real trends. As will be discussed in the limitations, more specimens will strengthen this pilot study.

5.3.3.2. Synthesis – A Comparison to the Literature

The values of the axial properties presented here are supported by similar findings in the literature. A recent study which measured in-vitro axial disc properties in various species of animals is the most comparable to ours[17]. The study measured a healthy lumbar porcine disc (average age 2 yrs) mean compressive stiffness of 2490±360 N/mm at 500 N of load, compared to our mean of approximately 1850±185 N/mm measured at 300N load. The higher stiffness they found is consistent with the fact they used older discs, and higher compressive loads. An in-vitro sheep model showed compressive stiffness of approximately 2400 N/mm, tensile stiffness of 720 N/mm and neutral zone displacements of 0.22 mm using loads of -400N to 300N[85]. Sheep and porcine discs are geometrically similar[17], so the results are again comparable to ours. The lower neutral zone displacement may be due to experimental differences, specifically the fact that they tested their specimens in a saline bath as opposed to being exposed to surrounding room conditions. Our results are higher than the mean compressive stiffness of 180 N/mm found in an in-vivo porcine model which measured compressive stiffness at 100-200N[87]. In-vivo, the constant uptake and expulsion of water, the use of a fully intact spine with

surrounding soft tissue (we tested a single FSU separated from the intact spine), and other physiologic responses may account for the much lower stiffness that was measured.

An increased compressive stiffness in discs showing advanced stages of degeneration compared to healthy ones is a widely reported finding in the literature.[73,84,87,122,133]. As the nucleus degenerates in-vivo, it loses its ability to hold water which is essential to resisting compressive loads in the spine. With the inability to bear compression by itself, the degenerated nucleus then transfers some compressive load bearing responsibility to the annulus or the posterior elements of the spine (i.e. facet joints)[35]. The degenerative stiffness increase is likely due to this load sharing. In early degeneration (grade 2 on the Pfirrmann scale), though, an initial decrease in stiffness has been found before the increase associated with more advanced grade degeneration[31,35]. We saw higher decreases in compressive stiffness of GAG degraded discs compared to healthy discs, and this may indicate that we have produced a disc state comparable to early degenerative stages, as expected. The relatively small percentage drop in compressive stiffness of healthy discs between test days (2-10%) is comparable to that seen in a previous study[85] which considered such small changes to be within acceptable repeatability limits.

NZ stiffness has been found to drop with GAG degradation and there is an associated neutral zone displacement increase[31,83]; these trends indicate a hypermobility of the disc at low loads with degeneration as described in section 5.3.3.1. The interaction between the nucleus and annulus is the key to the mechanical behaviour in this region. We unfortunately did not see such changes. Our variability in the neutral zone stiffness data

makes us question the validity or usefulness of measuring this property in axial testing protocols. The inter-specimen and between-test intra-specimen variability may mask actual differences between healthy and GAG degenerated discs. Further repeatability testing is needed to explore this.

In general, The percent changes in tensile, compressive, and neutral zone stiffness between days was relatively small (generally <10%), and we expect these to be smaller than the changes brought about by GAG degeneration; a recent study showed a percent change of approximately 40% in the compressive stiffness of discs after treatment with ChABC[182]. Future repeatability tests should be performed with and without soaking to see if soaking does contribute to the changes we saw. This potential effect of soaking may have masked mechanical changes brought on by the GAG degenerative process in the degenerated discs.

5.3.3.3. Strengths and Limitations of Healthy and GAG-degenerated Disc Mechanics and ACMRI Indices

The major strength of this study, as initially mentioned in section 5.1.3.2, is that we have a protocol in which each disc acts as its own healthy control. Although it was difficult for use to see differences in day-to-day property changes between healthy and degenerated specimens, we now know that we likely need to produce more GAG-degradation in order to highlight such differences. We have to overcome the 10% day-to-day variability in mechanical properties brought on by soaking and other variability sources.

The use of ACMRI as a surrogate measure of GAG is yet another strength of this work not previously mentioned. The use of ACMRI indices in mechanical tests provides an indirect, non-destructive GAG measurement technique. Currently, if GAG needs to be quantified, the disc must be destroyed for biochemical/histologic analysis. The effect of different treatments or multiple tests on GAG content of the *same* disc cannot be measured. With ACMRI, multiple GAG measurements can be taken without destroying the disc. ACMRI allows the study of the effects of multiple loading scenarios, focusing on how changes in frequency, rate, magnitude, or direction of loading contribute to GAG degradation over time, in the same specimen.

The major limitation to our mechanical study is the small number of specimens which inhibited our ability to represent the overall population of healthy and degenerated discs. Unfortunately, due to time constraints and difficulty in obtaining MRI time, we could not test and image more specimens. We were able to use our initial measurements to run a power study, though, which shows 15 specimens per group will be needed for a larger study. We have used this study to determine protocol changes and improvements, though, which is necessary in the protocol development stages of any research.

5.3.4. Recommendations from Healthy and GAG-degenerated Disc Mechanics and ACMRI Indices

The results from the study here led to the following protocol improvement recommendations.

1. Inject a higher concentration and volume of ChABC into the degenerated discs. We want to ensure that the mechanical changes due to degeneration are clearly distinguishable from those brought about by other sources of variation.
2. Once a full study is undertaken, 15 specimens per group should be included. This will be necessary to measure significant differences between healthy and degenerated groups. It may also improve the correlations between disc mechanics and ACMRI indices.

5.4. Protocol Development 2: Repeatability with Loading Rig 2

Following the results of the previous sections, the aim of this study was to improve upon the repeatability of our initial loading protocol, as well as to better assess the effect of soaking on disc mechanics. To do this, a new rig was used to load specimens. This rig, which allowed for flexion-extension of the specimen during testing, permitted us to better determine the disc balance point compared to our methods in protocol development 1. The rig would better help us to simulate pure compression. To differentiate variability in disc mechanics caused by soaking and that caused by other experimental factors, consecutive repeatability tests were run with and without soaking between them.

5.4.1. Materials and Methods for Protocol Development 2

For this repeatability study, 3 lower thoracic porcine disc specimens were used, all from the same spine. Thoracic discs were readily available, and the repeatability should not be affected by the use of a thoracic or a lumbar specimen, as long as both are consistently prepared and loaded in the same way (i.e. once posterior elements are removed, there should not be any confounding factors that would change repeatability outcome).

Specimens were first thawed for 12 hours after removal from a -20°C freezer. Single FSUs were removed from the intact thoracic spine with a saw. All soft tissue was then removed to expose bone for the potting process. Both the inferior and superior vertebrae were then potted in a dental stone using a circular mould; the upper and lower moulds were visually aligned so they were concentric, and a spirit level was used to ensure the

moulds were parallel to each other. After potting, discs were sprayed with saline, covered in saline soaked gauss, and stored at 4-5°C overnight until the day of testing. The following day, specimens were removed from the fridge. In order to focus only on the disc, we decided to remove the posterior elements. A ronger was used to remove the them, with care being taken not to damage the disc.

In order to test loading repeatability and the effect of soaking on mechanics, each specimen underwent 3 tests on day 1, was soaked for 12 hours, and tested once more each. A timeline is shown in Figure 5.10

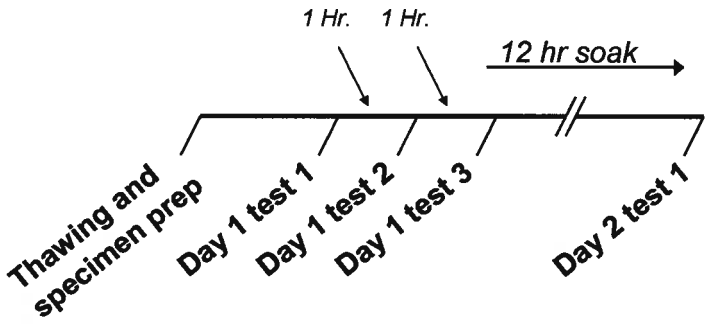

Figure 5.10: Timeline for protocol development 2 repeatability test. Each specimen underwent the same treatments.

A different testing machine (Instron 8874, MA, USA) than the first protocol development was used because it provided a better load control system than did the Instron Dynamight. Load control was used to ensure all specimens experienced the same load, an issue which we had with the position control protocol. Specimens were first placed on the Instron so the anterior-posterior axis of the disc was aligned with the flexion/extension direction of the loading rig (Figure 5.11). The balance point of the disc was then found by

applying up to 200N of force on the superior vertebra, and watching to determine if flexion or extension was occurring. During this, the rig was allowed to translate along the anterior-posterior axis of the disc and simultaneously rotate. The specimen was carefully repositioned after each load application until the point where no flexion-extension and no translation of the rig occurred. The balance point was defined as this position. The exact location of the specimen on the Instron was then marked so it could be repeatedly placed during consecutive tests.

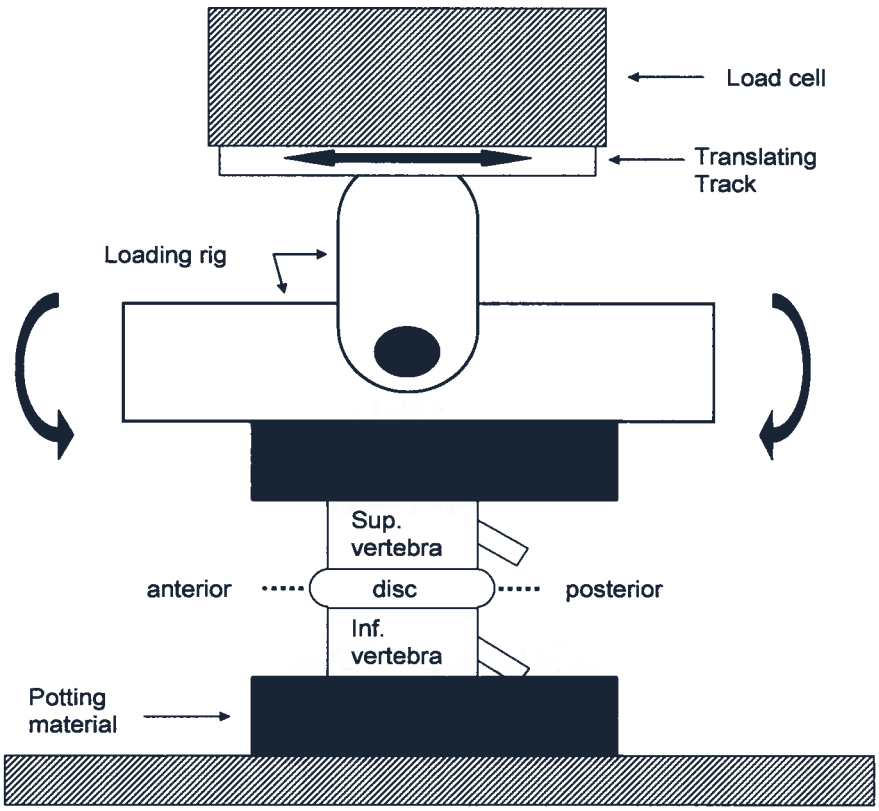

Figure 5.11: Loading schematic with the new rig. Thick arrows represent the loading rig's degrees of freedom: It was able to translate on a track attached to the load cell, and rotate about a pin (to simulate flexion-extension)

The loading protocol consisted of 20 cycles of load-controlled compression up to 500N in compression. The loading rate was 0.1 Hz (a slower rate than the 1 Hz used in protocol development 1), and load-displacement data was collected at 50 Hz. On day 1, after each test, specimens were covered in saline soaked gauss and stored at 4-5°C for one hour, after which the next test was performed. For each specimen, three tests were performed on the first day. Following test 3, each specimen was stored at 4-5°C until soaking began. All specimens were then placed in a phosphate buffered saline bath for 12 hours, following which they were tested with the same protocol as day 1 tests. The 12 hour soak mimics the time necessary for ChABC degeneration to occur. ChABC will be used in future studies which will aim to identify biomechanical differences between healthy and GAG-degenerated discs.

Only compressive stiffness was measured for these tests. Stiffness was measured as a linear regression of the 35 points surrounding 300N; once the differences in loading and sampling frequency are considered, the 35 points encompasses the same loading range as 7 points did in loading protocol 1 (range of approximately 80 N). For each specimen, stiffness of the 20th cycle was compared between all tests on both days, and the percent differences were reported.

5.4.2. Results for Protocol Development 2

The compressive stiffness for each test and each specimen can be seen in Table 5.5 and Figure 5.12. The repeatability of the compressive stiffness measurements was substantial,

with 4% being the largest percent difference when comparing test 1 of each specimen to the other 3.

Table 5.5: Compressive stiffness (N/mm) for 3 specimens, each undergoing 4 repeatability mechanical tests. Tests 1-3 represent the same day tests, while test represents testing after 12 hours of soaking.

	Test number			
	1	2	3	4 (after soaking)
Specimen 1	2698	2584	2665	2605
Specimen 2	2727	2776	2681	2626
Specimen 3	2694	2684	2637	2634

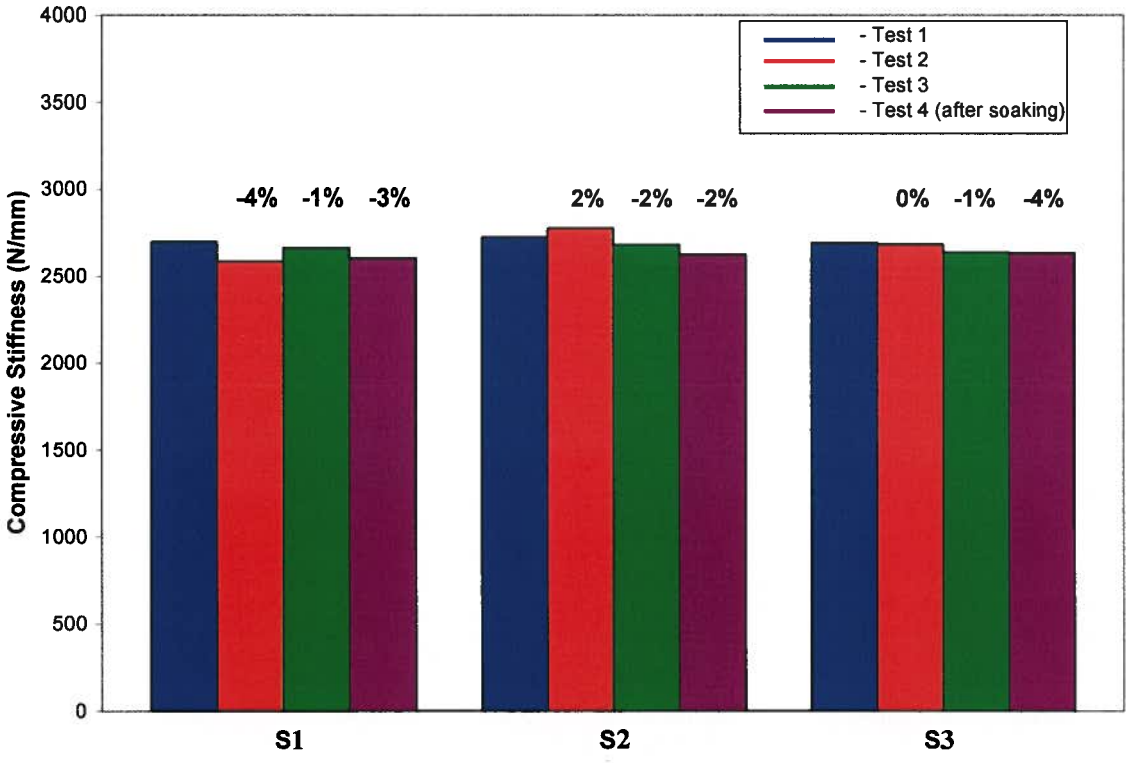

Figure 5.12: Compressive stiffness comparison for mechanical repeatability tests of 3 specimens. The percentages above each bar represent the percent difference of that test with respect to the same specimen's test 1 stiffness.

Soaking did not appear to change the stiffness of the specimens any more than repeated tests without soaking. Stiffness measurements were larger than those measured in protocol development 1.

5.4.3. Discussion for Protocol Development 2

Using a new rig and a new specimen preparation method, we found a much improved repeatability in the measurement of compressive stiffness compared to that in protocol development 1. Soaking, which we hypothesized to be the largest source of mechanical property variation in protocol development 1, did not appear to affect the results with this new protocol.

5.4.3.1. Repeatability of Loading Protocol 2

The mechanical identification of the discs' balance points and the use of a one degree of freedom rotational rig were likely the most significant reasons our repeatability was so much improved in this study. These two factors helped reduce moments on the disc, which was necessary to help ensure the disc experienced pure compression. In protocol development 1, flexion-extension moments could have been developed during testing because of the 2 rigid boundary conditions. If soaking affected the rotational mechanics of the disc, it would have appeared that there was a change in the supposed axial properties we measured in that protocol; for example, a reduced rotational stiffness due to soaking would have appeared as a reduced compressive stiffness in our measurements. In protocol 2 we are more confident that we measured the true compressive stiffness of the

disc. Our results here indicate that rotational stiffness was likely affected by soaking, because removal of some moments improved repeatability substantially.

Removal of the posterior elements of the disc may have improved repeatability as well. Soaking or mechanical testing could have affected the mechanics of the joints in protocol development 1, which again would have resulted in a change in the mechanical properties we measured. Removal of the posterior elements allowed us to focus more on disc mechanics without contribution of other structures.

Finally, the use of a lower loading frequency may have helped improve repeatability as well. The 0.1 Hz frequency used in this protocol simulates a static load. The slower load application may have reduced variability caused by excessive movement due to high speed loading (i.e. such as the 1 Hz loading frequency in protocol 1).

5.4.3.2. Strengths and Limitations of Loading Rig and Protocol 2

The repeatability improvement discussion in the previous section outlines the two major strengths of this protocol compared to protocol 1: The reduction in rotational moments by mechanical determination of the balance point and the one degree of freedom rig, and the removal of posterior elements so disc mechanics are measured independent of facet joint contributions.

Another strength of this protocol is the use of a load control protocol. The load control ensured that all discs experienced the same forces during testing, which meant we could

measure stiffness in the same loading regions for all discs. This was an issue in protocol 1, in which the maximum loads the discs transmitted varied from specimen to specimen.

The major limitation of this protocol is its inability to measure neutral zone mechanics. As explained in section 5.3.3.2, neutral zone mechanics change in early disc degeneration, and measuring such changes may be important in understanding the progression of degeneration. The variable neutral zone stiffness values we found in protocol development 1 made us question the validity of measuring that property in axial loading. Changes to the loading protocol introduced in this section may help remove variability in neutral zone measurements, though.

5.5. Overall Recommendations for Future Study

The research in chapter 5 focused on the creation of a protocol which will be used to compare intervertebral disc mechanics in healthy and degenerated discs (degenerated by ChABC), and compare mechanics to GAG concentration (using ACMRI as an indirect GAG measure). The steps taken to test and improve a protocol development have given us insight into what will help strengthen such a study. These recommendations follow:

1. The loading rig affects the repeatability of mechanical measurements, and it is important to reduce this variability as much as possible. We recommend the use of the one-degree of rotational rig for two reasons: it allows the balance point of the disc to be manually determined, and it removes flexion-extension moments during testing. Alterations to this rig to allow it to act in tension will also allow neutral zone mechanics to be studies. If this is done, another repeatability study mimicking that in section 5.4.1 should be undertaken to study neutral zone mechanics variability.
2. Stiffness and neutral zone displacement should be calculated with a linear regression of a number of data points, encompassing at least an 80 N range. If measured, neutral zone stiffness should be determined as the tangent to a 6^{th} order polynomial fit to the load displacement data, at the point of minimum slope.
3. Posterior elements of the disc should be removed. This likely helped repeatability in our work, and it will help emphasize degenerative mechanical changes in the disc by removing the mechanical contribution of the facet joints.

4. From our work, we cannot say whether the concentration and volume of ChABC was sufficient enough to cause measurable mechanical response changes. The literature shows that a higher concentration will change disc mechanics, though. A study should be undertaken to measure mechanics of discs injected with at least 3 different levels of ChABC concentrations. This has been done once in the literature[31], but will need to be repeated here because a different loading rig and protocol setup is being used.
5. We have focused on axial properties of the disc, but rotational properties will also change with degeneration. Future studies should consider measuring axial as well as rotational kinematics to give more insight into the degenerative process.
6. A full study should be undertaken in conjunction with points 3 and 4 above. It should employ the 2 day testing protocol explained throughout chapter 5. This study should first measure disc mechanics in all healthy discs; each disc should then be degraded with different concentrations of ChABC (at least 3), and mechanics measured again. The discs should then be imaged using the ACMRI protocol. With this data, relative GAG concentration, measured non-destructively, can be compared with disc mechanics to assess the feasibility of using ACMRI as a replacement for destructive GAG measurements in biomechanical studies. With only two groups (healthy and degenerated), a power analysis showed 15 specimens should be used per group, so we have a guideline for a full study such as this.

5.6. Conclusions

In the work presented here, we aimed to develop a mechanical testing protocol for the intervertebral disc. For this, we assessed measurement and calculation repeatability, and suggested improvements in protocol and loading rig design which will strengthen future studies. Future researchers should use our recommendations to design a study aimed at comparing disc mechanics in healthy discs and discs degraded with ChABC, and correlate mechanical properties with ACMRI indices. The mechanics of disc degeneration and their reliance on GAG concentration is important in understanding the progression and prevention of disc degeneration.

6. Conclusions

In our primary study, we determined the feasibility of using anionic contrast agent MRI (ACMRI) to image glycosaminoglycan degeneration of the intervertebral disc. We furthered our work in a protocol development study investigating correlations of ACMRI to the axial mechanics of healthy and GAG-degenerated discs. Our research questions and findings are summarized below.

6.1. Summary of findings

Research question 1*: In order to create an in-vitro model for testing the feasibility of ACMRI in the intervertebral disc, what is the best anatomical preparation method to ensure equilibrium contrast agent diffusion occurs into the in-vitro disc in a reasonable amount of time during undisturbed soaking?*

It was not clear how best to prepare in-vitro intervertebral disc specimens to ensure full diffusion of contrast agent, or how long contrast agent would take to equilibrate. We therefore used a 10 hour dynamic MRI scan to image discs prepared by 3 different methods while soaked in contrast agent. We were able to measure contrast agent uptake (increase in signal intensity) into the discs. When the full intact lumbar spine was soaked after the removal of soft tissue, we saw minor enhancement beyond the peripheries of the disc after 10 hours. The next preparation method involved the separation of the intervertebral disc from its superior and inferior vertebrae as close to the disc as possible. Again, we saw little enhancement beyond the periphery of the disc after 10 hours, and no enhancement in the central regions of the disc. The final method involved using a

diamond drill bit to remove the excess bone from the superior and inferior planes of the disc, thus exposing the endplates. After 10 hours of soaking in contrast agent, we saw a 750% increase in signal intensity in the central nucleus. The central nucleus signal intensity vs. time curve had almost, but not quite, reached equilibrium at this point. We decided this was the method to use for remainder of our research.

Our diffusion time findings are within the range of previous in-vitro diffusion studies. The endplate is the primary path of diffusion of fluids in-vivo, so we expected that exposing it would improve contrast diffusion. Answering research question 1 was essential to designing the study to answer research question 2 below.

Research question 2: *Are MRI T1 relaxation times after equilibration of anionic contrast agent sensitive to glycosaminoglycan differences in the intervertebral disc?*

The ability of anionic contrast agent MRI to identify glycosaminoglycan degeneration in the intervertebral disc has not been studied in a controlled setting. To assess this, we compared T1 relaxation times before and after contrast agent uptake in-vitro in healthy and glycosaminoglycan-degraded porcine lumbar intervertebral discs. We found that post-contrast T1 times were significantly lower in the nucleus pulposus of GAG-degraded discs ($p<0.01$), while there was no difference in the pre-contrast T1. There was also a significantly greater drop in T1 from pre- to post-contrast images in the nucleus of the degenerated discs ($p<0.01$) indicating a larger uptake of contrast agent compared to the healthy disc groups. These findings supported our hypothesis that contrast agent would accumulate more in the GAG-degenerated disc. GAG degeneration reduces the

fixed negative charge density in the semi-fluid nucleus so there is less negative electrostatic repulsion of the contrast agent. More of the negatively charged contrast is therefore able to diffuse to regions of depleted GAG than in the healthy discs and T1 is reduced in relation to the concentration of contrast agent. For the number of specimens we tested, we found no statistically significant differences in the post-contrast T1 or ΔT1 values in the anterior annulus region of healthy and degenerated discs. This was expected due to the relatively low fluid retention capability and low GAG content of the outer annulus.

Objective 3: *To create an axial mechanics testing protocol which will be used to detect differences between healthy and GAG-degenerated disc mechanics, and correlate the mechanical properties with ACMRI indices.*

The mechanical properties of the intervertebral disc are altered by the degenerative process and such changes can initiate a cycle of further degeneration. Determining mechanical changes caused by GAG depletion can help us better understand the progressive nature of disc degeneration. We therefore aimed to develop a mechanical testing protocol which would eventually be used to study mechanical effects of disc degeneration. We determined that the use of a one rotational degree of freedom rig, combined with posterior element removal will help improve repeatability of axial stiffness measurements. Further, the method of calculating mechanical properties did not change the values for compressive, tensile, and neutral zone displacement to a large degree, but was important when calculating neutral zone stiffness. A full study should be

undertaken which compares disc mechanics at various stages of GAG degeneration, and ACMRI indices can be used to quantify these levels.

6.2. Strengths and Limitations

Our use of a controlled in-vitro experiment is the greatest strength of our research. Unlike other quantitative MR studies, we were able to image degeneration after specifically targeting depletion of the GAG molecules using ChABC. Previous quantitative MRI research has measured T1 with and without contrast, T1ρ, and T2 as measures of in-vivo disc degeneration; these measures are unable to identify single aspects of degeneration (i.e. just GAG degeneration) and/or are performed in an environment characterized by a number of uncontrolled morphologic and biochemical changes. By isolating GAG depletion, we have showed the ability of ACMRI to detect early degeneration.

The main limitation of our study is it reveals nothing about the ability of intervertebral disc ACMRI to work in-vivo. Because of constant fluid exchange in the intervertebral disc, obtaining equilibrium contrast agent diffusion into the disc is likely the main barrier to using ACMRI in-vivo. Previous studies have suggested that diffusion will occur in a reasonable time[128,142,171], however, which suggests strongly that ACMRI is clinically feasible.

6.3. Steps Required for the Development of ACMRI In-vivo

The potential for ACMRI to measure GAG content in-vivo has been recently studied with encouraging results[171], and further in-vivo development will help optimize the technique. The development of a contrast agent injection protocol with dynamic MRI to assess the uptake of contrast agent in-vivo is the first step which should be undertaken in the development of an in-vivo ACMRI protocol. As shown in dGEMRIC research, protocol changes such as exercise after injection of contrast agent and injection dose will affect the uptake of contrast agent into cartilage[36]. Assessing such protocol variables in the disc will assist in minimizing diffusion times. Optimizing MRI scans to provide high resolution images in relatively short times will also be needed. Patient comfort is essential in MRI imaging so minimizing the time they spend in the scanner should be a primary concern. However, high resolution images are also desired as we would like to identify localized areas of GAG depletion. Once these two steps are complete, research should focus on measuring ACMRI indices in discs representing the spectrum of Pfirrmann degenerative grades. This will give an indication of the ability of ACMRI to quantify degeneration. Further, this work may lead to the development of a more continuous and quantifiable scale of disc degeneration able to consistently identify early stages of the disease. Finally, research should aim to correlate ACMRI with clinical symptoms of back pain. Medical imaging research has yet to find identify a consistent radiologic marker for lower back pain. ACMRI may provide more insight into this. In-vivo ACMRI has the potential to advance our understanding of intervertebral disc degeneration and should therefore be developed in future research.

6.4. Clinical Significance

ACMRI's potential to image GAG degeneration in-vivo has important clinical significance. Because GAG reduction is a characteristic of early disc degeneration, ACMRI has the potential to identify patients who may be at risk of developing more severe degeneration. Conservative therapeutic techniques (i.e. physiotherapy) in the early stages of degeneration may be a key in preventing some cases of lower back pain. As therapeutic techniques often focus on GAG restoration, ACMRI's non-destructive nature will be an asset in determining the effectiveness of such therapies. In severe cases of degeneration where spinal surgery is required, ACMRI may be useful in confirming the spinal level of the disc which needs to be operated on. It may be able to replace the invasive and more dangerous provocative discography which is still used for this purpose.

In conclusion, there are important implications of non-invasively measuring intervertebral disc GAG health, and our work has brought the research one step closer to that phase. Clinical work aims to maintain and improve patient quality of life, and future ACMRI research may help to isolate ways to achieve that in those suffering from debilitating low back pain caused by intervertebral disc degeneration.

References

1. Adams M.A. MDS, Wagstaff J., Goodship A.E. Abnormal stress concentrations in lumbar intervertebral discs following damage to the vertebral bodies: a cause of disc failure? Eur Spine J 1993;1:214-21.
2. Adams MA, Freeman BJ, Morrison HP, et al. Mechanical initiation of intervertebral disc degeneration. Spine 2000;25:1625-36.
3. Adams MA, Hutton WC. The effect of posture on diffusion into lumbar intervertebral discs. J Anat 1986;147:121-34.
4. Adams MA, McMillan DW, Green TP, et al. Sustained loading generates stress concentrations in lumbar intervertebral discs. Spine 1996;21:434-8.
5. Adams MA, Roughley PJ. What is intervertebral disc degeneration, and what causes it? Spine 2006;31:2151-61.
6. Ahmed AM, Duncan NA, Burke DL. The effect of facet geometry on the axial torque-rotation response of lumbar motion segments. Spine 1990;15:391-401.
7. Akansel G, Haughton VM, Papke RA, et al. Diffusion into human intervertebral disks studied with MR and gadoteridol. AJNR Am J Neuroradiol 1997;18:443-5.
8. Andersson GB. Epidemiological features of chronic low-back pain. Lancet 1999;354:581-5.
9. Antoniou J, Pike GB, Steffen T, et al. Quantitative magnetic resonance imaging in the assessment of degenerative disc disease. Magn Reson Med 1998;40:900-7.
10. Aprill C, Bogduk N. High-intensity zone: a diagnostic sign of painful lumbar disc on magnetic resonance imaging. Br J Radiol 1992;65:361-9.
11. Auerbach JD, Johannessen W, Borthakur A, et al. In vivo quantification of human lumbar disc degeneration using T(1rho)-weighted magnetic resonance imaging. Eur Spine J 2006;15 Suppl 15:338-44.
12. Bashir A, Gray ML, Burstein D. Gd-DTPA2- as a measure of cartilage degradation. Magn Reson Med 1996;36:665-73.
13. Bashir A, Gray ML, Hartke J, et al. Nondestructive imaging of human cartilage glycosaminoglycan concentration by MRI. Magn Reson Med 1999;41:857-65.
14. Battie MC, Videman T. Lumbar disc degeneration: epidemiology and genetics. J Bone Joint Surg Am 2006;88 Suppl 2:3-9.
15. Battie MC, Videman T, Gibbons LE, et al. 1995 Volvo Award in clinical sciences. Determinants of lumbar disc degeneration. A study relating lifetime exposures and magnetic resonance imaging findings in identical twins. Spine 1995;20:2601-12.
16. Beattie PF, Meyers SP, Stratford P, et al. Associations between patient report of symptoms and anatomic impairment visible on lumbar magnetic resonance imaging. Spine 2000;25:819-28.
17. Beckstein JC, Sen S, Schaer TP, et al. Comparison of animal discs used in disc research to human lumbar disc: axial compression mechanics and glycosaminoglycan content. Spine 2008;33:E166-73.
18. Benjamin M, Ralphs JR. Biology of fibrocartilage cells. Int Rev Cytol 2004;233:1-45.

19. Benneker LM, Heini PF, Anderson SE, et al. Correlation of radiographic and MRI parameters to morphological and biochemical assessment of intervertebral disc degeneration. Eur Spine J 2005;14:27-35.
20. Berry H, Hutchinson DR. Tizanidine and ibuprofen in acute low-back pain: results of a double-blind multicentre study in general practice. J Int Med Res 1988;16:83-91.
21. Berry JL, Moran JM, Berg WS, et al. A morphometric study of human lumbar and selected thoracic vertebrae. Spine 1987;12:362-7.
22. Best BA, Guilak F, Setton LA, et al. Compressive mechanical properties of the human anulus fibrosus and their relationship to biochemical composition. Spine 1994;19:212-21.
23. Boden SD, Davis DO, Dina TS, et al. Abnormal magnetic-resonance scans of the lumbar spine in asymptomatic subjects. A prospective investigation. J Bone Joint Surg Am 1990;72:403-8.
24. Boos N, Boesch C. Quantitative magnetic resonance imaging of the lumbar spine. Potential for investigations of water content and biochemical composition. Spine 1995;20:2358-65; discussion 66.
25. Boos N, Dreier D, Hilfiker E, et al. Tissue characterization of symptomatic and asymptomatic disc herniations by quantitative magnetic resonance imaging. J Orthop Res 1997;15:141-9.
26. Boos N, Rieder R, Schade V, et al. 1995 Volvo Award in clinical sciences. The diagnostic accuracy of magnetic resonance imaging, work perception, and psychosocial factors in identifying symptomatic disc herniations. Spine 1995;20:2613-25.
27. Boos N, Wallin A, Gbedegbegnon T, et al. Quantitative MR imaging of lumbar intervertebral disks and vertebral bodies: influence of diurnal water content variations. Radiology 1993;188:351-4.
28. Boos N, Wallin A, Schmucker T, et al. Quantitative MR imaging of lumbar intervertebral disc and vertebral bodies: methodology, reproducibility, and preliminary results. Magn Reson Imaging 1994;12:577-87.
29. Boos N, Weissbach S, Rohrbach H, et al. Classification of age-related changes in lumbar intervertebral discs: 2002 Volvo Award in basic science. Spine 2002;27:2631-44.
30. Bottomley PA, Hardy CJ, Argersinger RE, et al. A review of 1H nuclear magnetic resonance relaxation in pathology: are T1 and T2 diagnostic? Med Phys 1987;14:1-37.
31. Boxberger JI, Sen S, Yerramalli CS, et al. Nucleus pulposus glycosaminoglycan content is correlated with axial mechanics in rat lumbar motion segments. J Orthop Res 2006;24:1906-15.
32. Bozzao A, Gallucci M, Masciocchi C, et al. Lumbar disk herniation: MR imaging assessment of natural history in patients treated without surgery. Radiology 1992;185:135-41.
33. Brinckmann P, Grootenboer H. Change of disc height, radial disc bulge, and intradiscal pressure from discectomy. An in vitro investigation on human lumbar discs. Spine 1991;16:641-6.
34. Brodin H. Paths of nutrition in articular cartilage and intervertebral discs. Acta Orthop Scand 1955;24:177-83.
35. Brown MD, Holmes DC, Heiner AD. Measurement of cadaver lumbar spine motion segment stiffness. Spine 2002;27:918-22.

36. Burstein D, Velyvis J, Scott KT, et al. Protocol issues for delayed Gd(DTPA)(2-)-enhanced MRI (dGEMRIC) for clinical evaluation of articular cartilage. Magn Reson Med 2001;45:36-41.
37. Bush K, Cowan N, Katz DE, et al. The natural history of sciatica associated with disc pathology. A prospective study with clinical and independent radiologic follow-up. Spine 1992;17:1205-12.
38. Caplan PS, Freedman LM, Connelly TP. Degenerative joint disease of the lumbar spine in coal miners--a clinical and x-ray study. Arthritis Rheum 1966;9:693-702.
39. Carragee E, Alamin T, Cheng I, et al. Are first-time episodes of serious LBP associated with new MRI findings? Spine J 2006;6:624-35.
40. Carragee EJ, Alamin TF, Miller JL, et al. Discographic, MRI and psychosocial determinants of low back pain disability and remission: a prospective study in subjects with benign persistent back pain. Spine J 2005;5:24-35.
41. Carragee EJ, Paragioudakis SJ, Khurana S. 2000 Volvo Award winner in clinical studies: Lumbar high-intensity zone and discography in subjects without low back problems. Spine 2000;25:2987-92.
42. Carrera GF, Williams AL. Current concepts in evaluation of the lumbar facet joints. Crit Rev Diagn Imaging 1984;21:85-104.
43. Chatani K, Kusaka Y, Mifune T, et al. Topographic differences of 1H-NMR relaxation times (T1, T2) in the normal intervertebral disc and its relationship to water content. Spine 1993;18:2271-5.
44. Chiu EJ, Newitt DC, Segal MR, et al. Magnetic resonance imaging measurement of relaxation and water diffusion in the human lumbar intervertebral disc under compression in vitro. Spine 2001;26:E437-44.
45. Cinotti G, David T, Postacchini F. Results of disc prosthesis after a minimum follow-up period of 2 years. Spine 1996;21:995-1000.
46. Deyo RA. Diagnostic evaluation of LBP: reaching a specific diagnosis is often impossible. Arch Intern Med 2002;162:1444-7; discussion 7-8.
47. Deyo RA. Drug therapy for back pain. Which drugs help which patients? Spine 1996;21:2840-9; discussion 9-50.
48. Deyo RA, Bass JE. Lifestyle and low-back pain. The influence of smoking and obesity. Spine 1989;14:501-6.
49. Drake R, Vogl W, Mitchell A. Gray's Anatomy for Studentsed: Churchill Livingstone, 2004.
50. Enker P, Steffee A, McMillin C, et al. Artificial disc replacement. Preliminary report with a 3-year minimum follow-up. Spine 1993;18:1061-70.
51. Eurell JA, Brown MD, Ramos M. The effects of chondroitinase ABC on the rabbit intervertebral disc. A roentgenographic and histologic study. Clin Orthop Relat Res 1990:238-43.
52. Finch P. Technology Insight: imaging of low back pain. Nat Clin Pract Rheumatol 2006;2:554-61.
53. Freemont AJ, Peacock TE, Goupille P, et al. Nerve ingrowth into diseased intervertebral disc in chronic back pain. The Lancet 1997;350:178.
54. Fritzell P, Hagg O, Wessberg P, et al. 2001 Volvo Award Winner in Clinical Studies: Lumbar fusion versus nonsurgical treatment for chronic low back pain: a

multicenter randomized controlled trial from the Swedish Lumbar Spine Study Group. Spine 2001;26:2521-32; discussion 32-4.
55. Frobin W, Brinckmann P, Kramer M, et al. Height of lumbar discs measured from radiographs compared with degeneration and height classified from MR images. Eur Radiol 2001;11:263-9.
56. Fry TR, Eurell JC, Johnson AL, et al. Radiographic and histologic effects of chondroitinase ABC on normal canine lumbar intervertebral disc. Spine 1991;16:816-9.
57. Frymoyer JW. Back pain and sciatica. N Engl J Med 1988;318:291-300.
58. Gallagher S. Trunk extension strength and muscle activity in standing and kneeling postures. Spine 1997;22:1864-72.
59. Gill K, Blumenthal SL. Functional results after anterior lumbar fusion at L5-S1 in patients with normal and abnormal MRI scans. Spine 1992;17:940-2.
60. Gold GE, Han E, Stainsby J, et al. Musculoskeletal MRI at 3.0 T: relaxation times and image contrast. AJR Am J Roentgenol 2004;183:343-51.
61. Griffith SL, Shelokov AP, Buttner-Janz K, et al. A multicenter retrospective study of the clinical results of the LINK SB Charite intervertebral prosthesis. The initial European experience. Spine 1994;19:1842-9.
62. Gunzburg R, Parkinson R, Moore R, et al. A cadaveric study comparing discography, magnetic resonance imaging, histology, and mechanical behavior of the human lumbar disc. Spine 1992;17:417-26.
63. Haig AJ, Geisser ME, Tong HC, et al. Electromyographic and magnetic resonance imaging to predict lumbar stenosis, low-back pain, and no back symptoms. J Bone Joint Surg Am 2007;89:358-66.
64. Hansson TH, Keller TS, Spengler DM. Mechanical behavior of the human lumbar spine. II. Fatigue strength during dynamic compressive loading. J Orthop Res 1987;5:479-87.
65. Hart LG, Deyo RA, Cherkin DC. Physician office visits for low back pain. Frequency, clinical evaluation, and treatment patterns from a U.S. national survey. Spine 1995;20:11-9.
66. Hickey DS, Aspden RM, Hukins DW, et al. Analysis of magnetic resonance images from normal and degenerate lumbar intervertebral discs. Spine 1986;11:702-8.
67. Hirsch C, Schajowicz F. Studies on structural changes in the lumbar annulus fibrosus. Acta Orthop Scand 1953;22:184-231.
68. Hiyama K, Okada S. Crystallization and some properties of chondroitinase from Arthrobacter aurescens. J Biol Chem 1975;250:1824-8.
69. Hutton WC, Murakami H, Li J, et al. The effect of blocking a nutritional pathway to the intervertebral disc in the dog model. J Spinal Disord Tech 2004;17:53-63.
70. Hutton WC, Toribatake Y, Elmer WA, et al. The effect of compressive force applied to the intervertebral disc in vivo. A study of proteoglycans and collagen. Spine 1998;23:2524-37.
71. Hutton WC, Yoon ST, Elmer WA, et al. Effect of tail suspension (or simulated weightlessness) on the lumbar intervertebral disc: study of proteoglycans and collagen. Spine 2002;27:1286-90.
72. Iatridis JC, Mente PL, Stokes IA, et al. Compression-induced changes in intervertebral disc properties in a rat tail model. Spine 1999;24:996-1002.

73. Iatridis JC, Setton LA, Foster RJ, et al. Degeneration affects the anisotropic and nonlinear behaviors of human anulus fibrosus in compression. J Biomech 1998;31:535-44.
74. Ibrahim MA, Haughton VM, Hyde JS. Effect of disk maturation on diffusion of low-molecular-weight gadolinium complexes: an experimental study in rabbits. AJNR Am J Neuroradiol 1995;16:1307-11.
75. Ibrahim MA, Haughton VM, Hyde JS. Enhancement of intervertebral disks with gadolinium complexes: comparison of an ionic and a nonionic medium in an animal model. AJNR Am J Neuroradiol 1994;15:1907-10.
76. Ibrahim MA, Jesmanowicz A, Hyde JS, et al. Contrast enhancement of normal intervertebral disks: time and dose dependence. AJNR Am J Neuroradiol 1994;15:419-23.
77. Ito M, Incorvaia KM, Yu SF, et al. Predictive signs of discogenic lumbar pain on magnetic resonance imaging with discography correlation. Spine 1998;23:1252-8; discussion 9-60.
78. Jackson RP, Cain JE, Jr., Jacobs RR, et al. The neuroradiographic diagnosis of lumbar herniated nucleus pulposus: II. A comparison of computed tomography (CT), myelography, CT-myelography, and magnetic resonance imaging. Spine 1989;14:1362-7.
79. Jarvik JG, Deyo RA. Diagnostic evaluation of low back pain with emphasis on imaging. Ann Intern Med 2002;137:586-97.
80. Jensen MC, Brant-Zawadzki MN, Obuchowski N, et al. Magnetic resonance imaging of the lumbar spine in people without back pain. N Engl J Med 1994;331:69-73.
81. Jensen MC, Kelly AP, Brant-Zawadzki MN. MRI of degenerative disease of the lumbar spine. Magn Reson Q 1994;10:173-90.
82. Johannessen W, Auerbach JD, Wheaton AJ, et al. Assessment of human disc degeneration and proteoglycan content using T1rho-weighted magnetic resonance imaging. Spine 2006;31:1253-7.
83. Johannessen W, Cloyd JM, O'Connell GD, et al. Trans-endplate nucleotomy increases deformation and creep response in axial loading. Ann Biomed Eng 2006;34:687-96.
84. Johannessen W, Elliott DM. Effects of degeneration on the biphasic material properties of human nucleus pulposus in confined compression. Spine 2005;30:E724-9.
85. Johannessen W, Vresilovic EJ, Wright AC, et al. Intervertebral disc mechanics are restored following cyclic loading and unloaded recovery. Ann Biomed Eng 2004;32:70-6.
86. Johnsson KE, Sass M. Cauda equina syndrome in lumbar spinal stenosis: case report and incidence in Jutland, Denmark. J Spinal Disord Tech 2004;17:334-5.
87. Kaigle A, Ekstrom L, Holm S, et al. In vivo dynamic stiffness of the porcine lumbar spine exposed to cyclic loading: influence of load and degeneration. J Spinal Disord 1998;11:65-70.
88. Kakitsubata Y, Theodorou DJ, Theodorou SJ, et al. Magnetic resonance discography in cadavers: tears of the annulus fibrosus. Clin Orthop Relat Res 2003:228-40.
89. Kato F, Iwata H, Mimatsu K, et al. Experimental chemonucleolysis with chondroitinase ABC. Clin Orthop Relat Res 1990:301-8.

90. Kendrick D, Fielding K, Bentley E, et al. Radiography of the lumbar spine in primary care patients with low back pain: randomised controlled trial. Bmj 2001;322:400-5.
91. Kettler A, Wilke HJ. Review of existing grading systems for cervical or lumbar disc and facet joint degeneration. Eur Spine J 2006;15:705-18.
92. Kjaer P, Leboeuf-Yde C, Korsholm L, et al. Magnetic resonance imaging and low back pain in adults: a diagnostic imaging study of 40-year-old men and women. Spine 2005;30:1173-80.
93. Kolstad F, Myhr G, Kvistad KA, et al. Degeneration and height of cervical discs classified from MRI compared with precise height measurements from radiographs. Eur J Radiol 2005;55:415-20.
94. Kurunlahti M, Kerttula L, Jauhiainen J, et al. Correlation of diffusion in lumbar intervertebral disks with occlusion of lumbar arteries: a study in adult volunteers. Radiology 2001;221:779-86.
95. Kurunlahti M, Tervonen O, Vanharanta H, et al. Association of atherosclerosis with low back pain and the degree of disc degeneration. Spine 1999;24:2080-4.
96. Kuslich SD, Ulstrom CL, Michael CJ. The tissue origin of low back pain and sciatica: a report of pain response to tissue stimulation during operations on the lumbar spine using local anesthesia. Orthop Clin North Am 1991;22:181-7.
97. Kwon BK, Vaccaro AR, Grauer JN, et al. Indications, techniques, and outcomes of posterior surgery for chronic low back pain. Orthop Clin North Am 2003;34:297-308.
98. Lane NE, Nevitt MC, Genant HK, et al. Reliability of new indices of radiographic osteoarthritis of the hand and hip and lumbar disc degeneration. J Rheumatol 1993;20:1911-8.
99. Leonardi M, Simonetti L, Agati R. Neuroradiology of spine degenerative diseases. Best Pract Res Clin Rheumatol 2002;16:59-87.
100. Lim CH, Jee WH, Son BC, et al. Discogenic lumbar pain: association with MR imaging and CT discography. Eur J Radiol 2005;54:431-7.
101. Lotz JC, Chin JR. Intervertebral disc cell death is dependent on the magnitude and duration of spinal loading. Spine 2000;25:1477-83.
102. Lu DS, Shono Y, Oda I, et al. Effects of chondroitinase ABC and chymopapain on spinal motion segment biomechanics. An in vivo biomechanical, radiologic, and histologic canine study. Spine 1997;22:1828-34; discussion 34-5.
103. Luoma K, Riihimaki H, Luukkonen R, et al. Low back pain in relation to lumbar disc degeneration. Spine 2000;25:487-92.
104. Luoma K, Vehmas T, Riihimaki H, et al. Disc height and signal intensity of the nucleus pulposus on magnetic resonance imaging as indicators of lumbar disc degeneration. Spine 2001;26:680-6.
105. MacGregor AJ, Andrew T, Sambrook PN, et al. Structural, psychological, and genetic influences on low back and neck pain: a study of adult female twins. Arthritis Rheum 2004;51:160-7.
106. Madan SS, Rai A, Harley JM. Interobserver error in interpretation of the radiographs for degeneration of the lumbar spine. Iowa Orthop J 2003;23:51-6.
107. Maigne JY, Rime B, Deligne B. Computed tomographic follow-up study of forty-eight cases of nonoperatively treated lumbar intervertebral disc herniation. Spine 1992;17:1071-4.

108. Maroudas A, Stockwell RA, Nachemson A, et al. Factors involved in the nutrition of the human lumbar intervertebral disc: cellularity and diffusion of glucose in vitro. J Anat 1975;120:113-30.
109. Marras WS, Rangarajulu SL, Wongsam PE. Trunk force development during static and dynamic lifts. Hum Factors 1987;29:19-29.
110. Martini FH, Timmons MJ. Human Anatomy. 2nd ed. Upper Saddle River, New Jersey: Prentice Hall, 1997.
111. Masuoka K, Michalek AJ, MacLean JJ, et al. Different effects of static versus cyclic compressive loading on rat intervertebral disc height and water loss in vitro. Spine 2007;32:1974-9.
112. McCarron RF, Wimpee MW, Hudkins PG, et al. The inflammatory effect of nucleus pulposus. A possible element in the pathogenesis of low-back pain. Spine 1987;12:760-4.
113. McNally DS, Adams MA. Internal intervertebral disc mechanics as revealed by stress profilometry. Spine 1992;17:66-73.
114. Merriam WF, Quinnell RC, Stockdale HR, et al. The effect of postural changes on the inferred pressures within the nucleus pulposus during lumbar discography. Spine 1984;9:405-8.
115. Mimura M, Panjabi MM, Oxland TR, et al. Disc degeneration affects the multidirectional flexibility of the lumbar spine. Spine 1994;19:1371-80.
116. Mixter WB, JS. Rupture of the intervertebral disc with involvement of spinal canal. New Engl J of Med 1934;211:210-5.
117. Miyamoto K, Masuda K, Kim JG, et al. Intradiscal injections of osteogenic protein-1 restore the viscoelastic properties of degenerated intervertebral discs. Spine J 2006;6:692-703.
118. Modic MT. Degenerative disc disease and back pain. Magn Reson Imaging Clin N Am 1999;7:481-91, viii.
119. Modic MT, Pavlicek W, Weinstein MA, et al. Magnetic resonance imaging of intervertebral disk disease. Clinical and pulse sequence considerations. Radiology 1984;152:103-11.
120. Murphy PL, Volinn E. Is occupational low back pain on the rise? Spine 1999;24:691-7.
121. Nachemson A. The load on lumbar disks in different positions of the body. Clin Orthop Relat Res 1966;45:107-22.
122. Nachemson A. Lumbar intradiscal pressure. Experimental studies on post-mortem material. Acta Orthop Scand Suppl 1960;43:1-104.
123. Newman MH, Grinstead GL. Anterior lumbar interbody fusion for internal disc disruption. Spine 1992;17:831-3.
124. Nguyen-minh C, Haughton VM, Papke RA, et al. Measuring diffusion of solutes into intervertebral disks with MR imaging and paramagnetic contrast medium. AJNR Am J Neuroradiol 1998;19:1781-4.
125. Nguyen-minh C, Riley L, 3rd, Ho KC, et al. Effect of degeneration of the intervertebral disk on the process of diffusion. AJNR Am J Neuroradiol 1997;18:435-42.
126. Nguyen AM, Johannessen W, Yoder JH, et al. Noninvasive quantification of human nucleus pulposus pressure with use of T1rho-weighted magnetic resonance imaging. J Bone Joint Surg Am 2008;90:796-802.

127. Nightingale T, MacKay A, Pearce RH, et al. A model of unloaded human intervertebral disk based on NMR relaxation. Magn Reson Med 2000;43:34-44.
128. Niinimaki JL, Parviainen O, Ruohonen J, et al. In vivo quantification of delayed gadolinium enhancement in the nucleus pulposus of human intervertebral disc. J Magn Reson Imaging 2006.
129. Norcross JP, Lester GE, Weinhold P, et al. An in vivo model of degenerative disc disease. J Orthop Res 2003;21:183-8.
130. Ogata K, Whiteside LA. 1980 Volvo award winner in basic science. Nutritional pathways of the intervertebral disc. An experimental study using hydrogen washout technique. Spine 1981;6:211-6.
131. Olmarker K, Rydevik B, Nordborg C. Autologous nucleus pulposus induces neurophysiologic and histologic changes in porcine cauda equina nerve roots. Spine 1993;18:1425-32.
132. Parker LM, Murrell SE, Boden SD, et al. The outcome of posterolateral fusion in highly selected patients with discogenic low back pain. Spine 1996;21:1909-16; discussion 16-7.
133. Parkkinen JJ, Lammi MJ, Helminen HJ, et al. Local stimulation of proteoglycan synthesis in articular cartilage explants by dynamic compression in vitro. J Orthop Res 1992;10:610-20.
134. Paul R, Haydon RC, Cheng H, et al. Potential use of Sox9 gene therapy for intervertebral degenerative disc disease. Spine 2003;28:755-63.
135. Peng B, Wu W, Hou S, et al. The pathogenesis of discogenic low back pain. J Bone Joint Surg Br 2005;87:62-7.
136. Perie D, Iatridis JC, Demers CN, et al. Assessment of compressive modulus, hydraulic permeability and matrix content of trypsin-treated nucleus pulposus using quantitative MRI. J Biomech 2006;39:1392-400.
137. Perlewitz TJ, Haughton VM, Riley LH, 3rd, et al. Effect of molecular weight on the diffusion of contrast media into cartilage. Spine 1997;22:2707-10.
138. Perry J, Haughton V, Anderson PA, et al. The value of T2 relaxation times to characterize lumbar intervertebral disks: preliminary results. AJNR Am J Neuroradiol 2006;27:337-42.
139. Pfirrmann CW, Metzdorf A, Zanetti M, et al. Magnetic resonance classification of lumbar intervertebral disc degeneration. Spine 2001;26:1873-8.
140. Puustjarvi K, Lammi M, Helminen H, et al. Proteoglycans in the intervertebral disc of young dogs following strenuous running exercise. Connect Tissue Res 1994;30:225-40.
141. Race A, Broom ND, Robertson P. Effect of loading rate and hydration on the mechanical properties of the disc. Spine 2000;25:662-9.
142. Rajasekaran S, Babu JN, Arun R, et al. ISSLS prize winner: A study of diffusion in human lumbar discs: a serial magnetic resonance imaging study documenting the influence of the endplate on diffusion in normal and degenerate discs. Spine 2004;29:2654-67.
143. Renkawitz T, Boluki D, Grifka J. The association of low back pain, neuromuscular imbalance, and trunk extension strength in athletes. Spine J 2006;6:673-83.

144. Riihimaki H, Mattsson T, Zitting A, et al. Radiographically detectable degenerative changes of the lumbar spine among concrete reinforcement workers and house painters. Spine 1990;15:114-9.
145. Risbud MV, Albert TJ, Guttapalli A, et al. Differentiation of mesenchymal stem cells towards a nucleus pulposus-like phenotype in vitro: implications for cell-based transplantation therapy. Spine 2004;29:2627-32.
146. Robbins SE, Morse MH. Is the acquisition of a separate view of the sacroiliac joints in the prone position justified in patients with back pain? Clin Radiol 1996;51:637-8.
147. Roberts S, Evans H, Trivedi J, et al. Histology and pathology of the human intervertebral disc. J Bone Joint Surg Am 2006;88 Suppl 2:10-4.
148. Roberts S, Urban JP, Evans H, et al. Transport properties of the human cartilage endplate in relation to its composition and calcification. Spine 1996;21:415-20.
149. Rohlmann A, Zander T, Schmidt H, et al. Analysis of the influence of disc degeneration on the mechanical behaviour of a lumbar motion segment using the finite element method. J Biomech 2006;39:2484-90.
150. Rossignol M, Lortie M, Ledoux E. Comparison of spinal health indicators in predicting spinal status in a 1-year longitudinal study. Spine 1993;18:54-60.
151. Roughley PJ. Biology of intervertebral disc aging and degeneration: involvement of the extracellular matrix. Spine 2004;29:2691-9.
152. Saal JA, Saal JS, Herzog RJ. The natural history of lumbar intervertebral disc extrusions treated nonoperatively. Spine 1990;15:683-6.
153. Sambrook PN, MacGregor AJ, Spector TD. Genetic influences on cervical and lumbar disc degeneration: a magnetic resonance imaging study in twins. Arthritis Rheum 1999;42:366-72.
154. Samosky JT, Burstein D, Eric Grimson W, et al. Spatially-localized correlation of dGEMRIC-measured GAG distribution and mechanical stiffness in the human tibial plateau. J Orthop Res 2005;23:93-101.
155. Sasaki M, Takahashi T, Miyahara K, et al. Effects of chondroitinase ABC on intradiscal pressure in sheep: an in vivo study. Spine 2001;26:463-8.
156. Sato K, Kikuchi S, Yonezawa T. In vivo intradiscal pressure measurement in healthy individuals and in patients with ongoing back problems. Spine 1999;24:2468-74.
157. Sauerland K, Raiss RX, Steinmeyer J. Proteoglycan metabolism and viability of articular cartilage explants as modulated by the frequency of intermittent loading. Osteoarthritis Cartilage 2003;11:343-50.
158. Scavone JG, Latshaw RF, Weidner WA. Anteroposterior and lateral radiographs: an adequate lumbar spine examination. AJR Am J Roentgenol 1981;136:715-7.
159. Silberstein CE. The Evolution Of Degenerative Changes In The Cervical Spine And An Investigation Into The "Joints Of Luschka". Clin Orthop Relat Res 1965;40:184-204.
160. Sivan S, Merkher Y, Wachtel E, et al. Correlation of swelling pressure and intrafibrillar water in young and aged human intervertebral discs. J Orthop Res 2006;24:1292-8.
161. Stafira JS, Sonnad JR, Yuh WT, et al. Qualitative assessment of cervical spinal stenosis: observer variability on CT and MR images. AJNR Am J Neuroradiol 2003;24:766-9.

162. Stokes IA, Iatridis JC. Mechanical conditions that accelerate intervertebral disc degeneration: overload versus immobilization. Spine 2004;29:2724-32.
163. Strayer A. Lumbar spine: common pathology and interventions. J Neurosci Nurs 2005;37:181-93.
164. Taylor VM, Deyo RA, Cherkin DC, et al. Low back pain hospitalization. Recent United States trends and regional variations. Spine 1994;19:1207-12; discussion 13.
165. Thompson JP, Pearce RH, Schechter MT, et al. Preliminary evaluation of a scheme for grading the gross morphology of the human intervertebral disc. Spine 1990;15:411-5.
166. Thornbury JR, Fryback DG, Turski PA, et al. Disk-caused nerve compression in patients with acute low-back pain: diagnosis with MR, CT myelography, and plain CT. Radiology 1993;186:731-8.
167. Tsantrizos A, Ito K, Aebi M, et al. Internal strains in healthy and degenerated lumbar intervertebral discs. Spine 2005;30:2129-37.
168. Urban JP. The role of the physicochemical environment in determining disc cell behaviour. Biochem Soc Trans 2002;30:858-64.
169. Urban JP, Holm S, Maroudas A, et al. Nutrition of the intervertebral disc: effect of fluid flow on solute transport. Clin Orthop Relat Res 1982:296-302.
170. Urban JP, Smith S, Fairbank JC. Nutrition of the intervertebral disc. Spine 2004;29:2700-9.
171. Vaga S, Raimondi MT, Caiani EG, et al. Quantitative assessment of intervertebral disc glycosaminoglycan distribution by gadolinium-enhanced MRI in orthopedic patients. Magn Reson Med 2008;59:85-95.
172. Van Schaik JP, Verbiest H, Van Schaik FD. The orientation of laminae and facet joints in the lower lumbar spine. Spine 1985;10:59-63.
173. Vernon-Roberts B, Pirie CJ. Healing trabecular microfractures in the bodies of lumbar vertebrae. Ann Rheum Dis 1973;32:406-12.
174. Videman T, Battie MC, Gibbons LE, et al. Associations between back pain history and lumbar MRI findings. Spine 2003;28:582-8.
175. Vresilovic EJ, Johannessen W, Elliott DM. Disc mechanics with trans-endplate partial nucleotomy are not fully restored following cyclic compressive loading and unloaded recovery. J Biomech Eng 2006;128:823-9.
176. Wallach CJ, Sobajima S, Watanabe Y, et al. Gene transfer of the catabolic inhibitor TIMP-1 increases measured proteoglycans in cells from degenerated human intervertebral discs. Spine 2003;28:2331-7.
177. Wang DL, Jiang SD, Dai LY. Biologic response of the intervertebral disc to static and dynamic compression in vitro. Spine 2007;32:2521-8.
178. White AA, 3rd, Panjabi MM. The basic kinematics of the human spine. A review of past and current knowledge. Spine 1978;3:12-20.
179. Wilke HJ, Rohlmann F, Neidlinger-Wilke C, et al. Validity and interobserver agreement of a new radiographic grading system for intervertebral disc degeneration: Part I. Lumbar spine. Eur Spine J 2006;15:720-30.
180. Williams A, Gillis A, McKenzie C, et al. Glycosaminoglycan distribution in cartilage as determined by delayed gadolinium-enhanced MRI of cartilage (dGEMRIC): potential clinical applications. AJR Am J Roentgenol 2004;182:167-72.

181. Yao H, Justiz MA, Flagler D, et al. Effects of swelling pressure and hydraulic permeability on dynamic compressive behavior of lumbar annulus fibrosus. Ann Biomed Eng 2002;30:1234-41.
182. Yerramalli CS, Chou AI, Miller GJ, et al. The effect of nucleus pulposus crosslinking and glycosaminoglycan degradation on disc mechanical function. Biomech Model Mechanobiol 2007;6:13-20.
183. Yoon ST, Park JS, Kim KS, et al. ISSLS prize winner: LMP-1 upregulates intervertebral disc cell production of proteoglycans and BMPs in vitro and in vivo. Spine 2004;29:2603-11.
184. Zigler JE. Lumbar spine arthroplasty using the ProDisc II. Spine J 2004;4:260S-7S.

Appendix A: Ethics, MRI Protocol, and Publication Inclusion Approval Forms

High Field Magnetic Resonance Imaging Centre

Protocol Proposal Form

Study Title

Evaluation of delayed gadolinium enhanced magnetic resonance imaging (dGEMRIC) as a more sensitive measure of intervertebral disc degeneration.

Principal Investigator

David R. Wilson, DPhil

Please return Protocol Proposal Form and all attachments to the following address:

Linda Chandler
Administrator
UBC High Field Magnetic Resonance Imaging Centre
M10, Purdy Pavilion
2211 Wesbrook Mall
Vancouver, BC V6T 2B5
[redacted]
Phone:[redacted] Fax: [redacted]

High Field Magnetic Resonance Imaging Centre

Protocol Proposal Form

Please Complete in Full	
UBC Ethical Review #	Pending
Approval Date (mm/dd/yy)	
Study Expiry Date (mm/dd/yy)	

Date: June 6, 2006

Study Title: Evaluation of delayed gadolinium enhanced magnetic resonance imaging (dGEMRIC) as a more sensitive measure of intervertebral disc degeneration

Principal Investigator: David R. Wilson, DPhil

Address: Room 3114, 910 West 10th Ave.
Vancouver, BC
V5Z 4E3

Phone: [redacted] **Fax:** [redacted] **Email:** [redacted]

Type of Study *(please mark all applicable categories)*

- [x] Anatomy
- [ ] Angiography
- [ ] Diffusion
- [ ] Kinematics
- [ ] Functional Imaging
  - *Number of functional runs for each subject* _____
  - *Approximate length of each functional run* _____
  - *High resolution 3D Anatomical Images (Y/N)* _____
- [x] Gadolinium Contrast
- [ ] Magnetization Transfer
- [ ] Perfusion
- [ ] Serial Study
  - *# of MR visits per subject* _____
  - *Time interval between MR visits:* _____
- [ ] Spectroscopy
  - [ ] *Single Voxel*
  - [ ] *2D CSI*
- [x] T_1 Relaxation
- [ ] T_2 Relaxation
- [ ] Other (please specify) _____

High Field Magnetic Resonance Imaging Centre

Protocol Proposal Form

Study Timeline

Requested Start Date (dd/mm/yy)	01/07/06
Number of Volunteers	N/A
Number of Controls	N/A
Number of Patients	N/A
Requested scanner time per MR session	2 hrs
Estimated End Date (dd/mm/yy)	01/10/06

Funding

Funding Sources	Current Grants
Are you requesting PILOT scanner time?	Yes

Why? To develop the dGEMRIC protocol used in the knee and hip in the intervertebral disc.

Number of PILOT hours requested (maximum 10 hours) 4

Collaborators

1. Joshua Levitz, M.ASc candidate
2. Brian Kwon, M.D. – Qualified Investigator
3.
4.
5.
6.
7.
8.

Protocol Proposal Form

ABSTRACT

Please provide an abstract of up to two pages in length of the proposed research including the background, specific aims and the significance of the project as well as the Research Plan. This abstract should provide enough detail to allow evaluation of scientific merit.

If necessary, please attach additional materials to support this proposal.

Study Title: Evaluation of delayed gadolinium enhanced magnetic resonance imaging (dGEMRIC) as a more sensitive measure of intervertebral disc degeneration.

Principal Investigator: David R. Wilson, DPhil

Lower back pain is one of the most common injuries in society today, affecting between 70-85% of the general population at some point during their lives. In the USA, back pain is the second most frequent reason for doctor visitations, the fifth ranking cause for hospital admissions, and the third ranking cause for surgical procedures. In terms of Workers' Compensation, LBP is also the most common and expensive cause of disability related to work, with an estimated annual cost of $11.7 billion for LBP compensation in the United States. These trends are also seen in other western countries. LBP can interfere with the most common daily activities such as walking stairs or standing from a chair. In people under the age of 45, it is the most common cause of activity limitation, and therefore is a great concern to an individual's overall quality of life.

Although the etiology of lower back pain is often idiopathic, intervertebral (IV) disc degeneration is often cited as a cause for pain, especially in the lumbar spine. Degeneration is often characterized by tearing of the outer region of the disc (the annulus fibrosus), bulging of the disc into the spinal canal, and an overall decrease in the disc height. These features are able to be directly diagnosed from a one or more of standard radiographs, CT, or MRI images, especially when more severe degeneration has already occurred. These diagnostic techniques are often qualitative in nature, and inter- and intra-observer variability has been cited to be a possible problem in diagnosis of degeneration. Biochemically, proteoglycan concentration decreases with degeneration, and this is not currently diagnosable with imaging techniques.

Severe pathological signs of degeneration, such as nerve root compression by a herniated disc, are consistent indicators of low back pain. The majority of patients with back pain, however, will not show such severe signs, and may or may not show some degree of the physical features described above. Further, the same features are often seen in healthy patients with no lower back

Protocol Proposal Form
ABSTRACT

pain. Diagnosis of the cause for LBP cannot be made in approximately 85% of affected individuals because symptoms and pathological changes are not closely associated. To improve the quality and sensitivity of diagnoses of LBP, more sensitive measures of disc degeneration are being studied.

In recent years, MRI imaging has become the dominant imaging modality used to assess IVD degeneration. Its ability to contrast soft tissue and its promising results in assessing cartilage degeneration in synovial joints is the reason for its expansion. In general diagnosis, sagittal T1 and T2 weighted images are obtained and axial images of specific regions of interest are also useful. T1 weighted images are used to assess gross anatomy, disc herniations, and stenosis (canal compression), and T2 weighted images are used to assess disc hydration and highlight annular tears. Fat or cerebrospinal fluid suppression inversion recovery (FLAIR) sequences can be employed to improve visualization of the disc/thecal sac borders. Contrast enhancement with a non-ionic gadolinium based agent is becoming more common today to both enhance the signal in clinical diagnosis, and to study diffusion into the disc in research settings. More recently, T1ρ studies have emerged and initial correlations have been found to lower back pain, but the research is still in its infancy stages. The T1ρ value does not give us an indication of what anatomically is causing the pain either, as opposed to dGEMRIC for example, in which we know what exact molecule we are targeting.

This study is aiming to develop a more sensitive measure of IVD degeneration based on dGEMRIC protocol used in synovial cartilage degeneration assessment. Decrease of proteoglycan concentration is an indication of IVD degeneration, and may be a factor involved in lower back pain. The application of this protocol in the intervertebral disc has not been tested. If developed and validated, the research will continue with clinical testing. The major goal of the research will be to examine the correlation between lower back pain and proteoglycan loss. Further studies may also look at the mechanical behaviour of the disc and proteoglycan health.

The study will begin with the MR imaging of cadaveric specimens bathed in GAD. A histological analysis will follow to validate the process; both a quantitative and qualitative assessment of the procedures will occur. If validated, we will be designing studies to assess the mechanical properties of the disc and their dependence on proteoglycan health.

High Field Magnetic Resonance Imaging Centre

Protocol Proposal Form

Please prepare a detailed description of the MRI protocol**, after consultation with the Imaging Centre staff.**

Protocol Details: Assessment of Cartilage Health:

Procedure: Inversion recovery turbo-spin echo T1 scans according to the 2D dGEMRIC protocol. The protocol for dGEMRIC has been established and tested in volunteers for the knee and hip and needs to be assessed for the intervertebral disc.

Initially, human or animal cadaveric specimens will be used (decision pending). They will be bathed in the GAD contrast agent prior to scanning. A histological validation will follow the imaging process.

3T MR Protocol Amendment:

Evaluation of delayed gadolinium enhanced magnetic resonance imaging (dGEMRIC) as a more sensitive measure of intervertebral disc degeneration

Intervertebral discs bathed in a paramagnetic contrast agent may allow the visualization of the biochemical makeup of the disc. The dGEMRIC protocol currently used in the hip and knee is being applied in the lumbar spine in-vitro.

To initially test the feasibility of this, a dynamic test in the 3T MRI is being requested as an addition to the original accepted proposal.

Objective: To dynamically monitor the uptake of the contrast agent $Gd(DTPA)^{2-}$ in the lumbar intervertebral discs of a porcine lumbar spine immersed in a contrast agent bath. This will allow us to determine the time to maximum enhancement of the three main elements of the disc (nucleus, annulus, and endplates) which will be the bathing time for the future disc imaging study (already approved)

Proposal: I would like to place a lumbar spine in a watertight container with $Gd(DTPA)^{2-}$ solution. This will be placed in the MRI and monitored over a series of 6-8 hours. I am proposing to use the MRI after regular working hours, and set the scanner up to take T1 weighted images; initially, images will be taken at regular 20 min intervals (depending on time needed per image set) for the first 2 hours, then once an hour for the remaining time.

Previous studies which have looked at contrast agent uptake in the disc in-vivo have found enhancement in the central nucleus take up to 6 hours, with the initial hour showing a fast uptake of the solution in the peripheral regions of the disc. Articular cartilage in-vitro studies have used bathing times as low as 1.5 hrs. It is difficult to hypothesize about the time need in-vitro due to the lack of blood flow (i.e. different method of diffusion into the disc in-vitro), and the size of the disc, but 6-8 hours should be sufficient for this pilot test.

Joshua Levitz
Department of Orthopaedic Engineering
VGH

The University of British Columbia
Office of Research Services,
Clinical Research Ethics Board – Room 210, 828 West 10th Avenue, Vancouver, BC V5Z 1L8

Certificate of Expedited Approval

Clinical Research Ethics Board Official Notification

PRINCIPAL INVESTIGATOR	DEPARTMENT	NUMBER
Wilson, D.R.	Orthopaedics	C06-0350

INSTITUTION(S) WHERE RESEARCH WILL BE CARRIED OUT

UBC Campus, UBC Hospital

CO-INVESTIGATORS:

Levitz, Joshua, Orthopaedics

SPONSORING AGENCIES

Unfunded Research

TITLE:

Evaluation of Delayed Gadolinium Enhanced Magnetic Resonance Imaging (dGEMRIC) as a More Sensitive Measure of Intervertebral Disc Degeneration

APPROVAL DATE	TERM (YEARS)	DOCUMENTS INCLUDED IN THIS APPROVAL:
14 July 2006	1	Protocol; Anatomical Materials Transfer Agreement dd 14 March 2005; Tissue Request Form dd 14 March 2005; Sciencecare Tissue Use Policy dd 14 March 2005

CERTIFICATION:

In respect of clinical trials:

1. The membership of this Research Ethics Board complies with the membership requirements for Research Ethics Boards defined in Division 5 of the Food and Drug Regulations.

2. The Research Ethics Board carries out its functions in a manner consistent with Good Clinical Practices.

3. This Research Ethics Board has reviewed and approved the clinical trial protocol and informed consent form for the trial which is to be conducted by the qualified investigator named above at the specified clinical trial site. This approval and the views of this Research Ethics Board have been documented in writing.

The documentation included for the above-named project has been reviewed by the Chair of the UBC CREB, and the research study, as presented in the documentation, was found to be acceptable on ethical grounds for research involving human subjects and was approved by the UBC CREB.

The CREB approval for this study expires one year from the approval date.

[redacted]

Approval of the Clinical Research Ethics Board by one of:
Dr. Gail Bellward, Chair
Dr. James McCormack, Associate Chair
Dr. John Russell, Associate Chair
Dr. Caron Strahlendorf, Associate Chair

THE UNIVERSITY OF BRITISH COLUMBIA

Clinical Research Ethics Board Office
210 – 828 West 10th Avenue,
Research Pavilion,
Vancouver Hospital,
Vancouver, BC
V5Z 1L8
Phone: 604-875-4149
Fax: 604-875-4167

14 July 2006

File No: C06-0350

Dr. D.R. Wilson
Orthopaedics
VCHA
Campus Mail

Dear Dr. Wilson:

Re: "Evaluation of Delayed Gadolinium Enhanced Magnetic Resonance Imaging (dGEMRIC) as a More Sensitive Measure of Intervertebral Disc Degeneration"

The application for ethical review for this study has been reviewed and approved by the UBC Clinical Research Ethics Board (CREB). However, before the Certificate of Approval can be released, you must submit the Vancouver Coastal Health Authority (VCHA) "Request for Approval To Conduct Research" form to Vancouver Coastal Health Research Institute (VCHRI).

The VCHA submission is required in order to identify any and all resources involved in your study. This form may be downloaded from the VCHRI web site at www.vchri.ca/s/ClinicalTrials-Forms.asp

The CREB office will be informed by VCHRI once all VCHA requirements have been met, at which time your UBC Clinical Ethics Certificate of Approval will be immediately released and emailed to you.

According to VCHA policy, your research cannot begin until VCHRI approves the study. This final approval will be issued in a letter from the Vice-President, Research, VCHA.

For further assistance, please call Stephania Manusha, Regional Manager, Clinical Trials Administration at 604-[redacted] or email [redacted] or Wylo Kayle, Assistant, Clinical Trials Administration at 604-[redacted] Ext [redacted] or [redacted].

Sincerely,

Brent Sauder,
Director, Office of Research Services

CC Ms Stephania Manusha, Regional Manager, Clinical Trials Administration.

The University of British Columbia
Office of Research Services
Clinical Research Ethics Board – Room 210, 828 West 10th Avenue, Vancouver, BC V5Z 1L8

ETHICS CERTIFICATE OF EXPEDITED APPROVAL: RENEWAL WITH AMENDMENTS TO THE STUDY

PRINCIPAL INVESTIGATOR:	DEPARTMENT:	UBC CREB NUMBER:
David R. Wilson	UBC/Medicine, Faculty of/Orthopaedics	H06-70350

INSTITUTION(S) WHERE RESEARCH WILL BE CARRIED OUT:

Institution	Site
Vancouver Coastal Health (VCHRI/VCHA)	UBC Hospital

Other locations where the research will be conducted:
N/A

CO-INVESTIGATOR(S):

Joshua L. Levitz

SPONSORING AGENCIES:

Unfunded Research - "Evaluation of Delayed Gadolinium Enhanced Magnetic Resonance Imaging (dGEMRIC) as a More Sensitive Measure of Intervertebral Disc Degeneration"

PROJECT TITLE:
Evaluation of Delayed Gadolinium Enhanced Magnetic Resonance Imaging (dGEMRIC) as a More Sensitive Measure of Intervertebral Disc Degeneration

The current UBC CREB approval for this study expires: July 27, 2008

AMENDMENT(S):	AMENDMENT APPROVAL DATE:
Addition of Primary Contact, Project Period, and Funding.	July 27, 2007

CERTIFICATION:
In respect of clinical trials:
1. The membership of this Research Ethics Board complies with the membership requirements for Research Ethics Boards defined in Division 5 of the Food and Drug Regulations.
2. The Research Ethics Board carries out its functions in a manner consistent with Good Clinical Practices.
3. This Research Ethics Board has reviewed and approved the clinical trial protocol and informed consent form for the trial which is to be conducted by the qualified investigator named above at the specified clinical trial site. This approval and the views of this Research Ethics Board have been documented in writing.

The Chair of the UBC Clinical Research Ethics Board has reviewed the documentation for the above named project. The research study, as presented in the documentation, was found to be acceptable on ethical grounds for research involving human subjects and was approved for renewal by the UBC Clinical Research Ethics Board.

Approval of the Clinical Research Ethics Board by one of:

Dr. Bonita Sawatzky,
Associate Chair

The University of British Columbia
Clinical Research Ethics Board
Office of Research Services
Room 210, Research Pavilion, 828 W. 10th Avenue, Vancouver, BC V5Z 1L8
Phone: (604) 875-4111 ext. 68918 Fax: (604) 875-4167

For Administrative Use Only		
REB File Number:	Date Received:	Initials:

APPLICATION FOR CLINICAL ETHICAL REVIEW

to be completed with reference to CREB Guidance Notes

All information requested on this form must be typewritten in the space provided. ***Incomplete submissions will not be reviewed by the CREB.***
(Do not leave any box blank--- indicate "not applicable" by typing N/A. Limited additional space is available under item 45.)

The Principal Investigator must have a UBC Faculty Appointment or a staff appointment at an affiliated institution.

1. Principal Investigator / Faculty Advisor (see Guidance Note #1)
Surname: **Wilson** Given Name(s): **David**
Academic Rank: **Assistant Professor**
UBC Faculty / Department: **Orthopaedics**
UBC Division (If applicable): **Orthopaedic Engineering**
Hospital Department (if applicable): **N/A**
Hospital Division (if applicable): **N/A**
Phone Number: [redacted] Fax Number: [redacted]
E-mail Address: [redacted]

2. After reviewing Guidance Note #2 , please indicate whether your proposal falls under the "minimal risk" criteria and can be considered for Expedited Review.
☒ Yes ☐ No

3. Have you included the CREB fee with this Application? Complete Page 12 of this application for all industry- sponsored research. (see Guidance Note #3)
☐ Yes ☒ No

4. Indicate the sites where the research will be carried out. (see Guidance Note #4)
☒ UBC Vancouver ☐ UBC Okanagan ☐ VCHA-VGH ☒ VCHA-UBCH ☐ C&W ☐ PHC ☐ BCCA ☐ AC ☐ Other:
Studies carried out at PHC must also be submitted to the PHC REB (see Introduction of Guidance Notes re: Reciprocal Review)

5. Title of Research Proposal (see Guidance Note #5):
Evaluation of delayed gadolinium enhanced magnetic resonance imaging (dGEMRIC) as a more sensitive measure of intervertebral disc degeneration.
Proposed Project Period (day/month/year): From: **01/06/06** To: **01/06/08**
Is this proposal closely linked to any other proposal previously/simultaneously submitted to the CREB? (see Guidance Note #5) ☐ Yes ☒ No
If **Yes**, describe relationship of this proposal to this primary study: **N/A**
REB File Number of primary study: **N/A**

6. Provide a full and accurate listing of all documents submitted with this Application for Ethical Review. List reference numbers, version numbers, and/or dates. **Incomplete submissions will not be reviewed.** (see Guidance Note #6)

	Correct # of copies included?		Reference # / Version # + Date
Protocol **(3 copies)**	☒ Yes		
Amendments to Full Protocol **(3 copies)**	☐ Yes	☒ N/A	
Peer Review Reports **(3 copies; see box 11)**	☐ Yes	☒ N/A	
Investigator's Brochure **(1 copy)**	☐ Yes	☐ N/A	
Application form **(signature copy + 19 copies*)**	☒ Yes	☐ N/A	
Advertisement to recruit subjects **(20 copies*)**	☐ Yes		
Letter of initial contact **(20 copies*)**	☐ Yes	☒ N/A	
Subject consent form **(20 copies*)**	☐ Yes	☒ N/A	
Normal/Control subject consent form **(20 copies*)**	☐ Yes	☒ N/A	
Tissue/Blood Banking consent form **(20 copies*)**	☐ Yes	☒ N/A	
Other consent forms **(20 copies*)**	☐ Yes	☒ N/A	
Assent form **(20 copies*)**	☐ Yes	☒ N/A	
Questionnaires, tests, interview scripts, etc. **(20 copies*)**	☐ Yes	☒ N/A	

*** If this application can be considered for Expedited Review (when "Yes" has been checked, under Question #2), only THREE (3) copies are required.**

7. Required Signatures (see Guidance Note #7)

Principal Investigator / Faculty Advisor:
I agree to abide by the Tri-Council Policy for Ethical Conduct for Research Involving Human Subjects.

Signature Date

Department Head / Dean:
I confirm that the Principal Investigator has the qualifications, experience, and facilities to carry out this research.

Signature Date

Printed Name

8. Provide the name of ONE contact person for ALL correspondence. The original Certificate of Approval will be mailed to the address given here. (see Guidance Note #8)

Name: **David R. Wilson**
Title: **Assistant Professor**
Address: **577-828 West 10th Ave**
Vancouver, BC
V5Z 1L8

Phone Number: [redacted]
Fax Number: **604-875-4851**
E-mail Address: [redacted]

9. Co-Investigators and Students: (Use box 45 if additional space is needed) (see Guidance Note #9)

9a. Complete 9a. If this is research for a graduate degree:

Surname (ALL CAPS): **LEVITZ** Given Name(s): **Joshua Adam** Name of Supervisor: **David R. Wilson** UBC Faculty / Department: **Mechanical Engineering** UBC Division (If applicable): **Ortho Eng. Research** Hospital Department (If applicable): Hospital Division (If applicable): Type of degree program: ☒ Masters ☐ Doctorate ☐ Resident ***I agree to abide by the Tri-Council Policy for Ethical Conduct for Research Involving Human Subjects*** Signature of Student/Resident Date Printed Name	Surname (ALL CAPS): Given Name(s): Name of Supervisor: UBC Faculty / Department: UBC Division (If applicable): Hospital Department (If applicable): Hospital Division (If applicable): Type of degree program: ☐ Masters ☐ Doctorate ☐ Resident ***I agree to abide by the Tri-Council Policy for Ethical Conduct for Research Involving Human Subjects*** Signature of Student/Resident Date Printed Name

9b. Other Co-Investigators

Surname (ALL CAPS): Given Name(s): Academic Rank: UBC Faculty / Department: UBC Division (If applicable): Hospital Department (If applicable): Hospital Division (If applicable):	Surname (ALL CAPS): Given Name(s): Academic Rank: UBC Faculty / Department: UBC Division (If applicable): Hospital Department (If applicable): Hospital Division (If applicable):
Surname (ALL CAPS): Given Name(s): Academic Rank: UBC Faculty / Department: UBC Division (If applicable): Hospital Department (If applicable): Hospital Division (If applicable):	Surname (ALL CAPS): Given Name(s): Academic Rank: UBC Faculty / Department: UBC Division (If applicable): Hospital Department (If applicable): Hospital Division (If applicable):
Surname (ALL CAPS): Given Name(s): Academic Rank: UBC Faculty / Department: UBC Division (If applicable): Hospital Department (If applicable): Hospital Division (If applicable):	Surname (ALL CAPS): Given Name(s): Academic Rank: UBC Faculty / Department: UBC Division (If applicable): Hospital Department (If applicable): Hospital Division (If applicable):

9c. Tri Council Policy Statement (TCPS) Tutorial

All graduate students and medical residents are expected to complete the TCPS Tutorial before submission. The CREB strongly recommends that the Principal Investigators and all co-investigators are familiar with the TCPS. (See Guidance Note #9.3)
Indicate completion of the TCPS tutorial below:

All graduate students ☒ Yes ☐ No

All medical residents ☐ Yes ☐ No

Principal Investigator ☒ Yes ☐ No

Other investigators ☐ Yes ☐ No

10. Funding Source and Status

10a. Provide the NAME of the funding source (see Guidance Note #10):

10b. Classify the type of funding:

☐ For-profit sponsor ☐ Grant ☐ Grant-in-aid ☐ UBC internal ☒ No funding ☐ Other

10c. What is the status of the funding?

☐ Awarded ☐ Pending

11. Peer Review

Has this research proposal received any independent scientific/methodological peer review? (see Guidance Note #11) ☐ Yes ☒ No

If **Yes**, provide details below. Include the names of committees/individuals involved in the review. State whether the peer review process is ongoing or completed.

11a. External Peer Review Details:

11b. Internal (UBC or hospital) Peer Review Details:

11c. If No, explain why no independent scientific/methodological review has taken place:

12. Regulatory Approvals and Registration

12a. Enter the name of any **investigational drug(s)**, or **marketed drug(s)** used outside of its approved indication (See Guidance Note #12.1) :

12b. Enter the name of any marketed drug(s) used **within** its approved indication:

12c. Enter the name of any **Natural Health Products** (See Guidance Note #12.1):

12d. Enter the name of any **new investigational devices, or marketed devices used in experimental mode**, that will be used outside of their approved indication (See Guidance Note #12.1):

12e. Enter the name of any **positron-emitting radiopharmaceuticals (PERs)** (See Guidance Note #12.1):

12f. For clinical trials involving investigational drugs/devices or marketed drugs/devices outside of their indications **(including natural health products and positron-emitting radiopharmaceuticals)**, indicate whether or not approval has been obtained from the appropriate federal regulatory agency for this purpose. (See Guidance Note #12)

☐ Yes Name of agency: Date of approval (day/month/year)

☐ No

☐ Request for Approval has been submitted. **(Please notify the CREB Office when approval is obtained.)**

☒ Not applicable

12g. Does your research involve the use of **human pluripotent stem cells?** ☐ Yes ☒ No

Certain types of research involving human pluripotent stem cells conducted under the auspices of institutions receiving Tri-Council funding is required to apply to the CIHR Stem Cell Oversight Committee (SCOC) for approval. (See Guidance Note #2.1.2.4)

12h. The International Committee of Medical Journal Editors (ICMJE) now requires **registration** for all clinical trials as defined by ***"Any research project that prospectively assigns human subjects to intervention and comparison groups to study the cause-and-effect relationship between the medical intervention and the health outcome"***. Medical intervention is to be interpreted broadly to include drugs, devices, surgical procedures, behavioural or management studies which have the intent to modify a health outcome. In general all Phase III studies will need to be registered. However, Phase I and some phase II studies are excluded (See Guidance Note #12.3)

Does this clinical study fall within the definition above? ☐ Yes ☒ No

If Yes: has it been registered? ☐ Yes ☐ No

If Yes:

Indicate the Authorized Registry used:

Enter your Clinical Trial unique identifier:

If **No**: If you have not yet registered your clinical trial, visit ClinicalTrials.gov or Controlled-trials.com

12i. Is there a requirement for this research to comply with United States regulations for research ethics? (See Guidance Note #1.1.3) ☐ Yes ☒ No

13. Research Proposal Summary

Summarize the research proposal under the following headings: **1) Purpose, 2) Hypothesis, 3) Justification, 4) Objectives, and 5) Research Method.** Under Research Method, please justify the use of placebo in this study, if it is placebo-controlled. See boxes 14 to 20 to avoid duplicating information. The CREB requires sufficient background information and clear details of the research design in order to assess the scientific merit of the proposal in relation to ethical issues. (see Guidance Note #13)

1)Purpose

To develop a sensitive method of imaging early degeneration in the intervertebral disc by assessing the feasibility of using dGEMRIC, an MRI protocol previously used to look at cartilage health in synovial joints.

2) Hypothesis

We hypothesize that with protocol alterations, the use of dGEMRIC in the intervertebral disc will succeed.

3) Justification

Detection of early intervertebral disc degeneration is difficult with the current diagnostic imaging techniques. Disc degenerative disease is often cited as a cause of lower back pain. An important indication of disc degeneration is a decrease in the glycosaminoglycan (GAG) content of the disc, a negatively charged molecule which contributes to the water retention and load bearing capabilities of the disc. A method which can detect early onset of the disease by quantifying GAG content in-vivo may allow early preventative techniques to be applied to patients, thus sustaining a healthier back for a longer period of time.

4) Objectives

The primary objective of this study is to determine whether dGEMRIC can be used to assess the health of the intervertebral disc.

5) Research Methods

A total of 25 Cadaveric Human and animal discs will be used in this study. The specimens will be obtained through Science Care Anatomical (2020 West Melinda Lane, PO Box 87119, Phoenix, AZ 85027 - 602 331-3641), who are accredited by the American Association of Tissue Banks . Further specimens may be obtained through the UBC Injury Biomechanics Lab (UBC, Department of Mechanical Engineering, 6250 Applied Science Lane). The specimens will be imaged within 24 hours or receiving them, to avoid degradation due to the freezing/thawing process, or other environmental factors.

Cadaveric discs will be immersed in a Gd-DTPA^{2-}(Magnevist; Berlex Laboratories, Wayne, NJ) contrast agent solution for a predetermined amount of time.. Following immersion, MR images of multiple slices of the disc will be taken. The MRI sequence to be used will be similar to the dGEMRIC protocol recently developed for the hip, and minor changes will be made as necessary. Images will be transferred to a workstation where a T1 map of the image will be generated using customized software available at the UBC High Field Magnetic Resonance Imaging Centre. Concentration of GAG can be found using the T1 values, and the map will allow for a qualitative analysis as well.

For validation of the imaging technique, histological analysis will follow. The discs will be dissected into thin axial slices approximating the same slices taken during the imaging procedure. A histological analysis of each slice will then occur; this will allow us to validate the data obtained from the MRI images by providing us with both a qualitative and quantitative assessment of GAG in the tissue. This analysis will use an upright light microscope available in the Department of Orthopaedic Engineering (828 West 10th ave, 5th Floor) as well as a spectrophotometer available at the Jack Bell Research Center.

Linear regression analysis will be used to correlate the GAG concentration found from MR images and that found from the absorbance procedure. A qualitative assessment will be performed using the MR images after fitting a T_1 colour map and from the histological staining which is performed. If validated, the use of this protocol will be used in future studies in vivo.

Following the validation, general mechanical properties of the intervertebral disc, such as stiffness, will be assessed using the cadaveric specimens. Correlations between these properties and GAG concentrations as assessed by MRI will be identified.

Human Subject Enrolment

14. Is this a multi-centre trial? ☐ Yes ☒ No

How many subjects, including controls, will be enrolled in the entire study, across all sites? **25**

Of these, how many will be participating at the local (UBC/institution) site? **25**

How many normal subjects will be enrolled in the study, across all sites? **0**

Of the normal subjects, how many will be participating at the local (UBC/institution) site? **0**

Inclusion and Exclusion Criteria

15. Describe who is being selected, and the criteria for their inclusion (see also Box 34, and Guidance Note #15). For research involving human pluripotent stem cells, provide a detailed description of the stem cells being used in the research (see Guidance Note #2.1.2.4).

Cadaveric lumbar intervertebral discs

16. Describe which subjects will be excluded from participation. (see Guidance Note #16)

N/A

Identification, Initial Contact and Recruitment of Subjects

17. Describe how potential subjects will be contacted and by whom (see Guidance Note #17) . In addition, describe how the potential subjects will be identified, including the source of the contact information (see Guidance Note #17.1.1 and Guidance Note #17.1.2). Outline who originally collected the contact information and for what purpose it was originally collected. Attach copies of initial letters of contact and any other recruitment documents. Note that CREB policy does not allow initial contact by phone, unless in the case of emergencies (see UBC CREB Policy #2 in Guidance Note #17.5.2). Initial contact should not be made by the subject's primary caregiver (see Guidance Note #17.2.1)

N/A

18. Describe the selection and/or recruitment procedures for normal subjects, if these differ from the above. Attach copies of initial letters of contact and any other recruitment documents.

N/A

Description of Procedures (Must be written in the space provided)

19. Which of the following procedures are involved in this study? (Check all that apply.)

☐ Drug administration	☐ Collection of blood	☐ Questionnaires
☐ Surgical procedures	☐ Collection of other tissue	☐ Home visits
☐ Experimental medical devices	☐ Individual interview	☐ Video/Audio Recording
☒ Imaging studies (e.g., X-ray, MRI)	☐ Group interview	☐ Use of medical records

20. Summary of Procedures: Describe any specific manipulations: type, quantity, and route of administration of drugs and radiation, operations, tests, use of medical devices that are prototypes or altered from those in clinical use, interviews or questionnaires. Also, specify what procedures in this project involve an experimental approach, in that there may be diagnostic procedures or treatment dictated by the protocol differing from those required for standard patient care. (see Guidance Note #20)

Each Cadaveric specimen will undergo the following:

1) Each disc will be immersed in approximately 1000 ml of Gd-DTPA^{2-}(Magnevist; Berlex Laboratories, Wayne, NJ) and will be equilibrated for at least 12h with constant stirring. Before and after the solution application, up to 10 MR axial images of each disc will be taken, using the dGEMRIC protocol recently developed for the knee and hip. All MR imaging will be carried out using the 3 Tesla Phillips Gyroscan scanner at the UBC High Field MR Centre.

***All users of the MRI will have undertaken a safety orientation given by an authorized UBC High Field MRI employee, and will have been screened to ensure contact with the MRI scanner is safe.**

2) Each disc will be digested in papain, and then will be analyzed for GAG concentration with dimethylmethylene blue (DMMB) assay. A spectrophotometer will be used to find absorbances in the tissue (which can be used to calculate GAG concentrations). The discs will then be soaked in a saline solution to remove the DMMB, after which they will be stained with Hematoxylin and Eosin, or Alciam blue. This will allow viewing of the proteoglycans under a light microscope available at the Department of Orthopaedics in the VGH Research Pavillion (828 West 10th Ave). Area fractions of GAG content can be extracted using this method.

***The workers coming in contact with the cadavers will have obtained an anatomy and histology lab safety orientation (as necessary) given by authorized lab employees to ensure their safety when working with the specimens.**

21. Does the study involve research to be carried out in physician's private offices? ☐ Yes ☐ No

22. Time Requirements (see Guidance Note #22)

22a. How much time (i.e., how many minutes/hours over how many weeks/months) will a **subject** be asked to dedicate to the project beyond that needed for normal care? **N/A**

22b. How much time (i.e., how many minutes/hours over how many weeks/months) will a **normal volunteer** (if any) be asked to dedicate to the project?
N/A

Risks and Benefits

23. Describe what is known about the **risks** of the proposed research. Include any information about discomfort or incapacity that the subjects are likely to endure as a result of the experimental procedure, along with the details of any known **side effects** which may result from the experimental treatment. (see Guidance Note #23)
N/A

24. Describe the **benefits** to the subject that would arise from his or her participation in the proposed research. (see Guidance Note #24)
N/A

Reimbursement and Remuneration

25. Describe any reimbursement for expenses or payments/gifts-in-kind (e.g. honoraria, gifts, prizes, credits) to be offered to the subjects. Provide full details of the amounts, payment schedules, and value of gifts-in-kind. (see Guidance Note #25)
N/A

Monitoring and Data Analysis

26. Describe the provisions made to break the code of a double-blind study in an emergency situation, and indicate who has the code. (see Guidance Note #26)

N/A

27. Describe data monitoring procedures while the research is ongoing. Include details of planned interim analyses, Data and Safety Monitoring Board, or other monitoring systems. (see Guidance Note #27)

N/A

28. Describe the circumstances under which the study could be stopped early. Should this occur, describe what provisions would be put in place to ensure that the subjects are fully informed of the reasons for stopping the study. (see Guidance Note #28)

N/A

29. Describe how the identity of the subjects will be protected both during and after the research study. (see Guidance Note #29)

The names of the donors of the cadaveric specimen will not be known to the researchers, and they will instead be labelled by numbers. Anonymity of the donors will be protected.

30. Explain who will have access to the data at each stage of processing and analysis, and what steps will be taken to safeguard the confidentiality of the data at each stage. (see Guidance Note #30)

The data will be secure within the Division of Orthopaedic Engineering Research at Vancouver General Hospital. Only members of the research team will have access to the data

31. Describe what will happen to the data at the end of the study, and what plans there are for future use of the data.

The data will be retained for two years after the publication of any results in a peer reviewed journal of any results and shredded or erased thereafter.

Informed Consent

32. Describe the consent process. Who will ask for consent? Where, and under what circumstances? (see Guidance Note #32 and Guidance Note #17.6)

Cadavers used in this study are those of individuals who have given informed consent for their bodies to be used in scientific research. The specimens will be obtained through Science Care Anatomical (2020 West Melinda Lane, PO Box 87119, Phoenix, AZ 85027 - 602 331-3641), who are accredited by the American Association of Tissue Banks . Further animal specimens may be obtained through the UBC Injury Biomechanics Lab (UBC, Department of Mechanical Engineering, 6250 Applied Science Lane).

33. How long will the subject have to decide whether or not to participate? If this will be less than twenty-four hours, provide an explanation. (see Guidance Note #17.6)

N/A

34. Will every subject be competent to give fully informed consent on his/her own behalf? (see Guidance Note #34) ☐ Yes ☐ No

If **Yes**, skip to Box 37. If **No**, provide details of the nature of the incompetence (for instance, young age, mental or physical condition).

N/A

35. If a subject is not competent to give fully informed consent, who will consent on his/her behalf? (See Guidance Note #34.1)

N/A

36. If a subject is not competent to give fully informed consent, will he/she be able to give **assent** to participate? ☐ Yes ☐ No

Explain how assent will be sought. Attach copies of the **assent form** as necessary. (see Guidance Note #36)

N/A

37. Describe any situation in this research in which the **renewal of consent** might be appropriate, and how this would take place. (see Guidance Note #37)

N/A

38. What provisions are planned for subjects, or those consenting on a subject's behalf, to have **special assistance**, if needed, during the consent process (e.g., consent forms in Braille, or in languages other than English)? (see Guidance Note #38)

N/A

Consent Forms

39. UBC CREB policy requires written consent in all cases. All of the following information must be included in the consent form and not fragmented into information sheets. Please check off items in the following list to show that these items have been incorporated into all consent forms. (see Guidance Note #39) **Note that a separate tissue/DNA banking consent form is required when consent to bank tissue (including blood)/DNA is requested but is independent from the subject's participation in the study (i.e., when the subject may refuse banking, but still participate in the study). Refer to Guidance Note 39.6.1).**

- ☐ Consent forms prepared on institutional letterhead (UBC department or hospital) or a facsimile.
- ☐ The title of the project.
- ☐ The Identity of the Principal Investigator and the co-investigators, and the name and telephone number of a contact person.
- ☐ A contact telephone number for emergencies, and an explicit statement that it operates 24 hours a day, seven days a week, when appropriate.
- ☐ Second-person pronouns (you/your child), when referring to subjects. Be consistent throughout all consent forms.
- ☐ A clear explanation of why the subject has been invited to participate in the study.
- ☐ An offer to answer any inquiries concerning the procedures, to ensure that they are fully understood by the subject.
- ☐ An explanation of who is sponsoring the study.
- ☐ A brief but complete description in lay language of the purpose of the study and of all research procedures. (Terms such as Phase 1, Phase II, Phase III, random assignment, placebo, double blind, etc. must be explained in lay language.)
- ☐ A statement of the total amount of time for participating in the research required of a subject, beyond that normally needed for standard care.
- ☐ A description of which subjects must be excluded from the study, to allow the subject to self-select out of the study. This list should be limited to exclusions which the potential subject is likely to be aware of him/herself.
- ☐ A statement of all known side effects, with either an estimate of the probability of their occurrences or a summary of the available data (e.g., "has been tested in 50 normal volunteers; 5 experienced nausea and vomiting").
- ☐ A statement describing what alternatives to participating in the research project are available to the subject (i.e., what other treatment options are available outside of the study).
- ☐ A statement describing the timely disclosure to subjects of information related to their continuing participation.
- ☐ Assurance that the identity of the subject will be protected, and a description of how this will be accomplished. (see Guidance Note #39.7.1)
- ☐ Assurance that the information collected will be kept confidential, an explanation of how this will be done, and a statement of who will have access to it. (see Guidance Note #39.7.1 and UBC CREB Policy #11)
- ☐ Details of payment for expenses and/or any other remuneration to be offered to the subjects, if any.
- ☐ A statement that subjects do not waive any of their legal rights by signing the consent form. (see Guidance Note #39.7.5)
- ☐ A statement of any actual or potential conflict of interest on the part of the researchers or sponsor.
- ☐ An unambiguous statement that the subject may decline to enter, or withdraw from, the experiment at any time without any consequences to continuing medical care. (see Guidance Note #39.7.8)
- ☐ A statement that if the subject has any concerns about his/her treatment or rights as a research subject, he/she may telephone the Director, Office of Research Services at the University of British Columbia, at 604-822-8598. (see Guidance Note #39.7.6)
- ☐ A statement acknowledging receipt of a copy of the consent form, including all attachments.
- ☐ A statement that the subject is consenting to participate (by signing).
- ☐ The signature and printed name of the subject consenting to participate in the research project, investigation, or study, the date of the signature.
- ☐ The signature and printed name of a witness, and the date of signature. (see Guidance Note #39.8.3)
- ☐ The signature and printed name of the P. I. (or qualified designated representative), and the date of the signature. (See Guidance Note #39.8.4)
- ☐ Page numbers ("page 1 of 3," "page 2 of 3," etc.).
- ☐ The version number and date of the consent form, as a footer at the bottom of each page.

Potential Conflict of Interest

40. Describe any restrictions regarding the disclosure of information to research subjects (during or at the end of the study) that the sponsor has placed on investigators, including those related to the publication of results. (see Guidance Note #40)

N/A

41. Describe any personal benefits that the investigators and/or their partners/immediate family members will receive, connected to this research study. In addition, include details of all remuneration associated with the project that the investigator(s) or research organization will receive, (i.e. fees and/or honoraria directly related to this study, such as those for subject recruitment, advice on study design, presentation of results, or conference expenses). (see CREB Policy #16: Conflict of Interest in Guidance Note #40.2)

There will be no personal benefits received by any of the investigators in the study.

42. Describe any current or recent (within the last two years) consultancy or other contractual agreements with the sponsor held by the investigators. (Include amounts.) (see Guidance Note #40.3)

N/A

43. Give details, if any of the investigators and/or their partners/immediate family members have direct financial involvement with the sponsor via ownership of stock, stock options, or membership on a Board. (see Guidance Note #40)

N/A

44. Give details, if any of the investigators and/or their partners/immediate family members hold patent rights or intellectual property rights linked in any way to this study or its sponsor. (see Guidance Note #40)

N/A

Additional Information

45. Use this space to provide information which you feel will be helpful to the CREB, or to continue any item for which sufficient space was not available.

N/A

The University of British Columbia
Clinical Research Ethics Board
Office of Research Services
Room 210, Research Pavilion, 828 W. 10th Avenue, Vancouver, BC V5Z 1L8
Phone: (604) 875-4111 ext. 68918 Fax: (604) 875-4167

FEE-FOR-SERVICE PAYMENT DETAILS

Study Title: **Evaluation of delayed gadolinium enhanced magnetic resonance imaging (dGEMRIC) as a more sensitive measure of intervertebral disc degeneration.**

Study Principal Investigator: **David R. Wilson**

Industry For-Profit Sponsors: Include the **$3000.00** fee with the application. It is the investigator's responsibility to communicate this requirement to their sponsor and collect the payment prior to CREB submission (see Guidance Note #3 for more information).

Mechanism for Submitting Fee

Please indicate which of the following methods of payment has been attached to this application:

	Method of Payment:	*For Administrative Use Only*	
		Date Received:	Initials:
☐	A cheque made payable to "University of British Columbia," attention "Clinical Research Ethics Board"		
☐	A Journal Voucher crediting a. Speedchart (EDJM) b. Account: 477500 c. Fund: F0000 d. Dept. ID: 354000 e. Project Grant: 35F40100 * Make sure to debit your Project Grant using Account 651204. When the cheque is received from the funder, please process as a cost recovery by using the same Project Grant and Account on the Cash Receipt form. . * Make sure the Journal Voucher is signed by an authorized signatory.		

CREB Protocol Outline

Project Title: Evaluation of delayed gadolinium enhanced magnetic resonance imaging (dGEMRIC) as a more sensitive measure of intervertebral disc degeneration.

Background

Lower back pain is one of the most common injuries in society today, affecting between 70-85% of the general population at some point during their lives[1]. In the USA, back pain is the second most frequent reason for doctor visitations, the fifth ranking cause for hospital admissions, and the third ranking cause for surgical procedures [3;13]. In terms of Workers' Compensation, LBP is also the most common and expensive cause of disability related to work, with an estimated annual cost of $11.7 billion for LBP compensation in the United States[10]. These trends are also seen in other western countries [1]. Patients experiencing chronic lower back pain (consistent pain over a period greater than 3 months), use the health services more often than most other patient groups[3]. LBP can interfere with the most common daily activities such as walking stairs or standing from a chair. In people under the age of 45, it is the most common cause of activity limitation, and therefore is a great concern to an individual's overall quality of life[1].

Although the etiology of lower back pain is often idiopathic, intervertebral (IV) disc degeneration is often cited as a cause for pain, especially in the lumbar spine[4;9]. Degeneration is often characterized by tearing of the outer region of the disc (the annulus fibrosus), bulging of the disc into the spinal canal, and an overall decrease in the disc height. These features are able to be directly diagnosed from a one or more of standard radiographs, CT, or MRI images, especially when more severe degeneration has already occurred[5-7]. These diagnostic techniques are often qualitative in nature, and inter- and intra-observer variability has been shown to be a possible problem in diagnosis of degeneration. [8;12].

Severe pathological signs of degeneration, such as nerve root compression by a herniated disc, are consistent indicators of low back pain. The majority of patients with back pain, however, will not show such severe signs, and may or may not show some degree of the physical features described above. Further. the same features are often seen in healthy patients with no lower back pain[2;9;11]. Diagnosis of the cause for LBP cannot be made in approximately 85% of affected individuals because symptoms and pathological changes are not closely associated[14]. To improve the quality and sensitivity of diagnoses of LBP, more sensitive measures of disc degeneration are being studied.

In recent years, MRI imaging has become the dominant imaging modality used to assess IVD degeneration. Its ability to contrast soft tissue and its promising results in assessing cartilage degeneration in synovial joints is the reason for its expansion. This study is aiming to develop a more sensitive measure of IVD degeneration based on an MRI protocol used in synovial cartilage degeneration assessment, called delayed Gadolinium Enhanced MRI of Cartilage (dGEMRIC). This protocol uses a contrast agent injection

into a subject, and measures the amount of molecules called glycosaminoglycans (GAG) in the tissue indirectly by measuring T1 values of the tissue (MR parameter). A reduction in the amount of this molecule, which is important to the water retention and load bearing capabilities of the disc, is an indication of IVD degeneration. The application of this protocol in the intervertebral disc has not been tested.

Objectives

To develop a sensitive method of imaging early degeneration in the intervertebral disc by assessing the feasibility of using the dGEMRIC protocol.

Hypothesis

We hypothesize that with some protocol alterations, the use of dGEMRIC in the IVD will succeed.

Research Procedures

For the initial feasibility study, 25 cadaveric intervertebral discs will undergo the following (refer to ethics form for how cadaveric specimens will be obtained):

1. MRI-based assessment of disc GAG content

   Each of the 25 discs will be immersed in a Gd-DTPA^{2-} (Magnevist; Berlex Laboratories, Wayne, NJ) contrast agent solution for approximately 12 hours with constant stirring to promote diffusion into the disc. Following immersion, MR images of multiple slices of the disc will be taken. The MRI sequence used will be similar to the dGEMRIC protocol recently developed for the hip, and minor changes will be made as necessary. Images will be transferred to a workstation where a T1 map of the image will be generated using customized software available at the UBC High Field Magnetic Resonance Imaging Centre. Concentration of GAG can be found using the T1 values, and the map will allow for a qualitative analysis as well. All MR imaging will be carried out using the 3 Tesla Phillips Gyroscan scanner at the UBC High Field MR Centre.

2. Histological Analysis:

   The discs will be dissected into thin axial slices approximating the same slices taken during the imaging procedure. A histological analysis of each slice will then occur; this will allow us to validate the data obtained from the MRI images by providing us with both a qualitative and quantitative assessment of GAG in the tissue. This analysis will use an upright light microscope available in the Department of Orthopaedic Engineering (828 West 10th ave, 5th Floor) as well as a spectrophotometer available at the Jack Bell Research Center.Mechanical Analysis

3. Mechanical Testing

   Once the dGEMRIC sequence has been optimized to the intervertebral disc, mechanical testing will occur. We will be comparing mechanical properties of the cadaveric specimens, such as stiffness, with the GAG concentration or T1 maps found from the MRI protocol previously explained.

Statistical Analysis

Linear regression analysis will be used to correlate the GAG concentration found from MR images and that found from the absorbance procedure. A qualitative assessment will be performed using the MR images after fitting a T1 colour map and from the histological staining which is performed.

Organization of Study

This study will be carried out under the supervision of the principal investigator, Dr. David Wilson. Data collection and analysis will be carried out by Joshua Levitz (graduate student).

Reference List

1. Andersson GB. Epidemiological features of chronic low-back pain. Lancet 1999;354:581-5.

2. Deyo RA. Diagnostic evaluation of LBP: reaching a specific diagnosis is often impossible. Arch Intern Med 2002;162:1444-7; discussion 1447-8.

3. Hart LG, Deyo RA, and Cherkin DC. Physician office visits for low back pain. Frequency, clinical evaluation, and treatment patterns from a U.S. national survey. Spine 1995;20:11-9.

4. Haughton V. Medical imaging of intervertebral disc degeneration: current status of imaging. Spine 2004;29:2751-6.

5. Haughton V. Imaging intervertebral disc degeneration. J Bone Joint Surg Am 2006;88 Suppl 2:15-20.

6. Jarvik JG and Deyo RA. Diagnostic evaluation of low back pain with emphasis on imaging. Ann Intern Med 2002;137:586-97.

7. Kettler A and Wilke HJ. Review of existing grading systems for cervical or lumbar disc and facet joint degeneration. Eur Spine J 2005.

8. Kolstad F, Myhr G, Kvistad KA, Nygaard OP, and Leivseth G. Degeneration and height of cervical discs classified from MRI compared with precise height measurements from radiographs. Eur J Radiol 2005;55:415-20.

9. Leonardi M, Simonetti L, and Agati R. Neuroradiology of spine degenerative diseases. Best Pract Res Clin Rheumatol 2002;16:59-87.

10. Murphy PL and Volinn E. Is occupational low back pain on the rise? Spine 1999;24:691-7.

11. Roughley PJ. Biology of intervertebral disc aging and degeneration: involvement of the extracellular matrix. Spine 2004;29:2691-9.

12. Stafira JS, Sonnad JR, Yuh WT et al. Qualitative assessment of cervical spinal stenosis: observer variability on CT and MR images. AJNR Am J Neuroradiol 2003;24:766-9.

13. Taylor VM, Deyo RA, Cherkin DC, and Kreuter W. Low back pain hospitalization. Recent United States trends and regional variations. Spine 1994;19:1207-12; discussion 13.

14. White AA 3rd and Gordon SL. Synopsis: workshop on idiopathic low-back pain. Spine 1982;7:141-9.